

Geophysical investigation of the Marble Hall Fragment of the Bushveld Complex

By

OLUSEYI KAYODE TIMMY BABAYEJU

Submitted in partial fulfillment of the requirements for the degree

of

Master of Science

in the Faculty of Science

University of Pretoria

Pretoria

December 1999

Geophysical investigation of the Marble Hall Fragment of the Bushveld Complex

By

OLUSEYI KAYODE TIMMY BABAYEJU

Submitted in partial fulfillment of the requirements for the degree

of

Master of Science

in the Faculty of Science

University of Pretoria

Pretoria

December 1999

DEDICATION

I dedicate this study to my entire family who have been full of prayers and support for me for as long as this research lasted.

ACKNOWLEDGEMENT

The completion of this research would not have been possible without the assistance of many others who contributed financially, logistically, critically and morally.

First, I thank the Lord Almighty, my creator and my redeemer for leading the way for me throughout the duration of this research project and for His grace in making meet with the favour of people in the study area.

I wish to acknowledge the financial contribution of the Foundation for Research and Development (FRD) now National Research Foundation (NRF) and Iron and Steel Corporation of South Africa (ISCOR) towards the success of this project. My special thanks goes in particular to ISCOR Geophysics for providing logistic support, equipment and personnel (Raymond Vonk, Willem, Steven and Thomas) on different occasions for the gravity measurement. I will like to express my most sincere appreciation to the indefatigable efforts and contribution of Mr Raymond Vonk, doubling as a field exploration adviser and as a friend throughout this research.

I thank Mr Fritz Van der Merwe of the Department of Land Survey for providing the GPS and assisting in the topographic data interpretation and the Council for Geoscience, with special recognition to Dr. Edgar Stettler, for providing initial interpretative advice, equipment and laboratory facility needed.

I heartily appreciate the literature support and expert opinions of Prof P.G. Ericksson and Prof P.J. Hattingh on specific aspects of the research. I equally prize the supportive roles of my colleagues and friends, Hammond, Alain, Asfaw, Maletsabisa, Mike, Bjorn, Kobus, Godfrey, Alain and my dear brother, Dr Abiodun Babayeju. I am greatly indebted to the amiable Miss Magdel Combrinck for her tireless and committed assistance for as long as this research lasted.

The friendly gestures and support of all the farmers in the Marble Hall area despite being victims of violent criminal attacks rampant on farms at the time is highly commended. My most profound thanks in this regard goes to Mr Hennie Roets for providing accommodation on his farm and opening all his territories for the research.

I express my most sincere gratitude to my co-supervisor, Prof S.A. De Waal for his positive criticism, suggestions and encouragement. These are highly valued and his kindly gestures will be appreciated for a long time.

Last, but most important of all, I am heartily grateful to my research supervisor, Prof W.J. Botha, for providing all the necessary tools for my study, for his critically positive ideas, for making me feel at home in the department, and for creating an Exploration Geophysicist out of me.

The effort of every other person not mentioned and who has contributed one way or the other to the success of this research is also appreciated.

I thank you all.

OPSOMMING

Die geologiese struktuur van die Marble Hall Fragment van die Bosveldkompleks in die Mpumalanga Provinsie is ondersoek met behulp van gravitasie en hoë-digtheid lugmagnetiese data. Tydens die gravitasieondersoek is 'n regionale ondersoek oor 731 vierkante kilometer gedoen. Altesaam 731 swaartemetings, met 'n 1 kilometer interval, is ingesamel oor die Transvaal Supergroep, die mafiese gesteentes en die omliggende graniet. Die magnetiese data is gevlieg op 'n hoogte van 60 meters met 'n 87 meter lynspasiëring. Verskeie filters is toegepas op die magnetiese data met behulp van OASIS Montaj sagteware, en die struktuurelemente in die Fragment is omlyn met eerste-afgeleide data.

Die Wonderkopverskuiwing in die noordweste en 'n beduidende noordsuid-strekkende verskuiwing aan die ooste begrens die Marble Hall Fragment aan beide kante. Die helling van die noordsuid-strekkende verskuiwing aan die oostekant van die Fragment kon nie vasgestel word nie omdat die verskuiwing nie dagsoom nie. Die sterk magnetiese anomalie wat in die oostelike flank van die Swartkop-Marble Hall-antiklien voorkom is die oppervlakmanifestasie van die Hekpoort Andesietformasie. Daarenteen is die oorsprong van 'n verskuifde, goedgedefinieerde halfmaanvormige liggaam, met 'n sterk magnetiese patroon, langs die Swartkop-Marble Hall antiklien, nie duidelik nie aangesien dit nie met enige geologiese dagsoomverskynsel gekorreleer kan word nie.

Twee-en-'n-half-dimensionele interpretasie van beide die gravitasie en magnetiese data is uitgevoer langs geselekteerde profiele. Uit die modelle is dit duidelik dat 'n digte magnetiese propvormige liggaam, geleë in die senter van die Marble Hall Fragment, in die gesteentes van die Transvaal Supergroep ingeplaas is. Die intrusiewe liggaam het 'n sentrale subvertikale

gedeelte en word omring op vlakke diepte deur subhorisontale plaatvormige liggame. As gevolg van die nie-eenduidigheid van die potesiaalveldmetodes kan die werklike diepte en dikte van die mafiese plate nie bepaal word nie, en dit is begryplik dat die plate moontlik dunner en nader aan die oppervlakte kan wees as wat die modelle aandui. Uit die modelle volg dit dat die mafiese gesteentes jonger is as die plooiing en, moontlik selfs, sommige van die verskuiwings. Die Fragment kan beskou word as geplooië vloer van Transvaal Supergroep wat as 'n horst na die intrusie van die Rustenburg Gelaagde Suite ingeplaas is.

ABSTRACT

The geological structure of the Marble Hall Fragment of the Bushveld Complex in Mpumalanga Province, was investigated using gravity and high density airborne magnetic data. The gravity investigation amounted to a regional survey over an area of approximately 750 square kilometres. A total of 731 measurements, at 1 kilometre intervals, were made of the gravitational attraction on the Transvaal Supergroup, the mafic rocks and the surrounding granite. The magnetic data was flown at a terrain clearance of 60 metres and 87 metres line spacing. Several filters were applied to the magnetic data using OASIS Montaj software and the structures observed on the Fragment were delineated using the first vertical derivative data.

The Wonderkop fault, in the north-west, and a major north-south trending fault to the east were shown to border the Fragment on either side. The dip of the north-south trending fault to the east of the Marble Hall Fragment, could not be determined because there is no surface expression of the fault. The high magnetic signature associated with the eastern limb of the Swartkop-Marble Hall Anticline, running from the south towards the east-north-east, is the surface expression of the Hekpoort Andesite Formation. However, the origin of a faulted, well defined, crescent shaped body, with high magnetic signature to the north, along the axis of the Swartkop-Marble Hall Anticline, is not obvious, because of non-compatibility with outcropping geology in the area.

Two and a half-dimensional interpretation of both the gravity and magnetic data were carried out along five selected profiles. From the models it is evident that a dense magnetic plug-like body, situated in the centre of the Marble Hall Fragment, was emplaced in the Transvaal Supergroup rocks. The intrusive body has a central sub-vertical core section surrounded at shallower levels

by sub-horizontal sill-like sections. Due to non-uniqueness in potential field situations, the exact depth and thickness of the mafic sills cannot be categorically stated, and it is conceivable that the sills might be thinner and closer to the surface than implied by the models. It follows from the models, that the intrusion of the Bushveld mafic rocks post-dates the folding and perhaps some of the faults in the Fragment. The Fragment could be seen as folded floor of Transvaal Supergroup that was emplaced as a horst after the intrusion of the Rustenburg Layered Suite.

TABLE OF CONTENTS

| | |
|-------------------|------|
| TITLE PAGE | i |
| DEDICATION | ii |
| ACKNOWLEDGEMENT | iii |
| OPSOMMING | v |
| ABSTRACT | vii |
| TABLE OF CONTENTS | ix |
| LIST OF FIGURES | xiii |
| LIST OF TABLES | xv |

CHAPTER ONE : INTRODUCTION AND OBJECTIVES

| | |
|-----------------------------|---|
| 1.1. INTRODUCTION | 1 |
| 1.2. OBJECTIVES | 2 |
| 1.3. LOCATION OF STUDY AREA | 3 |

CHAPTER TWO : THE GEOLOGY OF THE MARBLE HALL FRAGMENT AND ITS ENVIRONMENT

| | |
|--------------------------------------|---|
| 2.1. GEOLOGY OF THE BUSHVELD COMPLEX | 6 |
| 2.1.1. RUSTENBURG LAYERED SUITE | 6 |
| 2.1.1.1. MARGINAL ZONE | 8 |
| 2.1.1.2. LOWER ZONE | 9 |
| 2.1.1.3. CRITICAL ZONE | 9 |

| | | |
|----------|--|----|
| 2.1.1.4. | MAIN ZONE | 11 |
| 2.1.1.5. | UPPER ZONE | 11 |
| 2.1.2. | RASHOOP GRANOPHYRE | 12 |
| 2.1.2.1. | STAVOREN GRANOPHYRE | 12 |
| 2.1.2.2. | DIEPKLOOF GRANOPHYRE | 12 |
| 2.1.2.3. | ZWARTBANK PSEUDOGANOPHYRE | 13 |
| 2.1.3. | LEBOWA GRANITE SUITE | 13 |
| 2.1.4. | ROOIBERG GROUP | 14 |
| 2.1.5. | MAKECKAAN FORMATION | 14 |
| 2.2. | THE AGE OF THE BUSHVELD COMPLEX | 15 |
| 2.3. | MODE OF EMPLACEMENT AND SHAPE OF THE BUSHVELD COMPLEX: GEOPHYSICAL DATA | 16 |
| 2.4. | THE MARBLE HALL FRAGMENT | 17 |
| 2.4.1. | LOCALITY | 17 |
| 2.4.2. | THE GEOLOGY OF THE MARBLE HALL FRAGMENT | 18 |

CHAPTER THREE : GEOPHYSICAL DATA ACQUISITION

| | | |
|----------|--|----|
| 3.1. | INTRODUCTION | 22 |
| 3.2. | DATA ACQUISITION, GRAVITY | 24 |
| 3.2.1. | FIELD PROCEDURE | 24 |
| 3.2.1.1. | PREVIOUS WORK | 24 |
| 3.2.1.2. | CONDUCT OF PRESENT SURVEY AND DATA ACQUISITIONING | 25 |
| 3.2.1.3. | LABORATORY DETERMINATION OF DENSITIES OF ROCK SAMPLES | 32 |

| | | |
|----------|--|----|
| 3.2.2. | DESCRIPTION OF EQUIPMENT | 33 |
| 3.2.2.1. | DATA ACQUISITION, GRAVITY (SCINTREX AUTOGRAV GRAVIMETER -CG3) | 33 |
| 3.2.2.2. | DATA ACQUISITION, POSITIONING (TRIMBLE 4000 SSE GEODETIC SYSTEM SURVEYOR) | 38 |
| 3.2.2.3. | DATA ACQUISITION, MAGNETIC SUSCEPTIBILITY (KT-9 KAPPMETER) | 43 |
| 3.3. | DATA ACQUISITION, AIRBORNE MAGNETIC DATA | 45 |

CHAPTER FOUR : GEOPHYSICAL INTERPRETATION AND DISCUSSION

| | | |
|--------|---|----|
| 4.1. | DATA PROCESSING AND INTERPRETATION | 46 |
| 4.1.1. | INTRODUCTION | 46 |
| 4.1.2. | VERTICAL DERIVATIVE | 46 |
| 4.1.3. | ANALYTICAL SIGNAL | 47 |
| 4.1.4. | UPWARD CONTINUATION | 48 |
| 4.1.5. | DOWNWARD CONTINUATION | 48 |
| 4.1.6. | REDUCTION TO THE MAGNETIC POLE | 49 |
| 4.2. | MAGNETIC DATA PROCESSING AND INTERPRETATION | 50 |
| 4.2.1. | INTRODUCTION | 50 |
| 4.2.2. | TOTAL MAGNETIC INTENSITY CONTOUR MAP | 50 |
| 4.2.3. | VERTICAL DERIVATIVE | 58 |
| 4.2.4. | ANALYTICAL SIGNAL | 58 |
| 4.2.5. | UPWARD CONTINUATION | 58 |
| 4.2.6. | REDUCTION TO THE POLE | 59 |

| | | |
|----------|---|----|
| 4.3. | PROCESSING OF GRAVITY DATA | 59 |
| 4.3.1. | REDUCTION TO BOUGUER VALUES | 59 |
| 4.4. | INTERPRETATION OF POTENTIAL FIELD DATA | 60 |
| 4.4.1. | GENERAL | 60 |
| 4.4.2. | CORRELATE KNOWN GEOLOGY WITH OBSERVED GEOPHYSICAL ANOMALIES | 60 |
| 4.4.3. | STRUCTURAL INTERPRETATION OF MAGNETIC AND GRAVITY CONTOUR MAPS | 68 |
| 4.4.3.1. | GRAVITY | 68 |
| 4.4.3.2. | MAGNETICS | 69 |
| 4.4.4. | 2.5-D MODELING OF SELECTED PROFILES | 69 |
| 4.4.5. | LIMITATIONS | 88 |
| 4.5. | CONCLUSIONS | 89 |
| | REFERENCES | 92 |

LIST OF FIGURES

- Figure 1.1. Locality map of the Marble Hall Fragment (After Hunter, 1975)
- Figure 2.1. Geological map of the Bushveld Complex showing the location of the study area and the distribution of the main components of the complex.
- Figure 2.2. Simplified geological map of the Marble Hall Fragment. The relatively thin Black Reef Formation between the Chuniespoort and Bloempoot Formation is shown as part of the Chuniespoort Group.
- Figure 3.1. Locality map of the gravity base station at Marble Hall
- Figure 3.2. Photograph of gravity base station at Marble Hall
- Figure 3.3. Locality map of the gravity base station at Groblersdal
- Figure 3.4a. Gravity station locality map
- Figure 3.4b. Locality map identifying each gravity position by number
- Figure 3.5. The Autograv gravity meter
- Figure 3.6. The GPS system in the survey area
- Figure 3.7. The KT- 9 Kappmeter (Susceptibility meter)
- Figure 4.1. Total field magnetic contour data
- Figure 4.2. First vertical derivative
- Figure 4.3. Analytical signal
- Figure 4.4. Magnetic data upward continued to an elevation of 500m
- Figure 4.5. Magnetic data upward continued to an elevation of 1000m
- Figure 4.6. Magnetic data upward continued to an elevation of 2000m
- Figure 4.7. Magnetic data with a reduction to the pole filter applied
- Figure 4.8. Topography of the study area
- Figure 4.9. Bouguer gravity map

- Figure 4.10. Simplified outline of geology superimposed on downward continued total field magnetic data
- Figure 4.11. Features identified from the correlation of vertical derivative map with simplified Geology
- Figure 4.12. Bouguer gravity map with outline of simplified geology
- Figure 4.13. Bouguer gravity map with contour lines to emphasise the steepness of the gradient in some areas
- Figure 4.14. Total field magnetic map draped over the topography
- Figure 4.15. Vertical derivative map with interpreted structures
- Figure 4.16a. Relative localities of gravity profiles selected for 2.5-D modeling
- Figure 4.16b. Relative localities of magnetic profiles selected for 2.5-D modeling
- Figure 4.17. Topographic relief along profiles AA', BB' and CC'
- Figure 4.18a. Starting models for profiles AA' and BB'
- Figure 4.18b. Starting model for profile CC'
- Figure 4.19a. Geophysical model for profile AA' (i) the gravity and (ii) the magnetics.
- Figure 4.19b. Geophysical model for profile BB' (i) the gravity and (ii) the magnetics.
- Figure 4.19c. Geophysical model for profile CC' (i) the gravity and (ii) the magnetics.
- Figure 4.20a. Gravity data showing the localities of profiles finally selected for 2.5-D modeling after determining strike.
- Figure 4.20b. Magnetic data showing the localities of profiles finally selected for 2.5-D modeling after determining strike.
- Figure 4.21. Geological cross sections for gravity and magnetic data along profiles DD' and EE'
- Figure 4.22. Geophysical model for profile DD' (i) the gravity and (ii) the magnetics.
- Figure 4.23. Geophysical model for profile EE' (i) the gravity and (ii) the magnetics.

LIST OF TABLES

- Table 1. Lithostratigraphic subdivision and thicknesses of the Rustenburg Layered Suite in the eastern Bushveld Complex.
- Table 2. Lithostratigraphic subdivision of the successions in the Marble Hall Fragment and Dennilton Dome
- Table 3. Base station values
- Table 4. Densities of rocks obtained in the research area
- Table 5. Typical gravity data as recorded by the scintrex autograv in the investigation of the Marble Hall Fragment
- Table 6. A typical processed elevation data obtained from the software controlled 4000 SSE Geodetic Surveyor used in the investigation of Marble Hall Fragment.
- Table 7. Magnetic susceptibilities of rocks obtained in the research area

INTRODUCTION AND OBJECTIVES

1.1. INTRODUCTION

The Marble Hall Fragment represents one of the larger inliers of floor rocks in the Bushveld Complex. The Fragment is situated approximately 160 kilometres due north-east of Pretoria, in the direct vicinity of the town of Marble Hall, Mpumalanga Province.

Geological studies (De Waal, 1963; Snyman, 1958; Hartzler, 1994) showed that the Fragment forms a dome-like structure of folded supracrustal rocks of the Transvaal Supergroup. It is entirely surrounded by granite of the Lebowa Granite Suite, and, in the south-western part, overlain by flat-lying sedimentary rocks of the Karoo Supergroup. Several outcrops of basic intrusive occur in the Fragment. De Waal (1963) and Hartzler (1994) attempted to interpret the shape of these intrusions from outcrop information. However, the generally poor outcrops in this area, widely acknowledged as outstanding irrigation land, makes such interpretation speculative at best. The need for deep sensing techniques to help the situation is clearly required.

The geophysical investigation of the Marble Hall Fragment reported in this dissertation forms part of multidisciplinary Marble Hall Project conducted by the Department for Earth Sciences at the University of Pretoria. The National Research Foundation and ISCOR Mining jointly funded the project.

1.2 OBJECTIVES OF THE RESEARCH

The objectives of the Marble Hall Project are (De Waal, S.A. 1999 pers. comm.):

- To determine the structure and geology of the Marble Hall Fragment;
- To determine the possible link between the Marble Hall basic intrusives and other Bushveld-related intrusives, stratigraphically below the Rustenburg Layered Suite;
- To review the economic potential of the Fragment; and
- To contribute to the understanding of the intrusive mechanism and history of the Bushveld Complex.

The objectives of the geophysical investigation are:

- To add additional constraints to the existing geological interpretations of the structure of the Fragment, especially in areas covered by superficial deposits;
- To map the subsurface extent and structure of the basic intrusives; and
- To develop new possible geological models for the deep structure of the Fragment, based on the observed gravity and magnetic data.

These added constraints on the deep structure of the Marble Hall Fragment are useful to distinguish between a number of opposing hypotheses on the structural nature of the Marble Hall Fragment. The following are of importance:

The structural deformation observed relates to

- the intrusion of the Rustenburg Layered Suite,

- the intrusion of the Nebo granite, or
- predates these events.

The Marble Hall Fragment represents

- a diapir,
- upfolded floor, or
- detached folded floor.

1.3 LOCATION OF STUDY AREA:

The boundaries of the geophysical research area are formed by latitudes $24^{\circ} 50' 00''\text{S}$ and $25^{\circ} 06' 30''\text{S}$, and longitudes $29^{\circ} 10' 00''\text{E}$ and $29^{\circ} 25' 00''\text{E}$ (Figure 1.1). The study area covers approximately 750 km^2 and embraces a number of farm settlements, game reserves, nature reserves, privately owned game farms and a small town.

The major river in the area is the Olifants River which flows along the eastern boundary of the research area with some meandering towards the west in places. Other smaller rivers, such as Elands and Moos Rivers, drain the central portion of the project area providing good irrigation sources for the various farmlands. Canals of the Loskop Dam Irrigation Scheme, delivering water to the large stretches of arable land, are common in the area. In addition, there are a large number of water wells and boreholes drilled for domestic purposes.

The area is endowed with a range of hills with elevations in the survey area ranging between 960 and 1144.7 metres above mean sea level. The most prominent of these hills are found in the northern part of the survey area and along the eastern boundary of the Marble Hall Fragment. The hills in the northwest are underlain by the Makeckaan Formation of the Stavoren Fragment. The Marble Hall Fragment, has a relatively flat topography.

Major roads found in this area provide access to towns such as Roedtan and Pietersburg in the north, Dennilton in the south, Groblersdal in the south-east and Siyabuswa in the west. There are other minor roads, paths and trails which provide access to smaller settlements, farms and rivers.

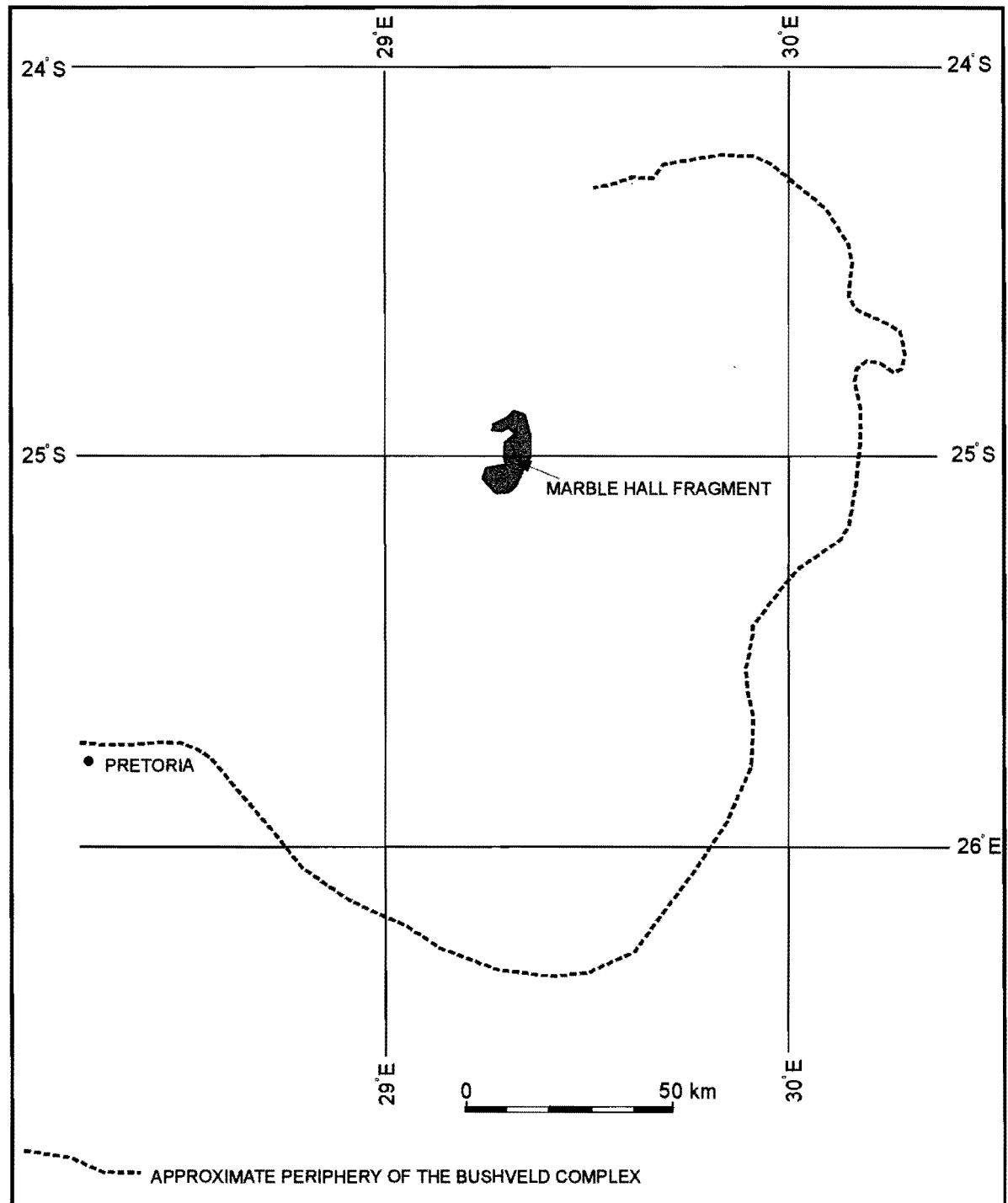


Figure 1.1 Locality map of the Marble Hall Fragment (After Hunter, 1975)

THE GEOLOGY OF THE MARBLE HALL FRAGMENT AND ITS ENVIRONMENT

2.1. GEOLOGY OF THE BUSHVELD COMPLEX

The Bushveld Complex is early Proterozoic in age and consists of three large suites of intrusive rocks, occupying a total surface area of approximately 65,000km². The Complex is known for its enormous concentrations of magmatic ores, a variety of pegmatitic and hydrothermal deposits, as well as industrial mineral deposits formed by the metamorphism of the floor rocks of the Complex (Cairncross and Dixon, 1995).

The three main lithological units of the Bushveld Complex are :

- Rustenburg Layered Suite
- Raseeb Granophyre Suite, and
- Lebowa Granite Suite.

A fourth suite, the Rooiberg Group of acid and basic volcanic rocks, was previously allocated to the Transvaal Supergroup (SACS, 1980), but is now accepted to be an integral part of the Bushveld Complex (Schweitzer *et al.*, 1995a, b).

2.1.1. Rustenburg Layered Suite

The Rustenburg Layered Suite is exposed in three, roughly crescent-shaped, outcrop areas, referred to as the Western, Eastern and Northern Lobes of the Bushveld Complex (Figure 2.1).

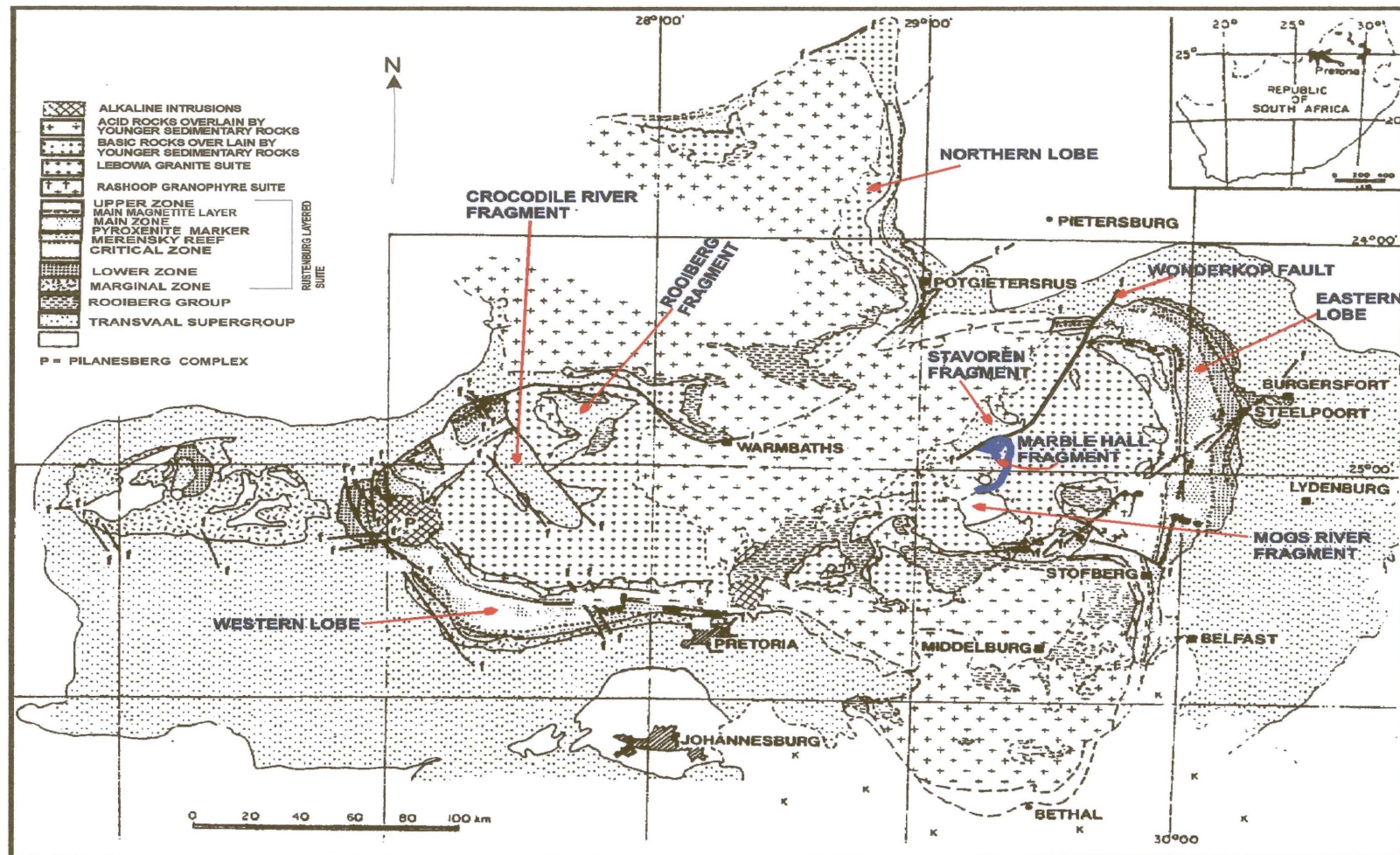


Figure 2.1. Geological map of the Bushveld Complex and environs showing the location of the study area and the distribution of the main components of the Complex (Adapted from Eales *et al.*, 1993).

The total exposed part of the Rustenburg Layered Suite covers an area of 12,200km². Measured thicknesses of close to 9000m are recorded in the eastern Bushveld, 7750m in the Western Bushveld and 7000m in the Potgietersrus area (Van der Merwe, 1976). The central area between the lobes is underlain by acid plutonic rocks of the Lebowa Granite and Rashoop Granophyre Suites, acid volcanics of the Rooiberg Group, and covered by supracrustal rocks of the Karoo Supergroup. Several inliers of floor rocks, as domes and diapirs (Cairncross and Dixon, 1995), are present in the Complex. The largest of these are the Crocodile River, Moos River and Marble Hall Fragments (Cairncross and Dixon, 1995).

The most significant outcrops of the basic and ultrabasic rocks of the Rustenburg Layered Suite are found in the Eastern Lobe of the Complex, where the complete succession of rock types from the base to the top is exposed (Vermaak and Gruenewaldt, 1986; Molyneux, 1974; Von Gruenewaldt, 1973; Cameron and Emerson, 1959; and Cameron, 1978). In the western part of the Complex, mapping by Vermaak (1970), Coertze (1970, 1974) and Young (1978), as well as deep drilling by mining companies (Vermaak, 1976) and the Geological Survey of South Africa (now the Council for Geoscience), show a comparable lithological succession to that in the east (Vermaak and Gruenewaldt, 1986).

The Rustenburg Layered Suite is subdivided into five zones viz :

2.1.1.1. Marginal Zone

This consists of plagioclase-orthopyroxene cumulates (norites), generally finer-grained than the interior of the complex and containing abundant country-rock xenoliths which defines the base of the sequence (Eales *et al.*, 1993). It has a varying thickness (Vermaak and Gruenewaldt, 1986; Teigler, 1990), reaching 250metres in the Western limb (Vermaak, 1976). Studies by Sharpe (1981) and Harmer & Sharpe (1985) on the marginal rocks of the

Rustenburg Layered Suite, led to the conclusion that for consistency the mafic rocks are conformable with the sedimentary units of the floor, but that there are abrupt discordances where the magma transgressed to higher stratigraphic levels.

2.1.1.2. Lower Zone

The Lower Zone overlies the Marginal Zone and it is dominated by olivine-rich cumulates (dunite, harzburgite) and orthopyroxenite (Eales *et al.*, 1993). This zone, previously called the Basal Zone, is composed mainly of four rock units namely Clapham Bronzitite (basal subzone), Rostock Bronzitite (lower bronzitite subzone), Jagdlust Harzburgite (harzburgite subzone), Serokolo Bronzitite (upper bronzitite subzone) (SACS, 1980). Table 1 gives the relative thicknesses of the units

2.1.1.3. Critical Zone

This is characterised by the regular and often fine-scale layering it displays. Dunites, harzburgites, pyroxenites, chromitites, norites and anorthosites are disposed in layers ranging in thickness from a few millimetres to many tens of metres (Eales *et al.*, 1993). The largest deposits of chromite in the world occur in the lower and upper Critical Zones of the main eastern and western lobes of the Bushveld Complex (Vermaak and Gruenewaldt, 1986). The lower (LG) group of chromitite layers occur within the essentially pyroxenitic or bronzitic lower Critical Zone, the upper (UG) group of chromitite layers occur exclusively within the essentially anorthositic to noritic Upper Critical Zone, while the middle (MG) group of chromitite layers occur at the pyroxenitic/anorthositic junction of the lower and upper Critical Zones (Vermaak and Gruenewaldt, 1986).

Table 1. Lithostratigraphic subdivision and thicknesses of the Rustenberg Layered Suite in the eastern Bushveld Complex (After Vermaak and Gruenewaldt, 1986)

| Formal Subdivision by SACS | | Lithology | Informal subdivision | | Approximate thickness (m) |
|----------------------------|---|--|----------------------|---|---------------------------|
| Rustenberg Layered Suite | Luipershoek Olivine Diorite | Diorite and olivine diorite. | Upper Zone | Subzone C | 2000 |
| | Ironstone Magnetite Gabbro Magnet Heights Gabbronorite | Magnetite gabbro with layers of magnetite, anorthosite and olivine gabbro. | | Subzone B Subzone A | |
| | Mapoch Gabbronorite Leolo Mountain Gabbronorite Winnaarshoek Norite-Anorthosite | Mostly homogenous gabbro and norite. | | Subzone C Subzone B Subzone A | |
| | Winterveld Norite Anorthosite Mooihoek Pyroxenite | Alternating layers of chromite, pyroxenite norite and anorthosite. Pyroxenite interlayered with chromite and dunite. | Critical Zone | Subzone B | 1000 |
| | | | | Subzone A | 500 |
| | Serokolo Bronzitite Jagdlust Harzburgite Rostock Bronzitite Clapham Bronzitite | Pyroxenite Harzburgite interlayered with pyroxenite and dunite. Pyroxenite Norite, feldspathic pyroxenite, Harzburgite layer near the base. | Lower Zone | Subzone D | 1600 |
| | | | | Subzone C Subzone B Subzone A | |
| | Shelter Norite | Norite, feldspathic pyroxenite, quartz norite, anorthosite norite. | Marginal Zone | | Up to 100 |

2.1.1.4. Main Zone

This overlying zone with a thickness of about 4000m for the larger part consists of a succession of relatively homogenous rocks which builds a very prominent mountain range known as Leolo Mountains stretching from Draaikraal in the south to the Olifants River in the north (Vermaak and Gruenewaldt, 1986). On the basis of layering and composition of the cumulus minerals, the Main Zone is coarser, less well defined than the often delicate, mm-scale layering of the Critical Zone and subdivided into three subzones (Molyneux, 1974 ; Von Gruenewaldt, 1973). Klemm *et al.*, 1985a; Cawthorn and McCarthy, 1985) proposed that the Main Zone appears to be devoid of any mineralisation though the pyroxenite marker has been thoroughly researched of late (Vermaak and Gruenewaldt, 1986). Table 1 gives the subdivision of the subzones.

2.1.1.5. Upper Zone

The base of the Upper Zone is defined by the first appearance of cumulus magnetite above the pyroxenite marker (Vermaak and Gruenewaldt, 1986; Eales *et al.*, 1993). This mineral makes its appearance as an intercumulus constituent in a prominent mottled anorthosite and is present as a cumulus mineral in nearly all the overlying rock types, right to the top of the Rustenburg Layered Suite. Pronounced layering is developed throughout this zone and is caused by varying proportions of cumulus minerals such as magnetite, olivine, plagioclase and pyroxene in the rocks (Vermaak and Gruenewaldt, 1986). Subdivision into three subzones is on the basis of the appearance of new cumulus minerals in the succession. The subdivisions are reflected in Table 1.

2.1.2. Rashoop Granophyre Suite

The Rashoop Granophyre Suite of the Bushveld Complex is subdivided by Walraven (1987a) into three different types.

2.1.2.1. Stavoren Granophyre

This granophyre is present throughout the Bushveld Complex and predates the basic rocks and granites of the Complex (Walraven, 1985). It is magmatic in origin and cogenetic with Rooiberg Group volcanics. It consists of medium to fine-grained rocks composed of K-feldspar, plagioclase and quartz together with hornblende, minor biotite and accessory iron oxide and zircon. It is characterised by micrographic intergrowths of quartz and feldspar. It includes sedimentary xenoliths where roof rocks are sedimentary, and spherulitic zones where they consist of Rooiberg Group volcanics (Hall, 1932, Walraven, 1985). The Stavoren Granophyre is well developed on the northern end of the Stavoren Fragment just off the northern boundary of the present study area.

2.1.2.2. Diepkloof Granophyre

This is texturally similar to the Stavoren Granophyre and restricted to the eastern part of the Bushveld Complex underlying volcanic rocks of Rooiberg Group (Walraven, 1985). It is cogenetic with granodioritic rocks present in similar geologic settings elsewhere in the Bushveld Complex and is presumed to have formed by the melting of volcanic roof rocks as a result of intrusion of basic rocks of the complex. It has the same age as the basic rocks (Walraven, 1985).

2.1.2.3. Zwartbank Pseudogranophyre

It is restricted to parts of the Bushveld Complex underlying the sedimentary rocks of Pretoria Group. It differs texturally from Stavoren and Diepkloof Granophyre and consists of intergrown quartz and feldspar indicative of replacement (Walraven, 1985). It is believed to have been formed by severe recrystallisation of sedimentary roof rocks as a result of intrusion of basic rocks of the Bushveld (De Waal, 1972, Walraven, 1985).

2.1.3. Lebowa Granite Suite

Field relationships, radiometric age determinations and geochemical studies have demonstrated the existence of several textural varieties of granites within the Bushveld Complex. Of importance to this study is the Nebo Granite that engulfs the Marble Hall Fragment.

The Nebo Granite forms a regional sill like intrusive of A-type granite (Kleeman and Twist, 1989; MacCaskie, 1983; McCarthy and Hasty, 1976; Hill *et al.*, 1996). It has an estimated thickness of some 2.5km (McCaskie, 1983). De Waal (1963), Snyman (1958) and Marlow (1976) described the main phase of this granite as red to grey in colour, coarse grained. Granular K-feldspar perthite, quartz and plagioclase are the major constituents, whereas hornblende, biotite and muscovite are minor constituents. Accessory minerals include opaque minerals, zircon, rutile and fluorite. Local granophyric and aplitic varieties are developed.

Walraven and Hattingh (1993) provide information on a dyke of Nebo Granite cutting the basic rocks of the Bushveld Complex, some 1500 m below the granite in the area north-west of Potgietersrus, in the northern lobe of the Complex. This dyke is believed to be a feeder to the main body of Nebo Granite (Walraven and Hattingh, 1993).

2.1.4. Rooiberg Group

These intercratonic volcanic rocks largely confined to the roof of the Bushveld Complex consist of nine magma types varying in composition from basalt to rhyolite (Hatton and Schweitzer, 1995). Basalts and andesites intercalated with dacites and rhyolites are found towards the base; rhyolite is the chief magma composition in the upper succession. According to Hatton and Schweitzer (1995), crustally contaminated plume magma synchronously intruded beneath the Rooiberg Group to produce the mafic rocks of the Rustenberg Layered Suite.

2.1.5. Makeckaan Formation

The Makeckaan Formation preserved in the Stavoren Fragment comprises lower and upper feldspathic sandstone members with large scale cross beds and ripple marks separated by mature, recrystallised quartzitic sandstones and micaceous wackes (Rhodes, 1972) or fluviodeltaic deposits (Schreiber, 1991). Hartzer (1994) described the Stavoren Fragment occupying a high-lying tract of land to the north and north-west of the Marble Hall dome as consisting of siliciclastic sedimentary and volcanic rocks of the upper part of the Pretoria Group and the lower part of the Rooiberg Group. It is covered by Karoo rocks towards the north and east (Hartzer, 1994).

The Stavoren Fragment has been subdivided physiologically by Hartzel (1994) into a plateau area containing the entire succession of the Upper Pretoria Group, culminating in Rooiberg lavas in the centre of the Rinkhalskop syncline and a range of hills that mark the Wonderkop fault zone. Several prominent pegmatitic quartz veins considered as late-stage differentiation products of Bushveld granitic magma (Wagner, 1927) form a series of high ridges in the eastern part of the fragment and some of these are clearly associated with the pre-existing fault planes linking up with the Wonderkop fault zone (Hartzel, 1994). These faults have important structural implications since the Transvaal succession in the fault zone consists of lower part of the Makeckaan subgroup.

The Makeckaan Formation has been brought into perspective in this study because it is part of the area embraced by this investigation and for its importance in the geophysical interpretation.

2.2. THE AGE OF THE BUSHVELD COMPLEX

Although grouped by SACS (1980) with the Bushveld Complex, the Stavoren Granophyre is considered to pre-date the basic layered rocks and granites of the complex (Walraven *et al.*, 1988). Based on its field relationships with the Bushveld layered rocks and granite as well as from genetic relationships with the lavas of the Rooiberg Group (Walraven, 1987a), it may be concluded that the Stavoren Granophyre must be as old as 2065Ma.

By combining all the concordant whole-rock data from the Upper Zone presented by Hamilton, 1977), Sharpe (1985) and Kruger *et al.* (1987) and assigned blanket errors, the result obtained gave an isochron of 2061 ± 27 Ma which is the preferred age for the mafic rocks of the Bushveld Complex (Walraven *et al.*, 1988).

Walraven and Hattingh (1993) indicated a crystallisation age of 2054.4 ± 1.8 Ma for the Nebo Granite from the new age determinations of zircon from the Nebo Granite using the Pb-evaporation technique.

The inter cratonic Rooiberg Group is one of the largest accumulations of silicious volcanic rocks (Schweitzer *et al.*, 1995a, b) and is largely confined to the roof of the Bushveld Complex. The age has been put at 2.06 Ga (Hatton and Schweitzer, 1995).

Despite the large range of ages obtained for the granites and basic layered rocks of the Bushveld Complex, much of the recent work strongly supports an emplacement age in the range of 2060 – 2050 Ma and such ages are also evident from the earlier U/Pb zircon age determinations (Walraven *et al.*, 1988)

2.3 MODE OF EMPLACEMENT AND SHAPE OF THE BUSHVELD COMPLEX: GEOPHYSICAL DATA

The structure of the Rustenburg Layered Suite was initially considered to be either that of a huge laccolith (Molengraaff, 1901; Jorssen, 1904; Mellor, 1906), or a number of smaller laccolithic intrusions (Molengraaff, 1902), or a lopolith (Daly and Molengraaff, 1924; Hall, 1932).

The geophysical technique first used to constrain geological models of the Basement Complex was gravity modelling (Cousins, 1959). Since then regional gravity surveys, ground and aeromagnetic surveys, time domain electromagnetic surveys, DC resistivity soundings and regional seismic reflection studies have been used (Meyer, 1987).

The latest models on the shape of the Rustenburg Layered Suite see the lobes as dipping tapering sheet terminating towards the centre (Kleywegt and Du Plessis, 1986) and tapering sills (Molyneux and Klinkert, 1978) with the ferrogabbros of the Upper Zone thinning towards the geographic centre of the Complex.

Earlier workers interpreted the Bushveld Complex as a number of discrete compartments (Smit, 1961; Smit *et al.*, 1962); a series of separate overlapping intrusions (Truter, 1955; Hattingh, 1983) or curved trough-like bodies, arranged around a central dome (Cousins, 1959) or Lebowa Granite Suite underlain by Transvaal Supergroup rocks (Meyer and De Beer, 1987). They concluded from the structural and geophysical models that the central portion is not underlain by the basic rocks of the Bushveld Complex.

Based on the interpretation of a regional gravity survey of eastern Transvaal, Hattingh (1980) also proposed that the mafic rocks of the Complex have a synformal morphology. He suggested the interpretation of gravity highs as intrusion centres for the mafic magma with the feeder zones being extremely narrow. Further interpretation indicated that the mafic rocks extend underneath felsite and sediments towards 29° 15' E; extending beneath the Bushveld Granite up to the Elandsplaagte Dome (Hattingh, 1980).

2.4. THE MARBLE HALL FRAGMENT

2.4.1. LOCALITY

The Marble Hall Fragment is situated approximately 160 kilometres due north-east of Pretoria. It forms a pear-shaped outcrop measuring approximately 30km in a northeast-southwesterly direction and approximately 20km in a northwest-southeasterly direction. The town of Marble Hall

is situated in about the centre of the Fragment and owes its name to marble occurrences in vicinity.

2.4.2. THE GEOLOGY OF THE MARBLE HALL FRAGMENT

The Marble Hall Fragment consists of severely deformed and metamorphosed rocks of the Transvaal Supergroup (Figure 2.2). It is entirely surrounded by Nebo Granite of the Lebowa Granite Suite and intruded by diorite. Towards the south it is partly covered by sedimentary rocks of the Karoo Supergroup.

The geological structure of the Marble Hall Fragment can be described as a north-west striking anticline, the Swartkop-Marble Hall Anticline (De Waal, 1970), that was refolded along a north-east striking anticlinal fold. The core of the north-east striking anticline forms a domal feature in the south-west of the area, known as the Elandslaagte Dome (Snyman, 1956). Mapping by Gau (1906), Wagner (1927), Wessels (1943), Lombaard (1931), Snyman (1956, 1958), De Waal (1963, 1970) and Hartzler (1994) led to the current lithological subdivision as given in Table 2.

For the sake of completeness the lithology below the Black Reef Quartzite for the Dennilton Dome is also included in Table 2. The reason for this is that the Bloempoot Formation is very poorly developed in the Marble Hall Fragment. However, these lower formations might also be present in the deeper parts of the Marble Hall Fragment and are therefore important in the geophysical interpretations.

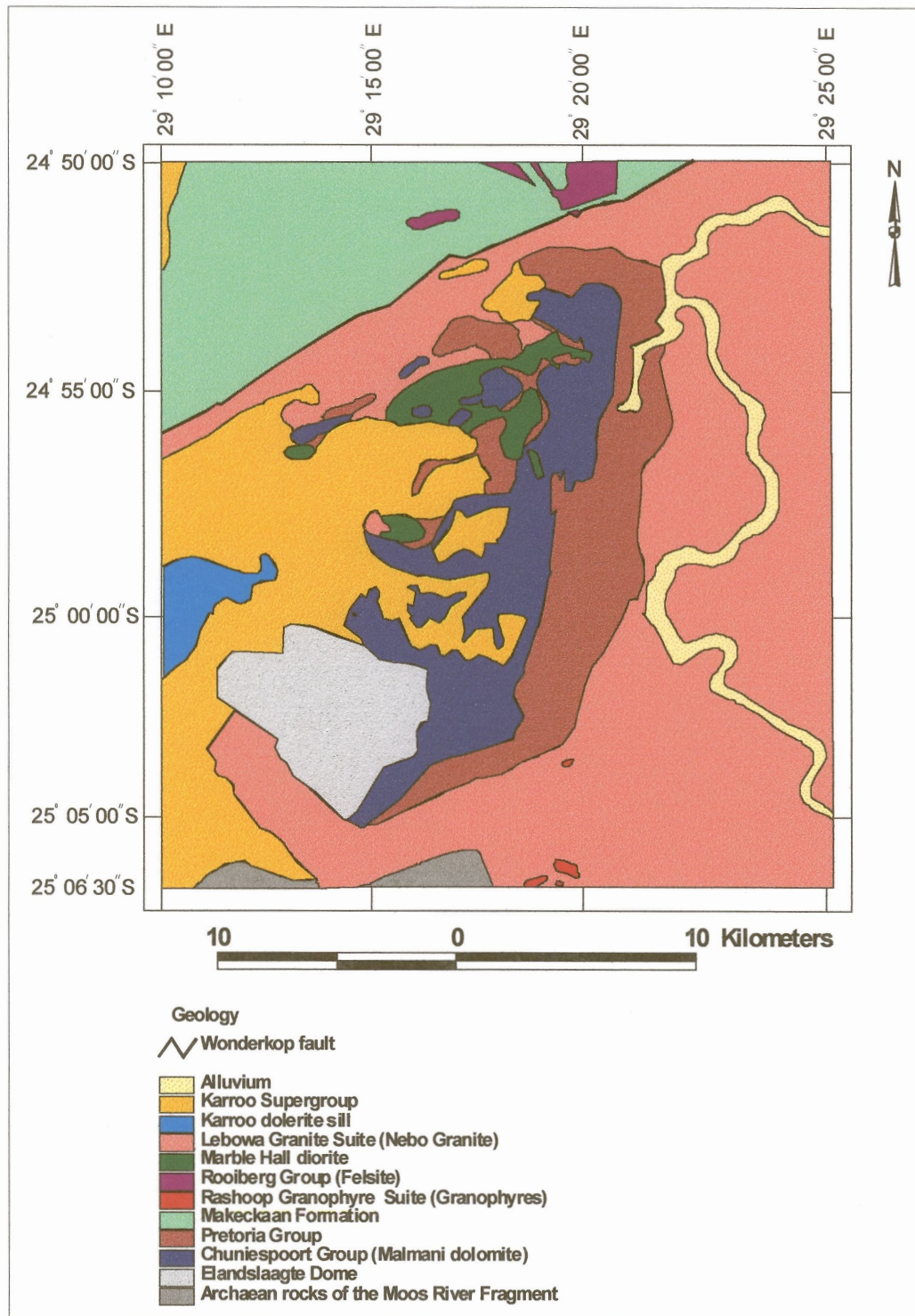


Figure 2.2. Simplified geology of the Marble Hall Fragment. The relatively thin Black Reef Formation between the Chuniespoort Group and Bloempoot Formation is shown as part of the Chuniespoort Group.



Table 2. LITHOSTRATIGRAPHIC SUBDIVISION OF THE SUCCESSIVE

FRAGMENT AND DENNILTON DOME (After Hartzer, 1994)

| LITHOLOGY | LITHOLOGIC SUBDIVISION | | THICKNESS | | |
|--------------------------------------|------------------------|--------------------|----------------------|------------------|---------|
| | | | Denilton Dome | Marble Hall Dome | |
| Lava, agglomerate, arenite, shale | Dulstroom Fm. | Pretoria Group | Transvaal Supergroup | ± 183 m | |
| Shale, quartzite | Houtenbek Fm. | | | 160 m | |
| Quartzite | Steenkampsberg Fm. | | | ± 710 m | |
| Feldspathic arenite, shale | Nederhors Fm. | | | ± 320 m | |
| Arenite | Lakenvalei Fm. | | | 200 m | |
| Claystone | Vermont Fm. | | | 184 m | |
| Quartz arenite, limestone | Magaliesburg Fm. | | | 800 m | |
| Claystone, siltstone | Lydenburg Mb | | | 867 m + | 320 m + |
| Tuff | Machadodorp Mb. | | | | 128 m |
| Agglomerate | | | | | 64 m |
| Claystone, siltstone | Boven Mb | | | | 167 m |
| Quartz arenite | Daspoort Fm. | | | 60 m | 30 m |
| Claystone, siltstone | Strubenkop Fm. | | | ± 130 m | ± 80 m |
| Arenite | Dwaalheuwel Fm. | | | ± 48 m | 45 m |
| Lava | Hekpoort Fm. | ± 230 m | ± 255 m | | |
| Claystone, siltstone | | ± 230 m | ± 225 m | | |
| Quartz arenite | Klapperkop Mb | 69 m | 128 m | | |
| Claystone, siltstone | | ± 300 m | ± 490 m | | |
| Carbonate rocks | Scherp Arabie Mb | ± 70 m | 15 m | | |
| Claystone | | | 5 – 10 m | | |
| Conglomerate | Bevets Mb. | ± 20 m | 20 – 25 m | | |
| Claystone | | ± 50 m | 0 – 60 m | | |
| Iron Formation | Penge Fm. | ± 35 m | ± 25 m | | |
| Dolomite, limestone | Frisco Fm. | ± 135 m | ± 118 m | | |
| Chert-rich dolomite | Eccles Fm. | ± 245 m | 220 m | | |
| Dolomite, limestone | Lyttelton Fm. | ± 233 m | | | |
| Chert-rich dolomite | MonteChristo Fm. | ± 1160 m | | | |
| Limestone, dolomite | Oak Tree Fm. | ± 330 m | | | |
| Arenite, claystone | Black Reef Fm. | Chinuespoort Group | | 39 m | |
| Arenite, grit, siltstone | Stukje Mb. | | | 10 m | |
| Siltstone, arenite | Boshalala Mb. | | | 15 m | |
| Quart, arenite, grit | Klipfontein Mb. | | | 43 m | |
| Siltstone, arenite | Kalkput Mb. | | | 17 m | |
| Arenite, siltstone | Rooiboskloof Mb. | | | 20 m | |
| Siltstone, claystone | La Casita Mb. | | | 5 m | |
| Quart arenite | Ruzawi Mb. | | | 114 m | |
| Claystone, Siltstone | Aquaville Mb. | | | 95 m | |
| Calcareous arenite, carbonate rocks | Celandine Mb. | Bloempoot Fm. | Transvaal Supergroup | 135 m | |
| Feldspathic and Calcareous arenite | Broekskeur Mb | | | 43 m | |
| Conglomerate | Uitzoek Mb. | | | | |
| Calcareous arenite | Oude Stad Mb. | | | 77 m | |
| Lava | Uitspanning Mb. | | | 45 m | |
| Claystone, siltstone, quartz arenite | Mpheleng Mb. | | | 175 m | |
| Lava | Moses River Mb. | | | 100 m | |
| Claystone, siltstone | Witpenskloof Mb. | | | 925 m | |
| Lava, tuff, granulite schist | Dennilton Fm. | | | ± 1500 m | |
| Gneiss | Vaalfontein Suite | | | | |
| Amphibolite, lava, schists | Terra Nostra Fm. | | | | |

De Waal (1970) described irregular bodies of diorite and albite diorite, classified with the upper portion of the Main Plutonic Phase (Upper Zone) of the Bushveld Igneous Complex and a sheet of pyroxene granulite of the Maruleng type that intruded the Transvaal System. The diorites are now interpreted to be related to the Bushveld sill complex below the Rustenburg Layered Suite (De Waal, 1999, pers.comm.) The precise shape of these sills can not be determined from surface outcrop (De Waal, 1970; Hartzel, 1994) and as stated earlier the main motivation for this geophysical investigation.

CHAPTER THREE

GEOPHYSICAL DATA ACQUISITION

3.1 INTRODUCTION

The gravity and magnetic geophysical techniques exploit the fact that variations in the physical properties of in-situ rocks give rise to variations in some physical quantity which may be measured remotely- at the surface of the ground or above it- without the need to touch, see or disturb the rock itself (Peterson and Reeves, 1985). These observed variations, when corrected appropriately and presented as two-dimensional (2-D) maps of “anomalies” over the earth’s surface, may be interpreted in terms of three-dimensional (3-D) subsurface variations of rock properties. These variations in physical properties must relate, to a greater or lesser extent, to the geology of the subsurface.

Both gravity and magnetic methods consist of three stages:

- (i) measurement of the specific field values at or above the ground surface (**data acquisition**);
- (ii) processing of the measured data (**data processing**)
- (iii) interpretation of the processed data in terms of rock property variations within the subsurface in accordance with known geology (**data interpretation**).

Gravity and magnetic techniques are often grouped together as the *potential field methods*. There are however some basic differences between them. Gravity is an inherent property of mass and the measured gravity field is only dependant on the subsurface density

distribution. The magnetic field is not only dependant on the type of minerals contained in a rock, but also on the inducing fields, both past and present. Density variations are relatively small, and the gravity effects of local masses are very small compared with the regional field of the earth as a whole, often in the order of 1 part in 10^6 to 10^7 . Magnetic variations on the other hand, are relatively large, in the order of 1 part in 10^3 .

The aeromagnetic method of geophysical surveying has been established in less than five decades as a powerful method in mining and petroleum exploration (Reford and Sumner, 1964). Many important discoveries can either directly or indirectly be credited to an aeromagnetic survey. The most distinguishing features of the aeromagnetic method, in comparison with other geophysical prospecting schemes, is the rapid rate of coverage and low cost per unit area explored (Peterson and Reeves, 1985).

The gravity method can be used to map and model any geological feature that will lead to a lateral variation in the density distribution of the subsurface material. These features can be relatively shallow, such as sinkholes in dolomitic terrain, giving rise to high frequency variations in the observed gravity field, or it can be relatively deep, such as subsurface salt domes, giving rise to low frequency variations in the observed gravity field.

Airborne magnetic surveys can be used to:

- (a) Delineate volcano-sedimentary belts under sand or other recent cover, or in strongly metamorphosed terrains where ancestral lithologies are otherwise unrecognisable. The combined use of gravity and magnetics is very helpful in this role. Important gold and base metal deposits have been found as a result of such programs (e.g. Reeves, 1985).

- (b) Identification and delineation of post-tectonic intrusives. Typical of such targets are zoned syenitic or carbonatite complexes, kimberlites, tin bearing-granites and mafic-ultramafic intrusives (e.g. Kimbell et al., 1984)
- (c) Recognition and interpretation of faulting, shearing, and fracturing not only as potential hosts for a variety of minerals, but also as an indirect guide to epigenetic, stress-related mineralisation in the surrounding rocks.
- (d) Interpretation of configuration and structure of magnetic basement underlying sedimentary basins applied to hydrocarbons and / or uranium exploration.
- (e) Direct detection of deposits of magnetic iron.
- (f) Identification of environments favorable for groundwater exploitation including fracture systems in crystalline rocks and bedrock aquifers under alluvial covers.

3.2. DATA ACQUISITION, GRAVITY:

3.2.1 FIELD PROCEDURE

3.2.1.1. Previous work:

During December of 1975, the Geological Survey of South Africa, in collaboration with the Institute for Geological Research on the Bushveld Complex, initiated a regional gravity survey in the Glibersdal-Lydenburg–Belfast area of the eastern Transvaal to gain more information on the structural relationships of the Bushveld Complex and to produce a gravity

map on a scale of 1 : 250000. For that survey, fourth order gravity base stations were established in the survey area at Globblersdal, Dullstroom, Machadodorp and Lydenburg. Gravimeter readings were taken at each base station and at the pendulum station at the Transvaal Museum in Pretoria, throughout a 24 hour period at each station. This resulted in a set of readings for each base station, from which absolute gravity values for the first-order gravity base stations were then calculated (Hattingh, 1980).

3.2.1.2. Conduct of present survey and data acquisition

The present survey constituted about 731 gravity observations, covering an area of approximately 25km by 30km. The gravity stations were distributed as evenly as possible on 1km grid spacing. The elevation of the gravity stations were determined mostly simultaneously with the gravity readings and when not done simultaneously, remote and fairly indelible spots marked with painted stones were selected to repeat either or both the gravity and elevation measurements should the need arise. In most cases, however, the elevation determination preceded the gravity measurement by some days and when these markers' positions were not found later for gravity measurements, new elevation measurements were taken and the last gravity reading re-observed to reduce error that could emanate due to long time drift effect.

All data were tied in to one of two base stations of which the absolute values were known. The one base station is at Marble Hall, Figure 3.1, the other at Groblersdal, Figure 3.3. A photograph showing the base station at Marble Hall is shown in Figure 3.2.

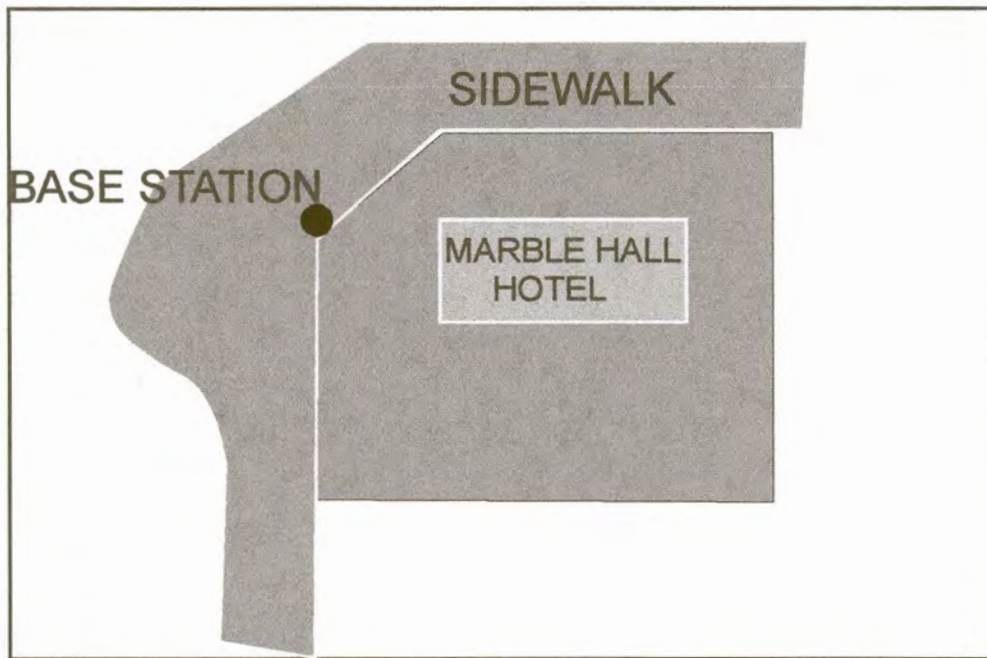


Figure 3.1: Locality map of the base station at Marble Hall



Figure 3.2: Photograph of base station at Marble Hall

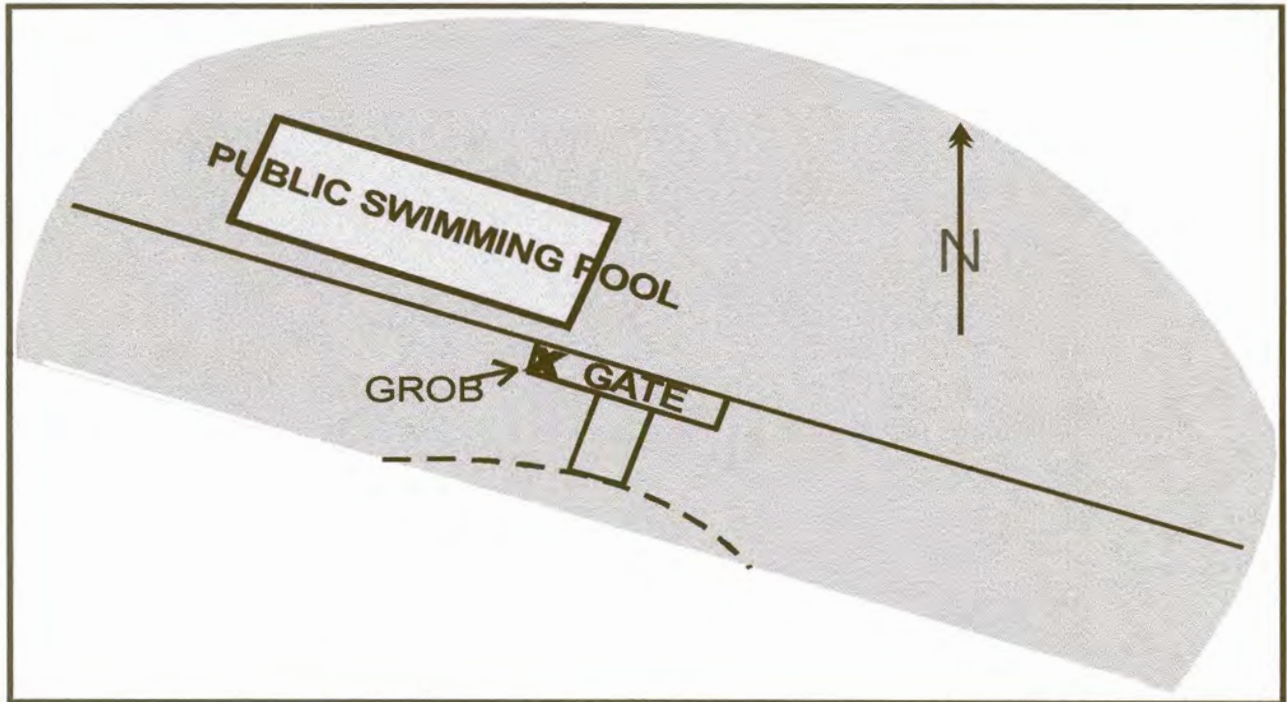


Figure 3.3: Locality map of gravity base station at Groblersdal

Data acquisition covered several areas with different settings with low and fairly high reliefs, nature reserves, dried river beds, farmlands, settlements and previously mined areas. The actual distribution of the gravity stations is shown in Figure 3.4a.

Each gravity position was identified by using a combination of numbers from 1 – 30 vertically and 01 – 25 horizontally reflecting the area coverage for the survey (approximately 25km by 30km) such that the stations are numbered 101,102,...125;1201, 1202...1225; 3001, 3002,...3025. Figure 3.4b shows the sequential numbering of the gravity stations.

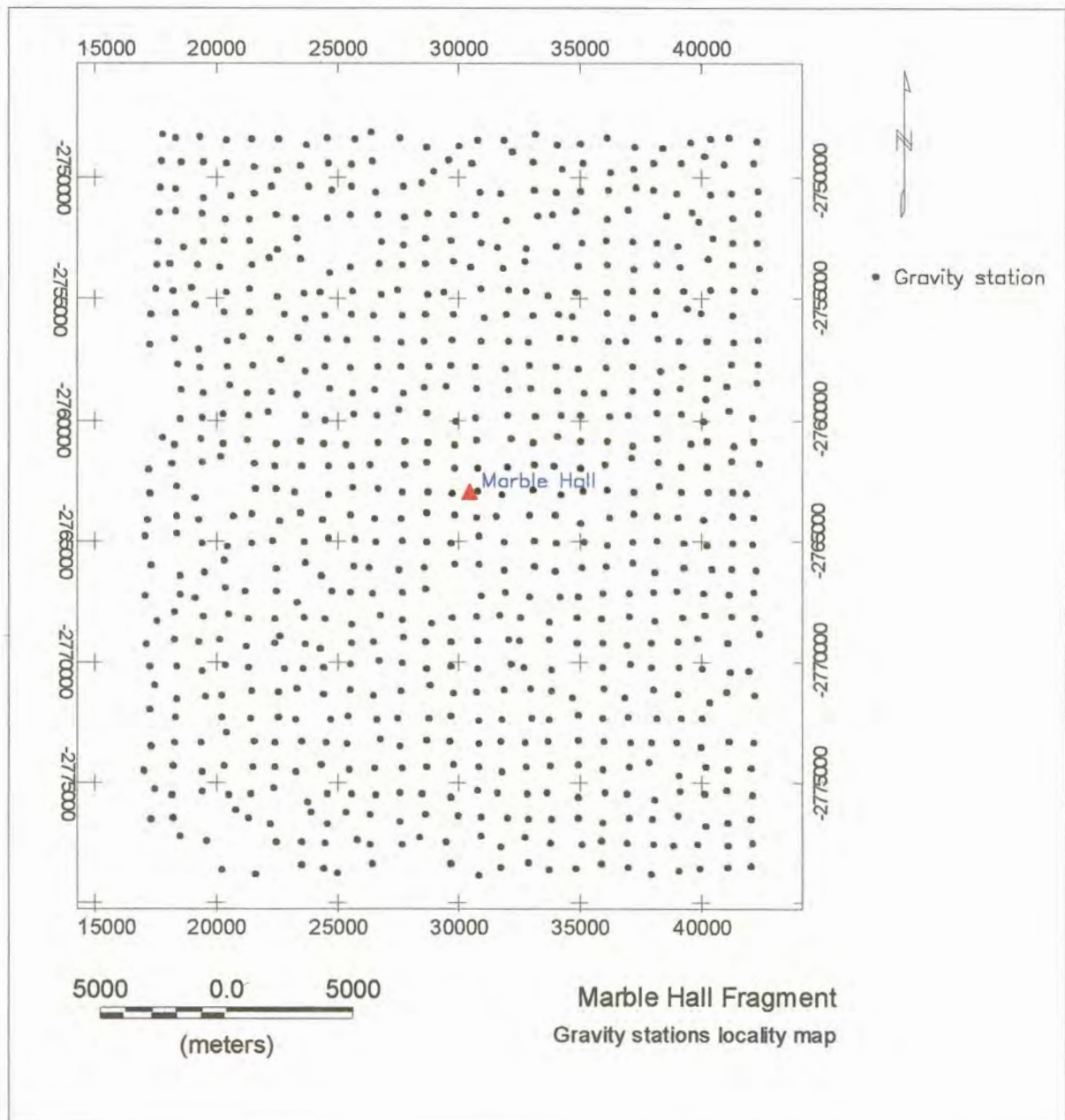


Figure 3.4a : Gravity station locality map

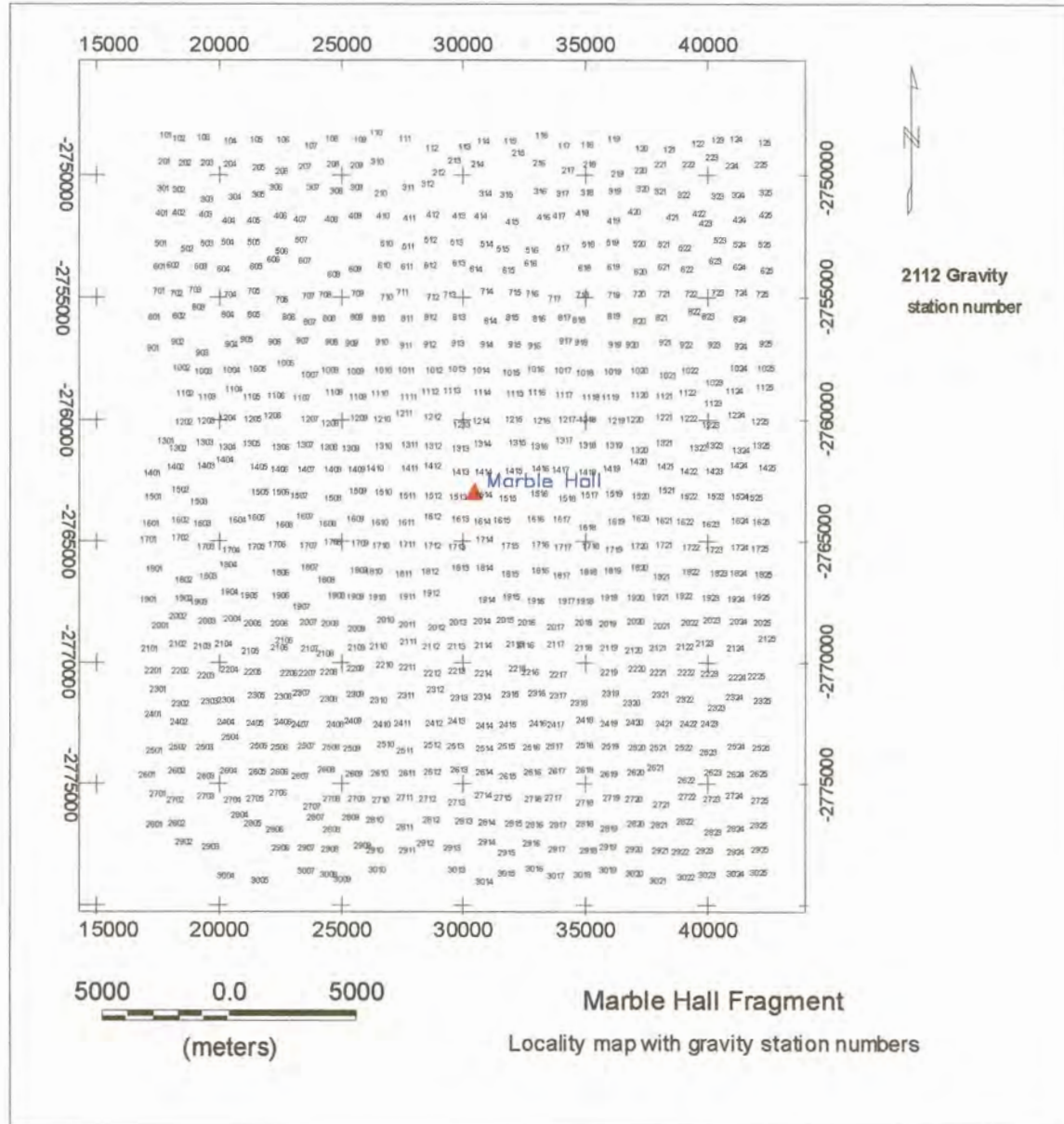


Figure 3.4b. Locality map identifying each gravity position by number

The survey commenced with the identification and location of two trigonometrical beacons within the research area. One was located in the northern part and the other in the southern part of the research area. These were to be used as control or reference points for the determination of the latitude, longitude and elevation position of each gravity station. The coordinates of these beacons are:

For the trigonometrical beacon used in the north, labeled Rooibok 51

$X = +2746031.40\text{m}$, $Y = -33290.53\text{m}$, $Z = 1117.7\text{m}$

For the trigonometrical beacon to the south of Marble Hall, named Mosesrivier Mond 58

$X = +2765779.90\text{m}$, $Y = -32414.33\text{m}$, $Z = 967.6\text{m}$

The coordinates and elevations used for these trigonometrical stations were for System Lo 29⁰ and were obtained from the list containing the coordinates of the South African Survey Grid and heights of beacons above mean sea level published by the Department of Public Works and Land Affairs, Directorate of Surveys and Mapping, issued on April 7, 1989.

Two other elevation control points named during the survey as Dam (located on Roets game farm) to the north and Bas1 (located close to a farmland) in the south of Marble Hall respectively were surveyed to and from Trig 58. The spatial coordinates and elevations calculated for these control points were used as references in calculating the elevations of several gravity stations in the survey area. The need to have four reference elevation positions arose because, for the fast static mode under which the differential GPS measurements were taken, the accuracy in measurement decreases beyond 12-15 km range. The additional stations were also used to reduce cumulative error that might result from little differences in determined elevation values.

Four gravity base stations numbered, -10, -1, -2, -3 corresponding to positions at Groblersdal, Dam, Lebowa and Marble Hall respectively were used for this gravity survey. The base stations and corresponding absolute gravity values are listed in Table 3. The absolute gravimeter station at Groblersdal determined by Hattingh (1977) was re-calibrated during the current survey and this constituted a first order base station to which the other three gravity base stations were tied. This was done in order to be able reduce the gravity values to the same datum as the countrywide survey and to tie this present survey to the previous surveys. Several readings were taken at each of these base stations at the commencement, during and at the end of each daily survey, in order to correct for long term drift effects. By using the scintrex autograv gravimeter, the absolute gravity value of the field stations were determined to an average accuracy greater than 0.03 mgal relative to the absolute gravity value of the first order base station at Groblersdal.

A software controlled Scintrex autograv (CG3) gravimeter supplied by the the Iron and Steel Corporation of South Africa (ISCOR) and 4000 SSE Trimble Geodetic Surveyor supplied by the Department of Land Survey, University of Pretoria, were used for the gravity and elevation determination respectively. An accuracy of 0.03 mgal or better was achieved for the gravity measurements while better than 7cm accuracy was achieved for the elevation determinations.

Table 3: Base station values

| Station ID | Name | Absolute gravity (mgal) |
|------------|-------------|-------------------------|
| -10 | Groblersdal | 978670.24 |
| -3 | Marble Hall | 978677.74 |
| -2 | Lebowa | 978656.48 |
| -1 | Dam | 978653.77 |

3.2.1.3. Laboratory determination of densities of rock samples

In the gravity method, the physical rock property is density, and density variations at all depths within the earth contribute to the broad spectrum of gravity anomalies (Paterson and Reeves, 1985). This density in turn depends on the porosity and gross mineralogy of rocks in bulk.

For the current research, several fresh rock samples from outcrops were taken at different locations and in some cases, four to five samples of the same lithological unit were taken at each location for density determination in the laboratory. The fresh samples were cut into two different geometric shapes viz cubic and cylindrical. At least 3 smaller samples of nearly uniform geometric shapes were obtained from each rock sample. Densities were determined at the South African Council for Geoscience. The densities are given in Table 4.

Table 4: Densities obtained for rocks in the research area.

| Rock Formation | | Density (g/cm ³) |
|----------------------|------------|---------------------------------|
| Makeckaan Formation | | 2,75 |
| Nebo Granite | | 2,67 |
| Pretoria Group | | 2,75 |
| Dolomite | | 2,85 |
| Bushveld basic rocks | Upper zone | 3,08 |
| | Main Zone | 2,95 |
| Bloempoot Formation | | 2,69 |
| Archaean Granite | | 2,67 |

3.2.2. DESCRIPTION OF EQUIPMENT

3.2.2.1. GRAVITY EQUIPMENT (SCINTREX AUTOGRAV GRAVIMETER- CG3)

The precision of data from a gravity survey depends upon the gravimeter and the accuracy of the spatial coordinates of the observation station. The following factors affect the ultimate precision of gravity data generated by a gravity survey (Seigel, 1993):

Instrumental factors

- Shocks and vibrations :
- Power-Down
- Extreme Temperature Shocks
- Elastic relaxation
- Levelling
- Calibration
- Long and Short Term drifts

External Factors:

- Seismic Noise
- Selection of Station Location
- Wind-Induced Vibration

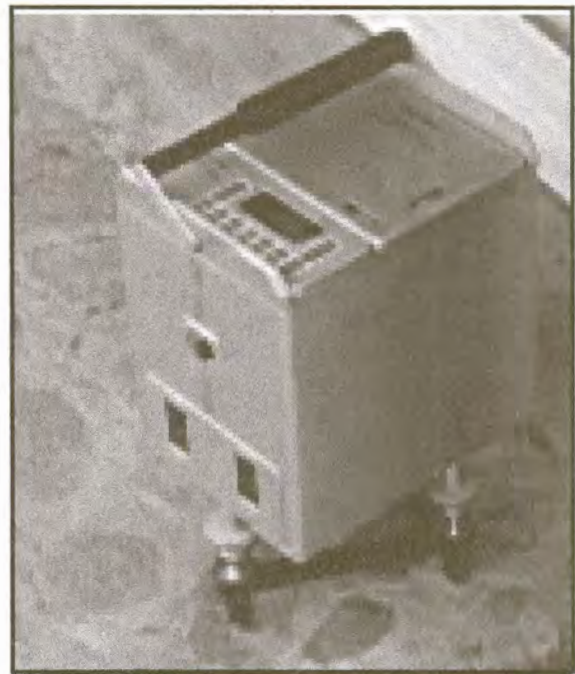


Figure 3.5: The Autograv gravity meter

- Atmospheric Pressure.

Based on all the above factors that can directly or indirectly militate against the quality of the data gathered in the field, the Scintrex autograv (CG3) supplied by the Iron and Steel corporation of South Africa (ISCOR) proved to be most robust. The choice of this equipment was not only based on its robustness and accuracy but also its operating speed. This was a major factor in lieu of the size and ruggedness of the survey area.

The Scintrex Autograv belongs to a new generation of land gravimeters matching or exceeding the precision of the previously top of the line LaCoste meters with the following more desirable characteristics (Seigel, 1993) :

- Straight forward to manufacture : The Autograv does not apply the astatic principle, with its critical dependence on dimensional precision.
- Mechanical Simplification : In the Autograv some of the mechanical complexity of the astatic meters are replaced with electronic circuitry to achieve the same high sensitivity, with the ease of replication and suitability for routine production inherent in the use of electronics. It also meant eliminating the use of micrometer screws and gears, with their mechanical imperfections.
- Tolerance of Rough Field Use : A fused quartz element, with its inherent super-elasticity, is utilized.
- Freedom from Ambient Temperature Variations.
- World wide Range : The Autograv has a resolution of 1 microgal, without the need for any mechanical reset mechanisms.
- High Precision Measurements : With a standard deviation of the order of 5 microgal or better.
- Electronic and Software Control of the Measurement: This carries with it freedom from the subjective judgement of the operator in making the measurement. It allows for many novel and useful features such as intelligent signal processing, correction for tilt errors

and tidal effects, etc. This implies the elimination of micrometer screws and gearboxes, with their mechanical imperfections and limitations of linearity, etc.

The gravitational force on the proof mass is balanced by a zero-length spring and a relatively small electrostatic restoring force. The position of the mass is sensed by a capacitive displacement transducer. An automatic feedback circuit applies a DC voltage to the capacitor plates, producing an electrostatic force on the mass, which brings it back to a null position. The feed-back voltage, which is a measure of the relative value of gravity at the reading system, is converted to a digital signal and then transmitted to the instrument's data acquisition system for processing, display and storage in solid state memory.

The inherent strength and excellent elastic properties of fused quartz, combined with limit-stops around the proof mass, permit the instrument to be operated without clamping. Further protection is provided by a durable shock mount system which supports the sensor within the housing.

The parameters of the gravity sensor and its electronic circuits are chosen so that the feedback voltage covers a range of over 7000 milligals without resetting. Low noise electronic design, including an auto-calibrating 23 bit analogue to digital converter, results in a resolution as high as 1 microgal, thus equipping the gravimeter for both detailed field investigations and large scale regional surveys (Seigel, 1993).

The sensor is enclosed in a sealed aluminium chamber to essentially eliminate the effect of external pressure changes. The most critical components, including the gravity and tilt sensors, are in a double oven, which reduces long-term external pressure changes by a factor of 100,000. A temperature sensor is in close proximity to the spring to provide a

compensation signal for residual temperature changes. Such residual changes are usually less than $1\text{m}^\circ\text{K}$. Some of the other, less critical electronic components are in an outer oven, thermostatically controlled to a fraction of a $^\circ\text{K}$.

The signal from the gravity sensor is sampled once a second and the samples are averaged for sufficient time (depending on the ambient noise conditions) to reduce the random error to the desired level. Noise rejection is assisted by an algorithm which statistically rejects individual high noise readings (Seigel, 1993).

Software controlled corrections are made, in real time, for

- long term drift of the sensor,
- residual sensor temperature variations,
- sun and moon tides,
- tilt of the sensor out of the vertical.

The CG-3 communicates with the outside world through an RS-232 port.

Table 5 shows a typical data printout, including

- station number,
- corrected gravity values,
- calculated standard deviation of one second samples,
- tilts out of the vertical (in arc seconds),
- internal residual sensor temperature variations in m°K
- residual tidal correction
- the number of one second gravity measurements which has been averaged
- the number of noisy readings rejected
- the time of the measurements.

Table 5. Typical gravity data as recorded by the Scintrex Autograv gravimeter in the investigation of the Marble Hall Fragment.

| | | | | | | | |
|------------------------|-----------------|-----------------------|--------------------------|--------|--------|-----------------|----------------|
| SCINTREX V4.1 | | AUTOGRAV / Field Mode | | R4.4 | | Ser No: 507282. | |
| Line: | 0. | Grid: | 1. | Job: | 0. | Date: 98/04/24 | Operator: 1. |
| GREF.: | 0. mGals | | Tilt x sensit.: | | 211.5 | | |
| GCAL.1: | 5781.241 | | Tilt y sensit.: | | 329.7 | | |
| GCAL.2: | 0. | | Deg.Latitude: | | -25.12 | | |
| TEMPCO.: | -0.1276 mGal/mK | | Deg.Longitude: | | -29.10 | | |
| Drift const.: | 0.787 | | GMT Difference: | | -2.hr | | |
| Drift Correction Start | Time: 12:18:20 | | Cal.after x samples: | | 12 | | |
| | Date: 98/04/20 | | On-Line Tilt Corrected = | | ** | | |
| ----- | | | | | | | |
| Station | Grav. | SD. | Tilt x | Tilt y | Temp. | E.T.C. | Dur # Rej Time |
| -10. | 2945.765* | 0.035 | -3. | -1. | 0.11 | -0.096 | 50 0 16:05:56 |
| -10. | 2945.770* | 0.036 | -3. | -1. | 0.12 | -0.096 | 54 0 16:07:02 |
| -10. | 2945.780* | 0.042 | -3. | -2. | 0.14 | -0.097 | 72 0 16:08:14 |
| -10. | 2945.830* | 0.032 | 0. | -3. | 0.09 | -0.097 | 42 0 17:13:58 |
| -10. | 2945.830* | 0.034 | -1. | -1. | 0.10 | -0.097 | 46 0 17:15:10 |
| -10. | 2945.835* | 0.024 | -1. | -1. | 0.11 | -0.097 | 24 0 17:16:12 |
| -10. | 2945.845* | 0.031 | -2. | -1. | 0.12 | -0.096 | 40 0 17:16:49 |
| -3. | 2953.305* | 0.039 | -3. | -0. | 0.10 | -0.102 | 61 1 16:34:48 |
| -3. | 2953.300* | 0.037 | -2. | -0. | 0.11 | -0.102 | 57 0 16:36:09 |
| -3. | 2953.295* | 0.048 | -0. | -2. | 0.11 | -0.102 | 94 1 16:41:10 |
| -1. | 2929.355* | 0.030 | -5. | -1. | -0.22 | 0.018 | 37 0 07:36:19 |
| -1. | 2929.375* | 0.049 | 0. | -1. | -0.20 | 0.020 | 97 0 07:37:20 |
| -1. | 2929.385* | 0.052 | -0. | -1. | -0.19 | 0.022 | 108 0 07:39:22 |
| -1. | 2929.250* | 0.036 | 0. | 8. | 0.08 | -0.061 | 51 0 15:02:15 |
| -1. | 2929.265* | 0.045 | -5. | 5. | 0.11 | -0.062 | 83 0 15:04:02 |
| -1. | 2929.280* | 0.034 | 1. | 1. | 0.12 | -0.064 | 48 0 15:06:30 |
| 1004. | 2918.705* | 0.034 | -1. | -8. | -0.15 | 0.116 | 48 0 09:36:49 |
| 1103. | 2919.455* | 0.038 | -3. | 11. | -0.14 | 0.122 | 60 0 09:50:12 |
| 1104. | 2922.255* | 0.044 | 2. | -4. | -0.16 | 0.108 | 77 0 09:21:34 |
| 1105. | 2927.120* | 0.041 | -3. | 9. | -0.19 | 0.098 | 69 0 09:06:58 |
| 1202. | 2919.110* | 0.033 | -1. | 2. | -0.11 | 0.128 | 44 0 10:10:06 |
| 1203. | 2923.445* | 0.044 | -0. | 4. | -0.10 | 0.130 | 81 0 10:21:23 |
| 1204. | 2926.885* | 0.044 | -13. | -11. | -0.09 | 0.131 | 77 1 10:31:10 |
| 1205. | 2933.000* | 0.035 | -8. | -2. | -0.21 | 0.086 | 50 0 08:50:57 |
| 1206. | 2936.300* | 0.006 | 0. | -3. | -0.28 | 0.061 | 5 0 08:21:29 |
| 1206. | 2936.325* | 0.048 | -4. | -6. | -0.23 | 0.062 | 93 0 08:21:47 |
| 1301. | 2918.695* | 0.042 | 2. | -5. | -0.01 | 0.123 | 71 0 11:21:26 |
| 1302. | 2922.310* | 0.044 | 5. | 4. | -0.01 | 0.104 | 78 0 11:59:45 |
| 1303. | 2927.210* | 0.046 | -10. | -5. | -0.07 | 0.131 | 86 0 10:52:02 |
| 1304. | 2933.980* | 0.040 | 1. | 8. | -0.08 | 0.131 | 64 0 10:44:13 |
| 1305. | 2937.320* | 0.040 | -2. | 9. | -0.24 | 0.071 | 64 0 08:32:57 |
| 1403. | 2932.740* | 0.048 | -8. | -12. | 0.02 | 0.088 | 92 0 12:21:41 |
| 1404. | 2939.375* | 0.046 | -6. | 0. | 0.05 | 0.063 | 86 0 12:50:44 |

The spatial coordinates of each station were obtained using a Trimble 4000 SSE geodetic surveyor. The system utilises the signal from Navstar satellites to compute the locations and the height at anytime of the day to great accuracy (at least 1cm accuracy).

3.2.2.2. DATA ACQUISITION, POSITIONING (TRIMBLE 4000 SSE GEODETIC SYSTEM SURVEYOR)

The Trimble 4000SSE Geodetic Surveyor Series is designed for high precision survey, positioning and navigational applications. This receiver continuously tracks L1 (Link 1) and L2 (Link 2) position code, when available, and utilizes cross-correlation measurements during periods of Anti-Spoof (AS) encryption. This enables dual-frequency code tracking, and thus, high precision measurements at all times. When used with another GPS Geodetic Surveyor and the GPSurvey™ Software Suite, three-dimensional coordinate differences between stations can be determined. Other outputs include : station position, normal section azimuth, slope distance, and vertical angle between the two survey points (Trimble Navigation Limited, 1992).

The 4000SSE offers surveys in Static, FastStatic™, Kinematic, and Pseudostatic modes. It also determines time, latitude, longitude, height and velocity. A navigation capability with over 99 way points is also available.

When used in differential GPS (DGPS) mode, RTCM (Radio Technical Commission for Maritime Surfaces) corrections can be generated at one unit and used by another to provide corrected positions at a one-fix-per-second rate. The 4000SSE receives L1 and L2 signals sent from the Global Positioning System (GPS) NAVSTAR satellites. The receiver automatically acquires and simultaneously tracks up to 9 GPS satellites. It precisely measures carrier and code phases (C/A and P, when available) and stores them in an internal, battery backed-up memory. The 4000SSE receiver continuously tracks P-code with 9 parallel channels when AS is off and utilizes Trimble's unique cross-correlation measurements during times of AS encryption. This enables the recovery of full-cycle L1 and

L2 phase signals and dual-frequency code tracking at all times (Trimble Navigation Limited, 1992).

GPS survey baselines are measured by recording GPS satellite data simultaneously with receivers positioned at each end of the baseline. Latitude, longitude, ellipsoidal height values, and the GPS satellite ephemeris data are referenced to the World Geodetic System (WGS-84).

The TRIMVEC Plus software computes

- slope distance accurate to :

Length : $5\text{mm} + 1 \text{ ppm} \times \text{baseline length}$

Azimuth : $1.0 \text{ sec} + 5 / \text{baseline in km}$

- vertical distance accurate to :

$1 \text{ cm} + 1 \text{ ppm} \times \text{baseline length}.$

For example, on a 10-kilometer line, a slope distance accurate to 1.5 cm may be expected.

The GPSurvey and TRIMVEC Plus software performs the data downloading and the processing and quality checking of the results. Interactive menus simplify the planning and scheduling of surveys. Loop-closure tests and transformations to state plane systems increase production quality and quantity.

Survey project can be scheduled and entered into the receiver prior to arriving at the job site to reduce field operations. On the other hand, last minute changes can be easily accommodated and surveys can be started with a single keystroke.

Position fix, time, satellite tracking data, and other quantities are displayed on the front-panel liquid crystal display. It must be noted that the real time position fixes displayed here have moderate accuracy and are not survey measurements. When the receiver is tracking a sufficient number of satellites, but not placed in a “survey mode”, the receiver automatically determines time and position and some other quantities without user action. This is its “**positioning mode**” (Trimble Navigation Limited, 1992).

The 4000SSE Geodetic System Surveyor also provides many advanced features such as Event Marker input, 1 PPS output, NMEA outputs, RTCM inputs and optional RTCM outputs, and an extended (99 waypoints) navigation feature. The receiver has dual I/O ports, three power ports, an event marker and 1 PPS port, and an optional external frequency input. While one I/O port is being used for sending or receiving the differential GPS corrections, the second can be used to store measurements for later post-mission analysis and archiving.

OPERATING ENVIRONMENT :

The Trimble 4000SSE Geodetic Surveyor can be used in all normal survey applications. However, the following can have an adverse influence on the results.

- High-Power UHF / TV Radio Signals:

High-power signals from a nearby radio or radar transmitter may overwhelm the sensitive receiver circuits. It is safer to try not to survey within a quarter mile of powerful radar, TV, or other transmitters. However, low-power two-way radio's don't interfere with 4000SSE operations.

- Temperature :

The receiver operates in air temperatures from -20° to $+55^{\circ}\text{C}$.

- Humidity:

The Surveyor is sealed and buoyant. A waterproof vent allows internal air pressure to adjust to altitude changes.



Figure 3.6: The GPS system in the survey area

The optional geodetic and kinematic antennas contain dessicant used to absorb moisture within the unit. The dessicant is contained in a plug that screws into the antenna base.

Figure 3.6 shows the equipment being adjusted at one of the trigonometric beacons in the survey area and Table 6 shows a typical processed data from the 4000SSE geodetic surveyor.

**Table 6. A typical processed elevation data obtained from the software controlled 4000SSE
Geodetic Surveyor used in the investigation of Marble Hall Fragment**

**** Adjusted Coordinates ****

Projection Group: User-defined TM

Zone Name: LO 29

Linear Units: meter

Angular Units: degrees

Datum Name: Kaap

| Station | Station | North | East | Ortho. | Ellip. |
|------------|----------|----------------|-------------|---------|-----------|
| Short Name | ID | | | Height | Height |
| 13060002 | 13060002 | -2760355.65843 | 22218.39329 | 0.00000 | 853.34238 |
| 13070001 | 13070001 | -2760247.41925 | 23171.72938 | 0.00000 | 865.72182 |
| 14060003 | 14060003 | -2761221.54190 | 22145.38343 | 0.00000 | 861.25141 |
| 14070018 | 14070018 | -2761222.45645 | 23194.96351 | 0.00000 | 871.04878 |
| 15060016 | 15060016 | -2762128.40748 | 22206.34655 | 0.00000 | 872.11923 |
| 15070017 | 15070017 | -2762283.65564 | 22926.09133 | 0.00000 | 878.45024 |
| 16040005 | 16040005 | -2763268.28467 | 20487.61432 | 0.00000 | 857.42884 |
| 16050004 | 16050004 | -2763167.22269 | 21234.56598 | 0.00000 | 869.63132 |
| 16060011 | 16060011 | -2763442.51089 | 22314.87709 | 0.00000 | 880.90067 |
| 17030015 | 17030015 | -2764342.29981 | 19216.37142 | 0.00000 | 869.26554 |
| 17040012 | 17040012 | -2764469.66483 | 20252.17219 | 0.00000 | 859.60835 |
| 17050006 | 17050006 | -2764341.07201 | 21207.59588 | 0.00000 | 868.83457 |
| 17060007 | 17060007 | -2764219.69336 | 22076.89075 | 0.00000 | 880.92143 |
| 17070010 | 17070010 | -2764271.77968 | 23311.46372 | 0.00000 | 894.31145 |
| 18020014 | 18020014 | -2765643.36704 | 18345.23561 | 0.00000 | 863.67391 |
| 18030013 | 18030013 | -2765486.44015 | 19320.97340 | 0.00000 | 876.15365 |
| 18070008 | 18070008 | -2765103.42954 | 23346.20727 | 0.00000 | 897.46639 |
| 18080009 | 18080009 | -2765805.70423 | 23986.27979 | 0.00000 | 904.06935 |
| DAM 0001 | DAM 0001 | -2755136.46000 | 27594.46000 | 0.00000 | 882.64000 |

***** End of Report *****

3.2.2.3. DATA ACQUISITION: MAGNETIC SUSCEPTIBILITY (KT-9 Kappameter)

The KT-9 kappameter is a state-of-the-art, hand-held field magnetic susceptibility meter for obtaining accurate and precise measurements from outcropping rocks, drill cores and rock samples. Special design features make the KT-9 superior in measuring uneven rock surfaces and well suited to automated drill-core logging with digital recording, Figure 3.7.

The KT-9 kappameter has many unique features which include :-

- (i) Easy to use : With a special measuring pin protruding from the centre of the measuring head. In order to take a reading, the pin is simply pressed against the sample to be measured. When the KT-9 is removed, it automatically displays the true measured susceptibility of the sample in SI units.
- (ii) Hi-sensitivity – The maximum sensitivity of the KT-9 is 1×10^{-5} SI units. The largest value that can be read is 999×10^{-3} SI units. The auto-ranging capability of the unit gives it the best sensitivity range available.
- (iii) True susceptibility – Unlike all other current commercial instrument which measure the apparent susceptibility, the KT-9's automated correcting routine displays the true susceptibility.
- (iv) Uneven samples – The measurement of magnetic susceptibility is dependent upon the volume of material being sampled. The presence of an uneven surface creates air space gaps due to the sensor sitting up on bumps. This causes serious errors in the measured susceptibility of all other currently available commercial units. The KT-9 overcomes this problem by spacing the sensor a fixed distance away from the

sample by means of a pin. The average of repeated measurements (placing the pin in different locations) averages the errors due to bumps to provide the true reading of the magnetic susceptibility. There is no reduction in the effective sensitivity of the KT-9 kappameter, because of the automatic compensation built into the unit.

- (v) Variable audio – In the scan mode, the KT-9 has a variable audio tone that is directly proportional to the measured susceptibility. This allows for quick scanning of a rock surface and visually correlate areas of varying susceptibility.
- (vi) Data averaging – The average of up to the 10 stored readings can also be displayed. This allows for very accurate measurement of uneven surfaces while in the pin mode, as well as improved data quality for smoother surfaces in the no-pin mode.
- (vii) Digital output to a computer – The KT-9 can be connected to a computer via the serial port and a special cable. The KT-9 can then be controlled completely from the computer in a special remote mode.

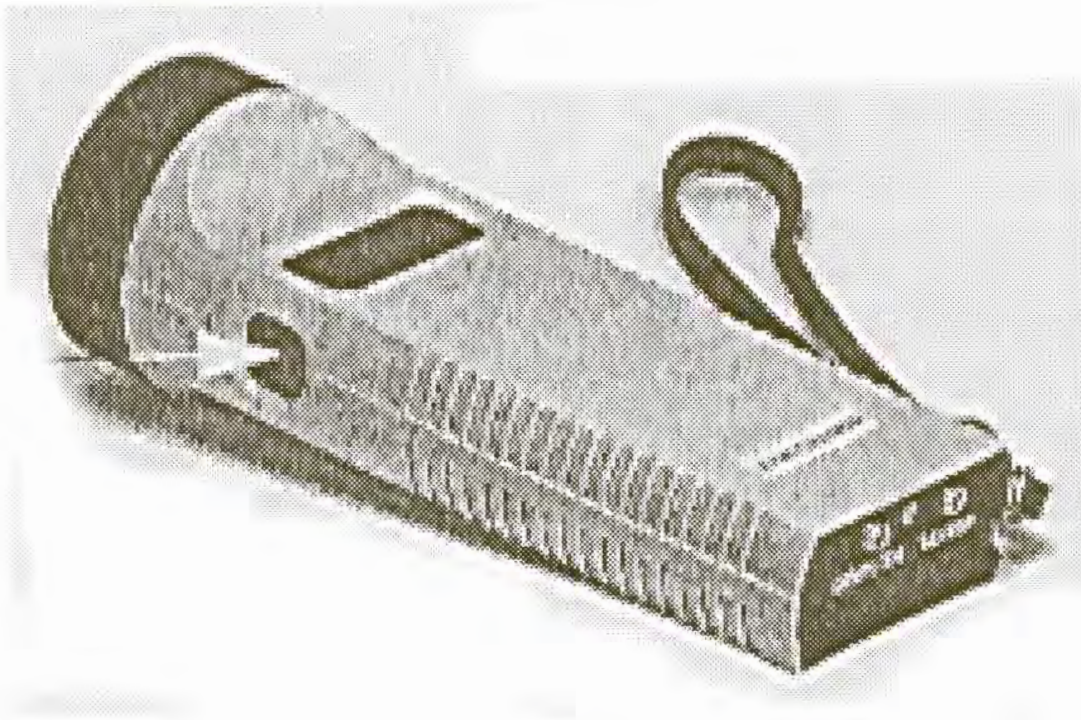


Figure 3.8. The KT- 9 Kappameter (Susceptibility meter)

3.3 DATA ACQUISITION, AIRBORNE MAGNETIC DATA

High density airborne magnetic data were purchased from the Council for Geoscience. The data were flown with a ground clearance of 60m and a line spacing of 87m.

CHAPTER FOUR

GEOPHYSICAL INTERPRETATION AND DISCUSSION

4.1. DATA PROCESSING AND INTERPRETATION

4.1.1. Introduction

Processing of potential field data entails the application of various filters to the data in order to accentuate certain chosen features as an aid in the interpretation of the data.

The process of quantitative interpretation of both gravity and magnetic anomalies endeavours to determine a source distribution whose anomalous field matches as closely as possible the actual field on the surface of measurement. The non-uniqueness of the potential field problem results in the introduction of constraints in the form of simplification of geometry, limits to size or depth, range limits on density or susceptibility, or whatever other parameters may seem justified in the context of what is known or can be reasonably inferred about the geologic environment (Paterson and Reeves, 1985).

A short discussion of the effects of the various filters used in the processing of the magnetic and/or gravity data used in this research project follows.

4.1.2. Vertical Derivative

Derivatives tend to sharpen the edges of anomalies and enhance shallow features.

The vertical derivative map is much more responsive to local influences than to broad or regional effects and therefore tends to give sharper picture than the map of the total field

intensity. Thus the smaller anomalies are more readily apparent in area of strong regional disturbances. In fact the first vertical derivative is used to delineate high frequency features more clearly where they are shadowed by large amplitude, low frequency anomalies. From GEOSOFT Inc., 1996;

$$L(r) = r^n$$

with : n = order of differentiation

4.1.3. Analytical signal

This is a filter applied to magnetic data and is aimed at simplifying the fact that magnetic bodies usually have a positive and negative peak associated with it, which in many cases make it difficult to determine the exact location of the causative body.

Nabighian (1972) has shown that for two-dimensional bodies, a bell-shaped symmetrical function can be derived which maximises exactly over the top of the magnetic contact. The three-dimensional case was derived in 1984 also by Nabighian. This function is the amplitude of the analytical signal. The only assumptions made are uniform magnetisation and that the cross section of all causative bodies can be represented by polygons of finite or infinite depth extent. This function and its derivatives are therefore independent of strike, dip, magnetic declination, inclination and remanent magnetism (Debeglia and Corpel, 1997).

The 3-D analytical signal, A , of a potential field anomaly can be defined (Nabighian, 1984)

$$A(x, y) = \left[\frac{\partial M}{\partial x} \right] \hat{x} + \left[\frac{\partial M}{\partial y} \right] \hat{y} + \left[\frac{\partial M}{\partial z} \right] \hat{z}$$

as:

With:

M = Magnetic field.

The analytical signal amplitude can now be calculated (Debeglia and Cotel, 1997) as:

$$|A(x, y)| = \sqrt{\left(\frac{\partial M}{\partial x}\right)^2 + \left(\frac{\partial M}{\partial y}\right)^2 + \left(\frac{\partial M}{\partial z}\right)^2}$$

4.1.4. Upward continuation

This is the calculation of the potential field at an elevation higher than that at which the field is measured and is applied to both magnetic and gravity data. The continuation involves the application of Green's theorem and is unique if the field is completely known over the lower surface (which is usually true for gravity and magnetic fields) and where all sources above the lower surface are known (usually all are zero). Upward continuation is used to smooth out near surface effects.

For upward continuation (where z is positive downward) (Telford, 1990)

$$F(x, y, -h) = \frac{h}{2\pi} \iint \frac{F(x, y, 0) \partial x \partial y}{\{(x - x')^2 + (y - y')^2 + h^2\}^{3/2}}$$

Where

$F(x', y', -h)$ = Total field at the point $P(x', y', -h)$ above the surface on which $F(x, y, 0)$ is known.

H = elevation above the surface

4.1.5. Downward continuation

Downward continuation is used to enhance features at a specified depth/elevation, lower than the acquisition level. This procedure accentuates near surface anomalies and can be used as an interpretation tool to determine the depth to a causative body. The filter can be

applied to both gravity and magnetic data. Downward continuation is done using the expression (Geosoft Inc., 1996):

$$L(r) = e^{hr}$$

With h the distance in meters to be continued downward.

4.1.6. Reduction to the magnetic pole

This is a method of removing the dependence of magnetic data on the angle of magnetic inclination. This filter converts data which have been recorded in the inclined earth's magnetic field to what the data would have looked like if the magnetic field had been vertical. A reduction to the pole transform will provide a symmetrical anomaly over a vertically dipping, non-remanent body and is again used as an interpretation aid under certain conditions. At low latitudes, however, an amplitude correction is required to prevent north-south signals from dominating the data. This filter can be described as (Geosoft Inc., 1996):

$$L(\theta) = \frac{1}{[\sin(I_a) + i \cos(I) \cdot \cos(D - \theta)]}$$

With:

- I geomagnetic inclination
- I_a inclination for amplitude correction ($I_a > I$)
- D geomagnetic declination

For two-dimensional structures, the anomaly peaks correlate very closely with the analytical signal peaks, indicating that the effect of remanent magnetism is relatively small.

4.2. MAGNETIC DATA PROCESSING AND INTERPRETATION

4.2.1. Introduction

Flight lines ran north-south and interpretation of the data was done in two stages:

- A basic interpretation delineating all major structural features.
- Cross sections along five selected profiles were modeled using 2,5D modeling software.

The basic interpretation was facilitated using the following filtered presentations of the data:

- The total field magnetic contour map, Figure 4.1
- The first vertical derivative contour map, Figure 4.2
- The analytical signal contour map, Figure 4.3
- Upward continued data (to 500m), Figure 4.4
- Upward continued data (to 1000m), Figure 4.5
- Upward continued data (to 2000m), Figure 4.6
- Reduction to the pole, Figure 4.7

4.2.2. *Total magnetic intensity contour map*

Figure 4.1 is a presentation map that gives the vector sum of all components of the magnetic field. In this study, the remanence observed in the mafic rocks was low and from laboratory determinations do not have any undue influence on the observed magnetic intensity used for the modeling. The total field magnetic contour map reveals the magnetic characteristics of the various lithological units in the study area. Unfortunately, the nature of a magnetic anomaly is a function of the strike of the body. For example, a north-south striking dolerite dyke will have a different associated magnetic anomaly than the same dyke striking east-west. The total field magnetic contour map is consequently primarily used to identify various lithologies.

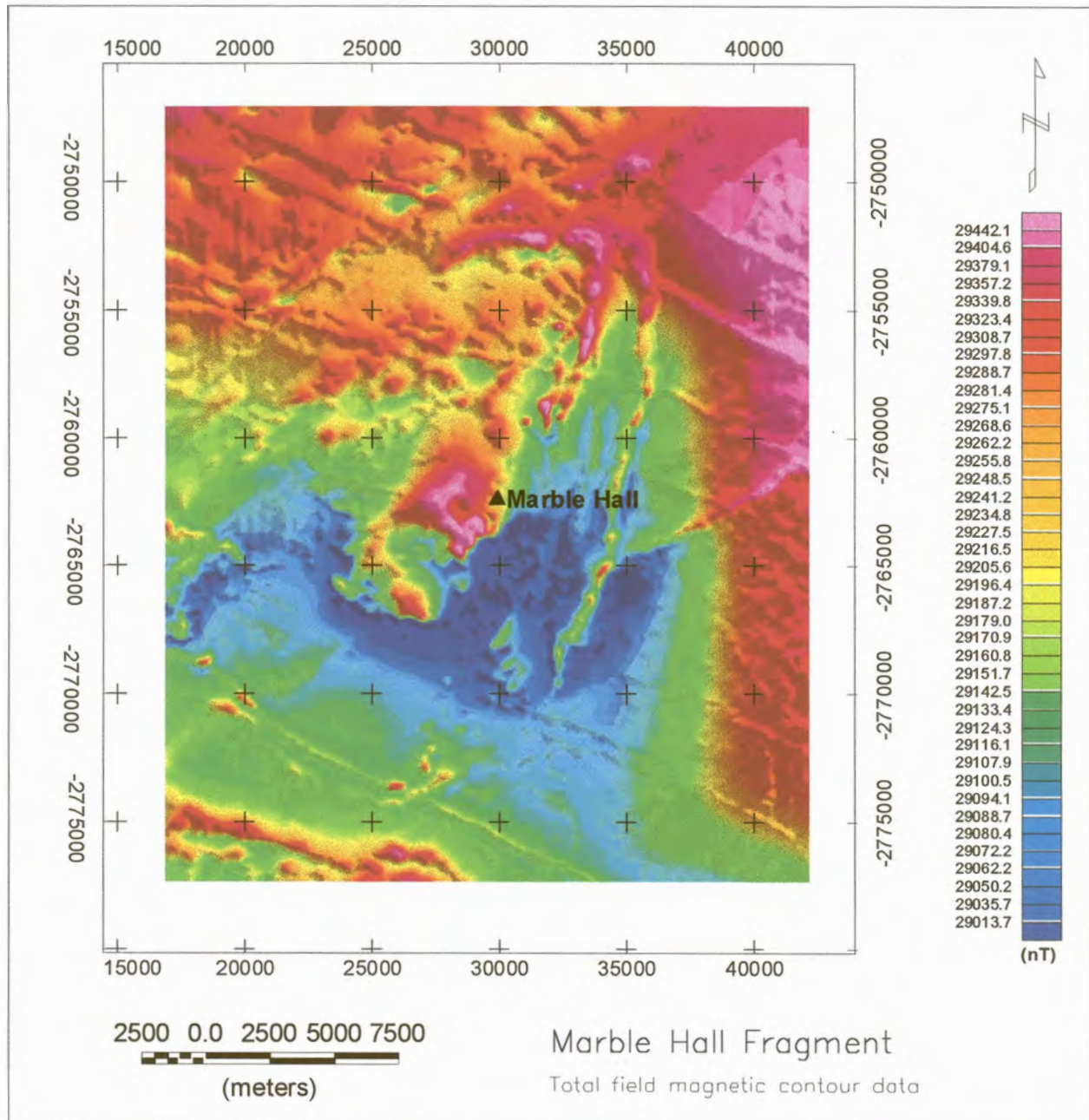


Figure 4.1 Total field magnetic colour contour data

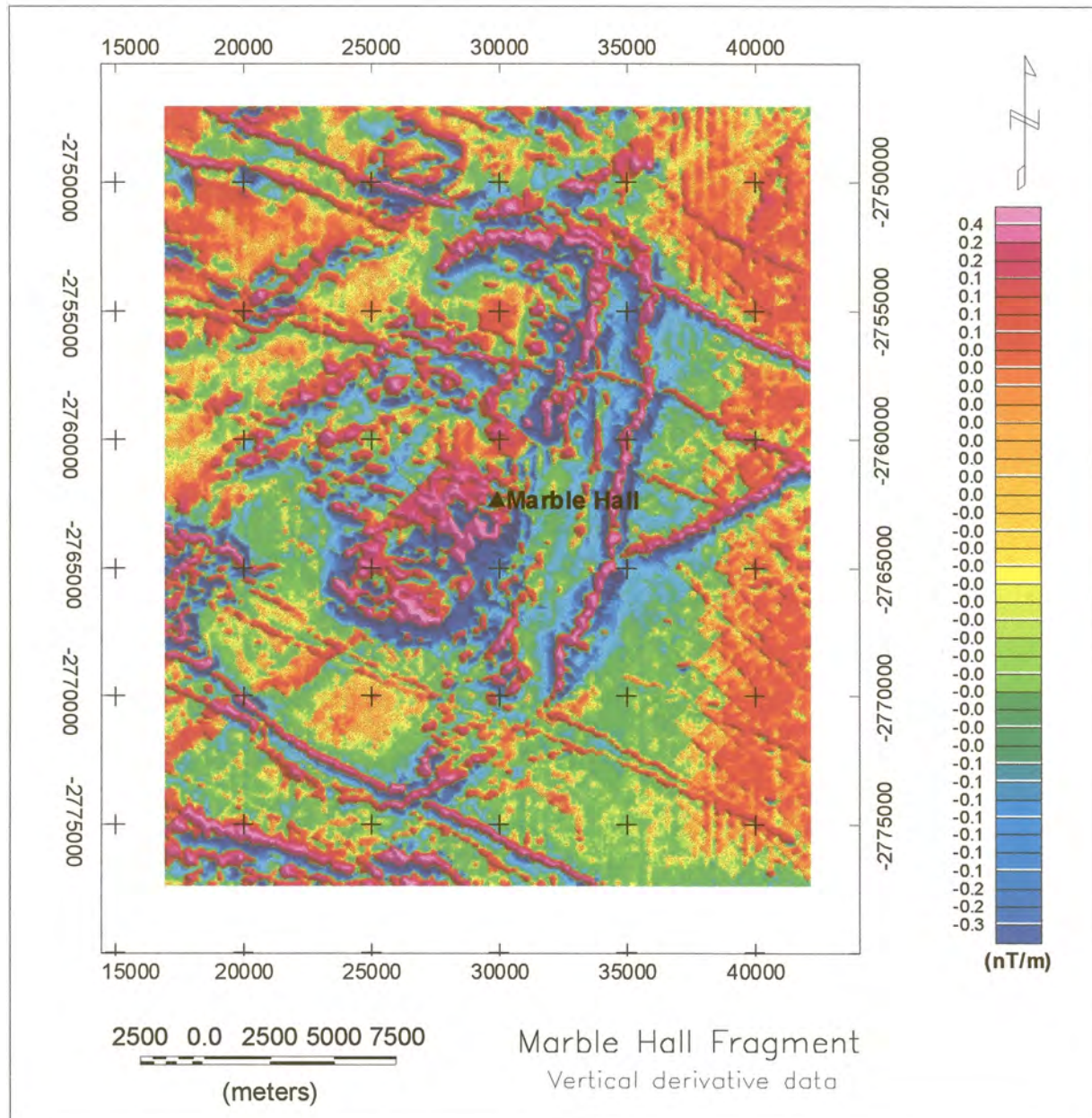


Figure 4.2. First vertical derivative

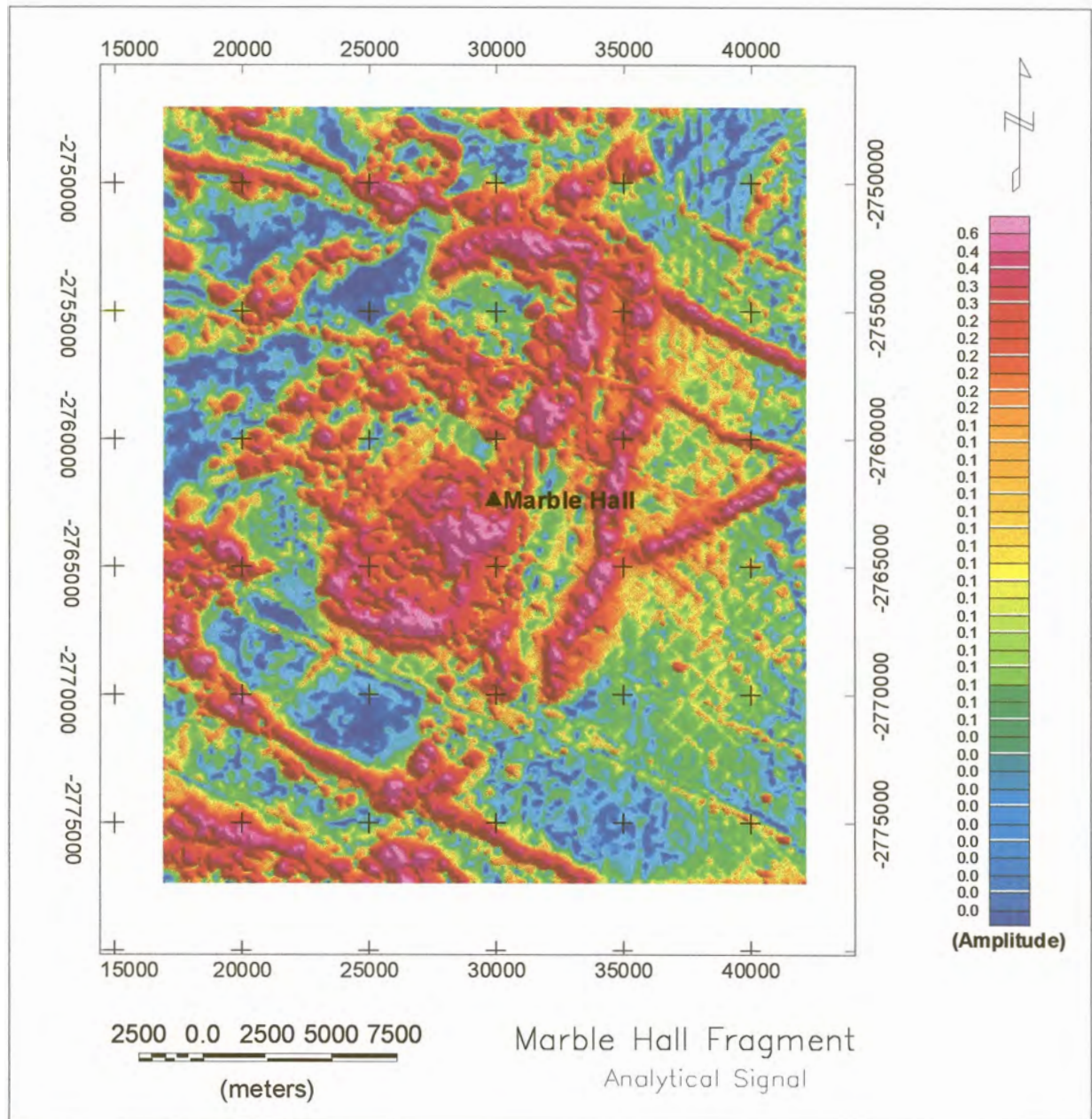


Figure 4.3. Analytical signal

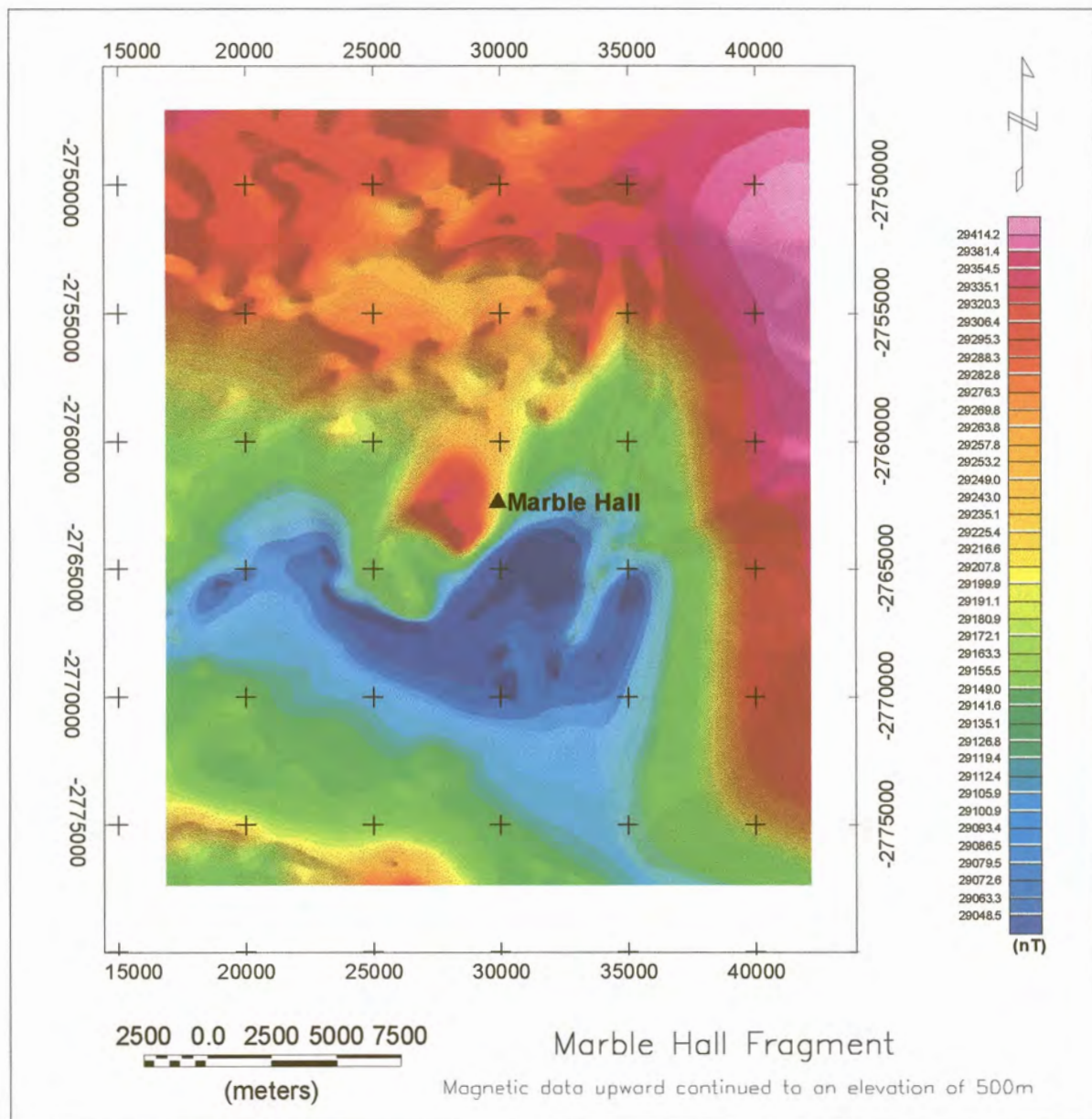


Figure 4.4. Magnetic data upward continued to an elevation of 500m

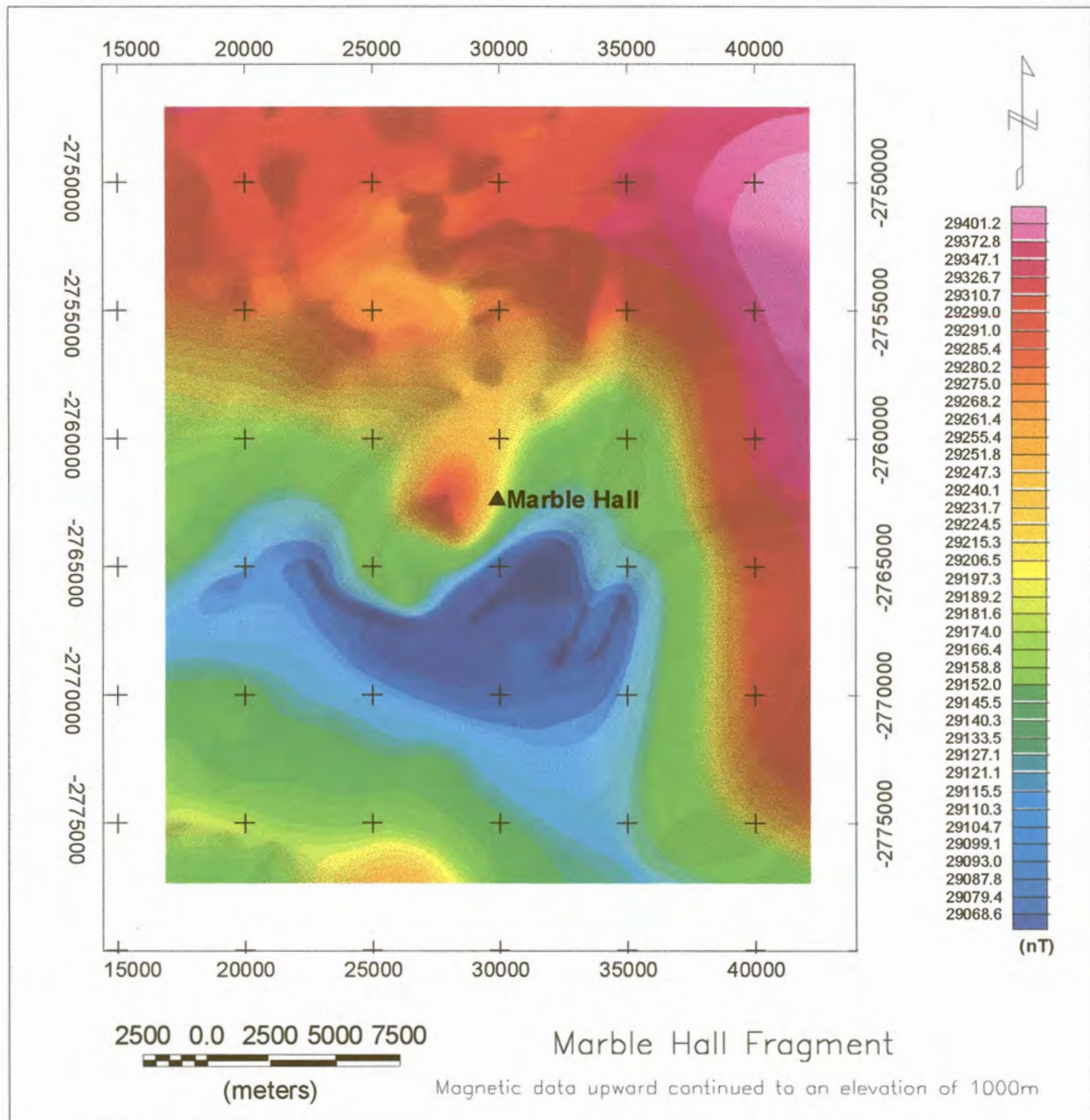


Figure 4.5. Magnetic data upward continued to an elevation of 1000 metres

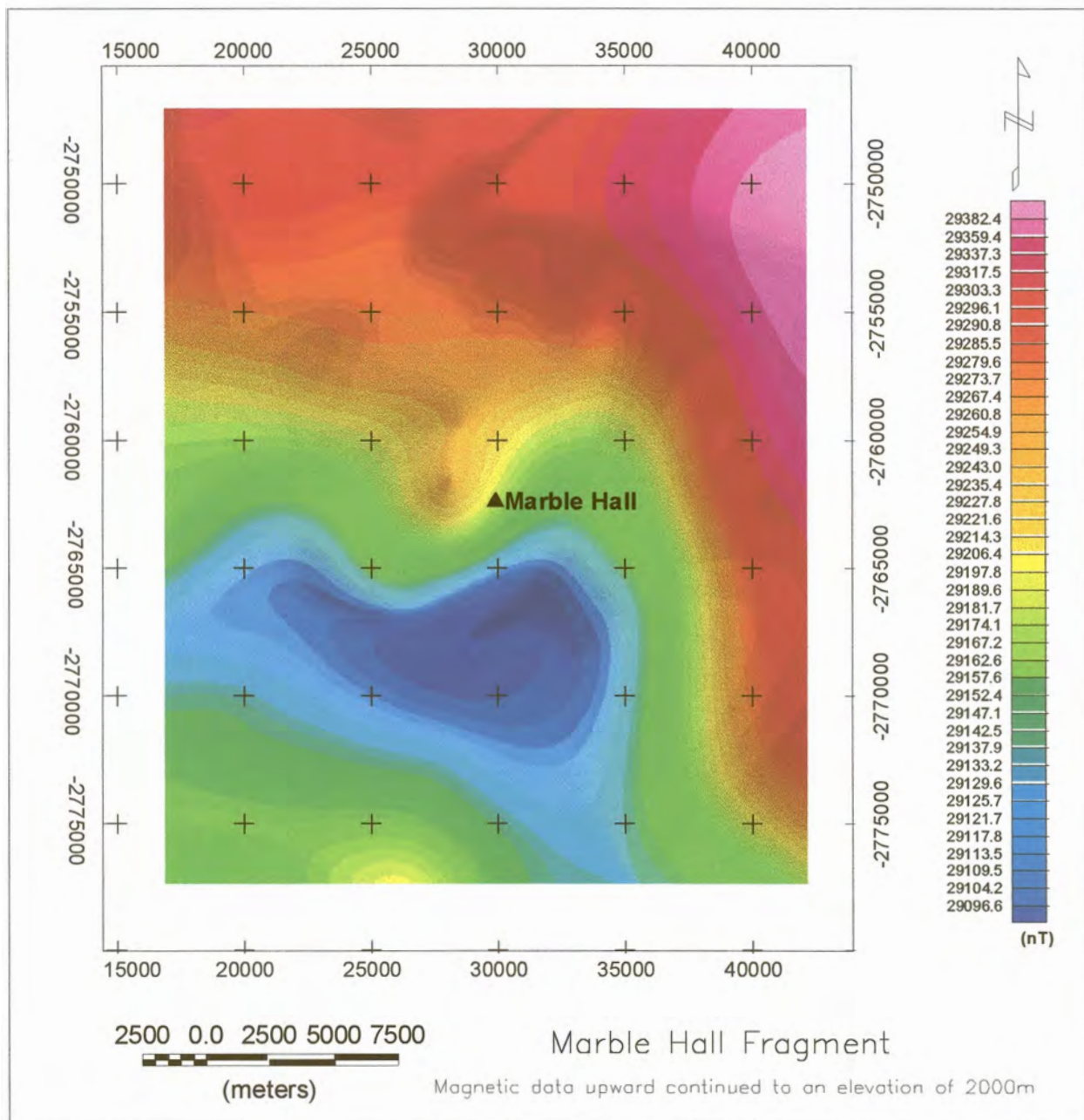


Figure 4.6 Magnetic data upward continued to an elevation of 2000 metres

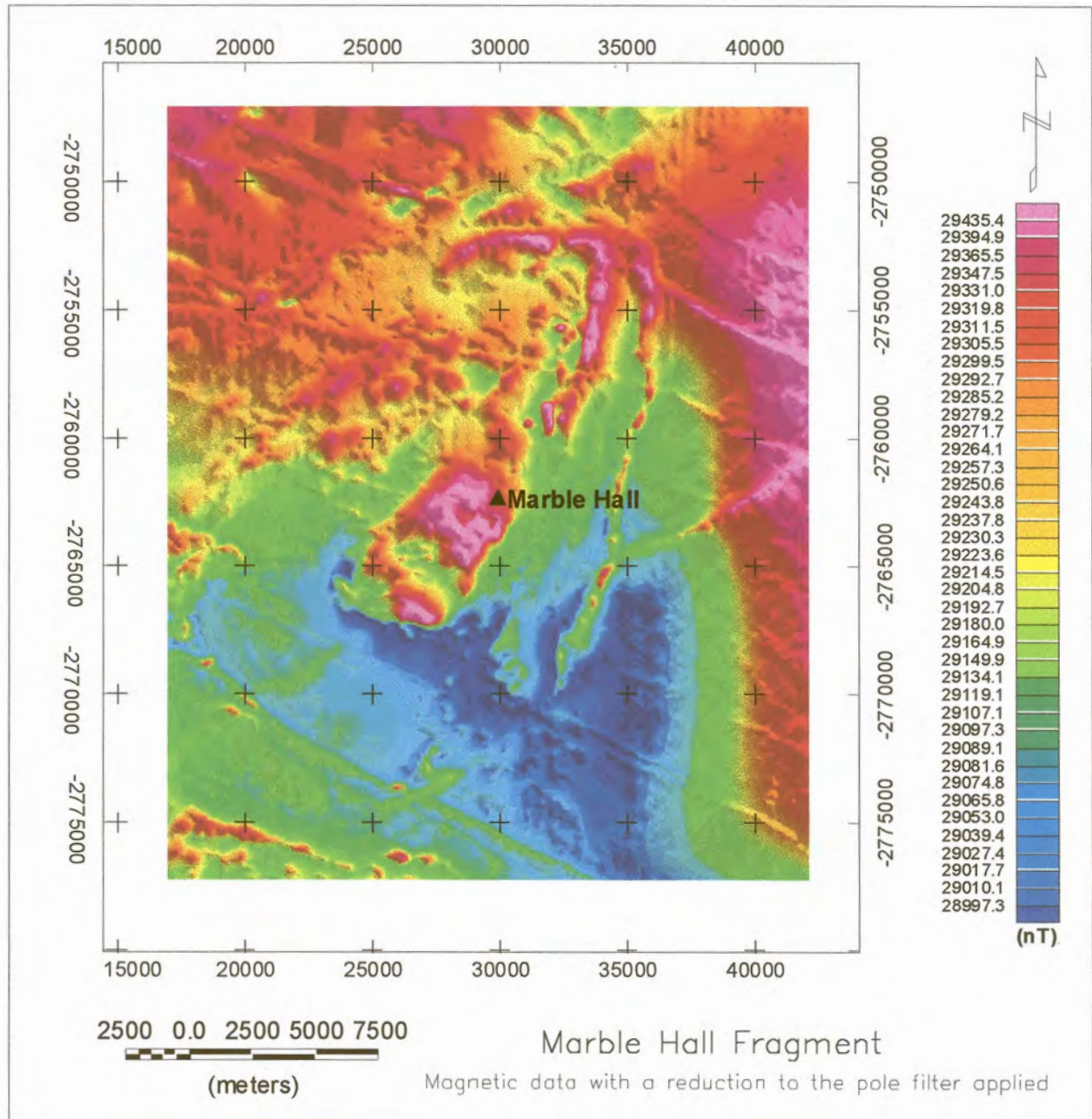


Figure 4.7 Magnetic data with a reduction to the pole filter applied

4.2.3. Vertical Derivative map

Comparison of the vertical derivative map (Figure 4.2), with the total field map (Figure 4.1), shows a marked increase in 'visibility' of structural features, especially in the southern part of the study area.

4.2.4. Analytical signal

This filter was applied to the airborne total magnetic field data. Comparing this map (Figure 4.3), with the total field magnetic contours (Figure 4.1), the difference is immediately obvious along the edges of the dolerite dyke in the south-west and the central portion of the Swartkop Marble Hall anticline. The analytical signal amplitude maximises over the edge of the magnetic structures. This map was used to delineate the edges of lithological units and to determine the centres of two-dimensional structural features.

4.2.5. Upward continuation

The total field data was upward continued to 500m (Figure 4.4), 1000m (Figure 4.5) and 2000m (Figure 4.6). Upward continuation to 500m did not have a significant effect on the original total field data. Upward continuation to 1000m did however have a significant filtering effect leaving only the fold closure of the Swartkop Marble Hall Anticline to the north, the magnetic highs at the central portion and the north-south lineament towards the eastern boundary. Upward continuation to 2000m reveals a marked distinction between any of the other upward continued data and the original data, in that the fold closures are no longer apparent and the magnetic high at the central part has disappeared leaving just a faint

outline. Also, the north south lineament to the eastern boundary is better defined. The magnetic low to the south of Marble Hall is more pronounced, and, finally, the highest magnetic signature (pink) is more confined to the extreme north eastern border.

4.2.6. Reduction to the Pole (RTP)

The reduction to the pole transform (Figure 4.7), resembles to a large extent the total field data except in the west where the Wonderkop fault appears to be better defined. In the northern part of the fragment where the faulting on the fold also seems to be better defined which would indicate that the influence of magnetic data on the angle of magnetic inclination has been removed. Thus, in removing the anomaly asymmetry caused by the magnetic inclination, the anomalies are better located relative to the causative bodies.

4.3. Processing of gravity data

4.3.1. Reduction to Bouguer values

Processing of the data to obtain the Bouguer values was done using the Oasis Montaj software from GEOSOF. First, the base station at Marble Hall was tied in to the absolute values known for the station at Groblersdal. Second, the other base station values were tied in to the absolute value calculated for the station at Marble Hall. These base stations were then tied to the International Gravity Standardisation Network values (Morelli et al., 1974) and were referred to the gravity formula based on the 1967 Geodetic Reference System (Moritz, 1968). Terrain corrections were not applied since the main area of interest for this research was fairly flat as is evident from the elevation contour map given in Figure 4.8. The Bouguer gravity map is shown in Figure 4.9.

4.4. Interpretation of potential field data

4.4.1. General

The interpretation of the data was done in three stages. These consisted of:

- Correlating geological units with features identified on the magnetic and gravity contour maps.
- Do a structural interpretation of the magnetic and gravity contour maps.
- Do a vertical profile interpretation along a number of profiles across the study area.

4.4.2. *Correlate known geology with observed geophysical anomalies.*

In the first stage a simplified outline of the geology was superimposed onto:

- the total field airborne magnetic data downward continued to ground level (Figure 4.10),
- the vertical derivative of the magnetic data (Figure 4.11),
- the bouguer gravity map (Figure 4.12),
- the bouguer gravity map with contour lines, emphasising the steepness of gradients in certain areas (Figure 4.13).

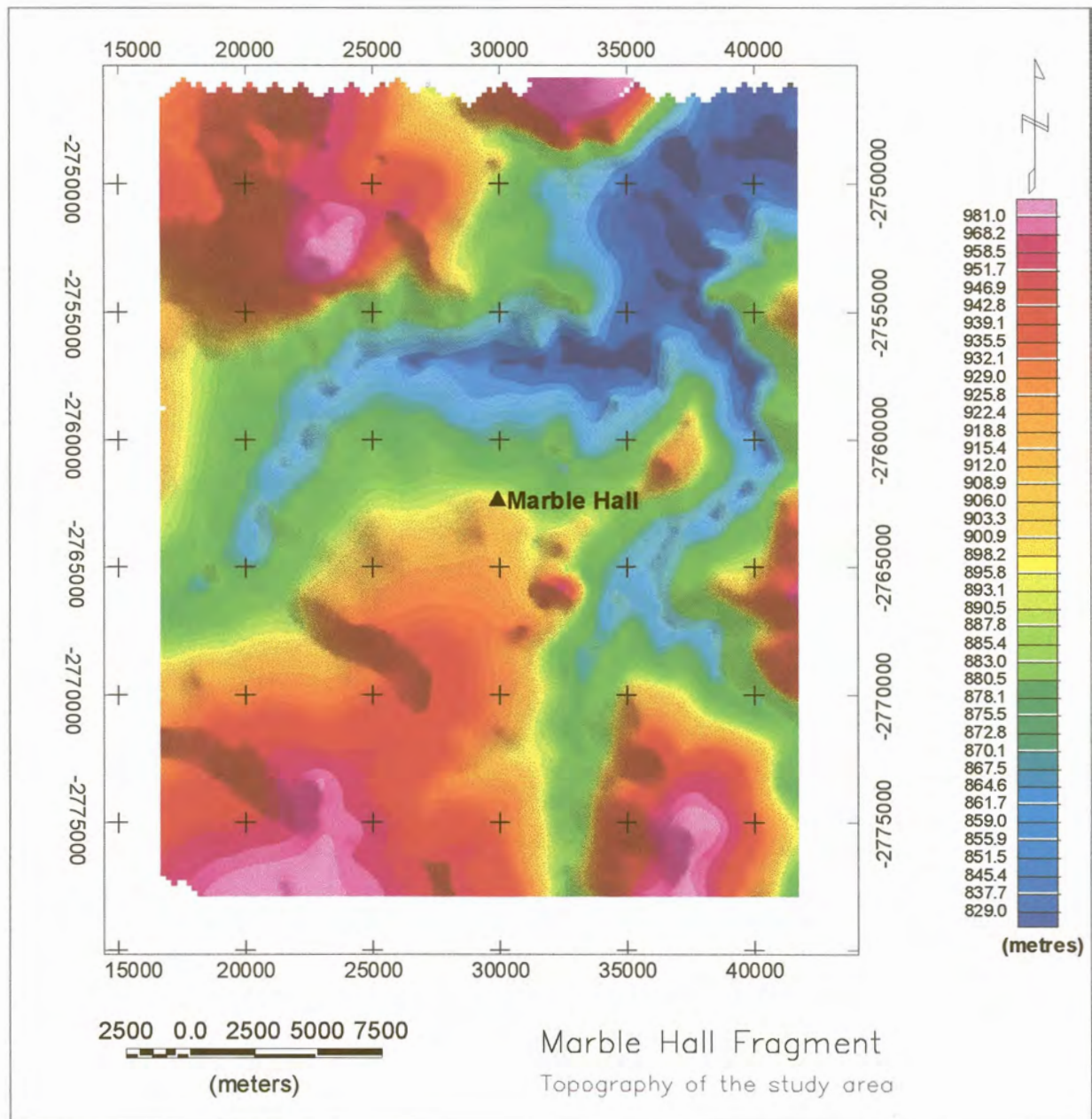


Figure 4.8. Topography of the study area

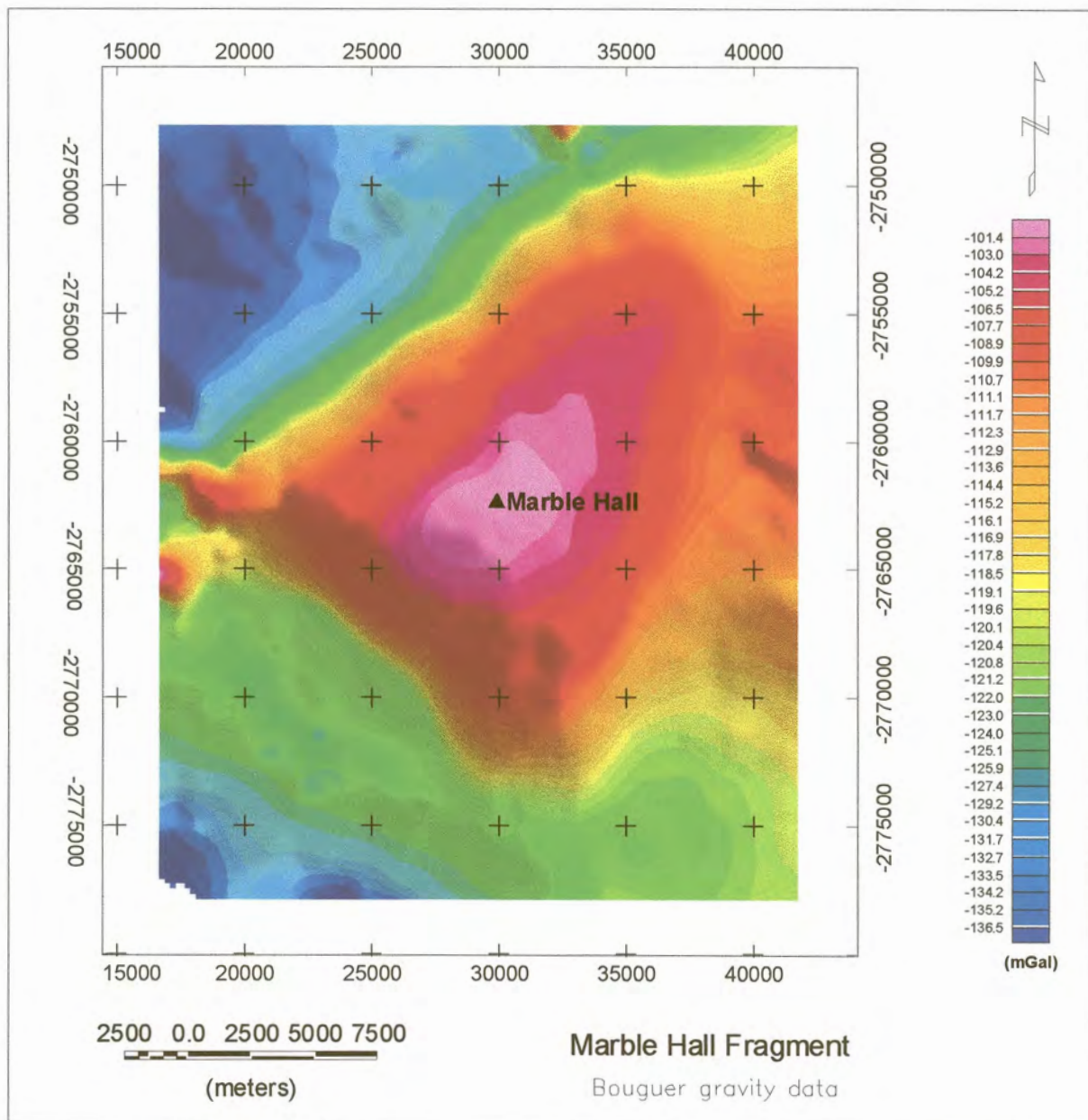


Figure 4.9 Bouguer gravity map

These maps were used to tie the geophysical data to known geological units and features.

The following units and features have been identified and the following numbers allocated.

1. Pretoria Series
2. Makeckaan Formation
3. Malmani dolomite
4. Karoo Supergroup
5. Elandslaagte Dome (Archaean rocks)
6. Wonderkop fault
7. Faults
8. Nebo Granite
9. Karro dolerite sills
10. Archaean rocks of the Moos River Fragment
11. Diorite
12. Dyke
13. Fold

To further facilitate the interpretation of the gravity map, the actual contour lines (Figure 4.13), were included on the colour coded gravity map. This gives a better visualization of the gradient in the observed gravity values.

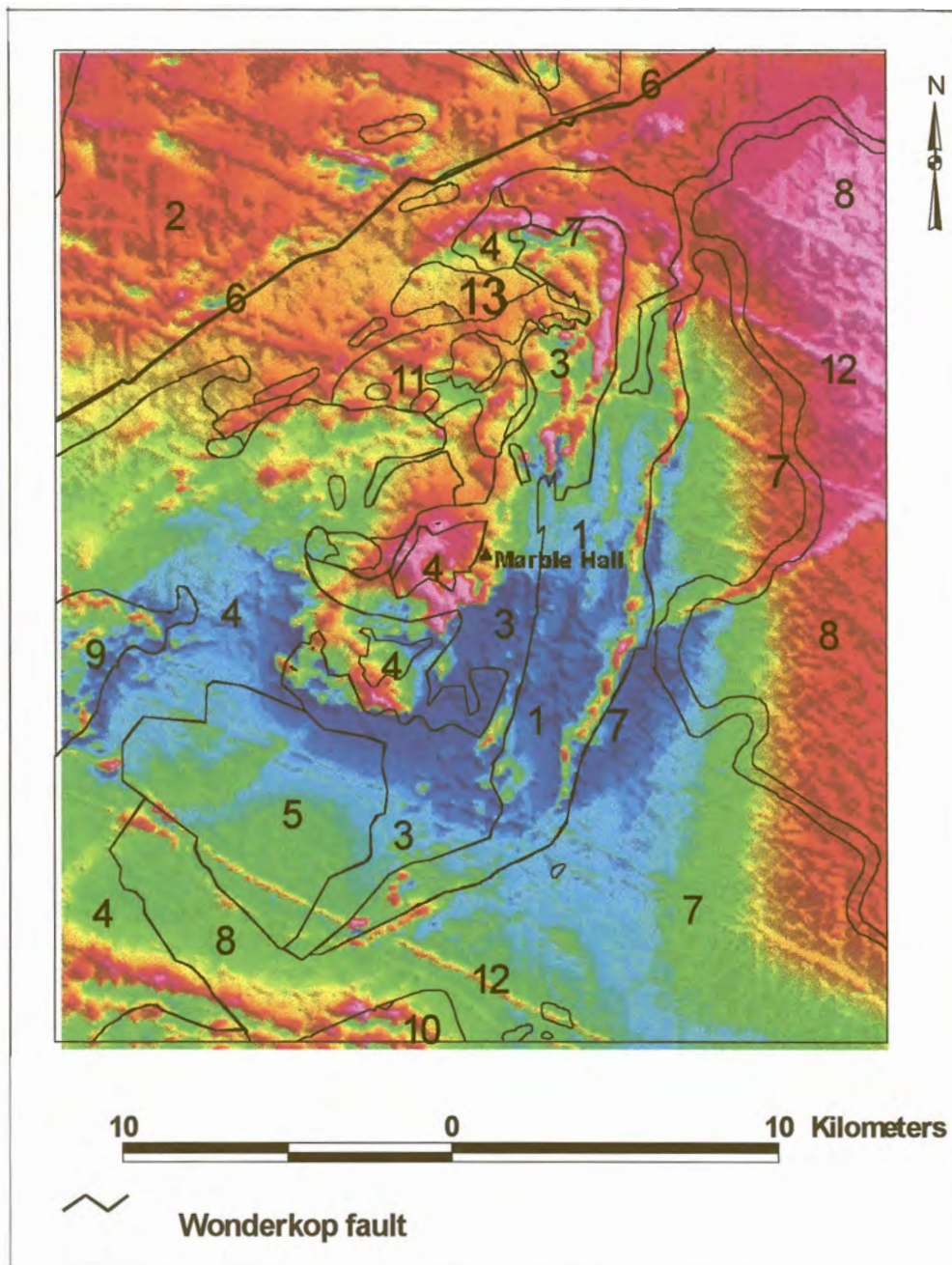


Figure 4.10. Simplified outline of geology superimposed on downward continued total field magnetic data

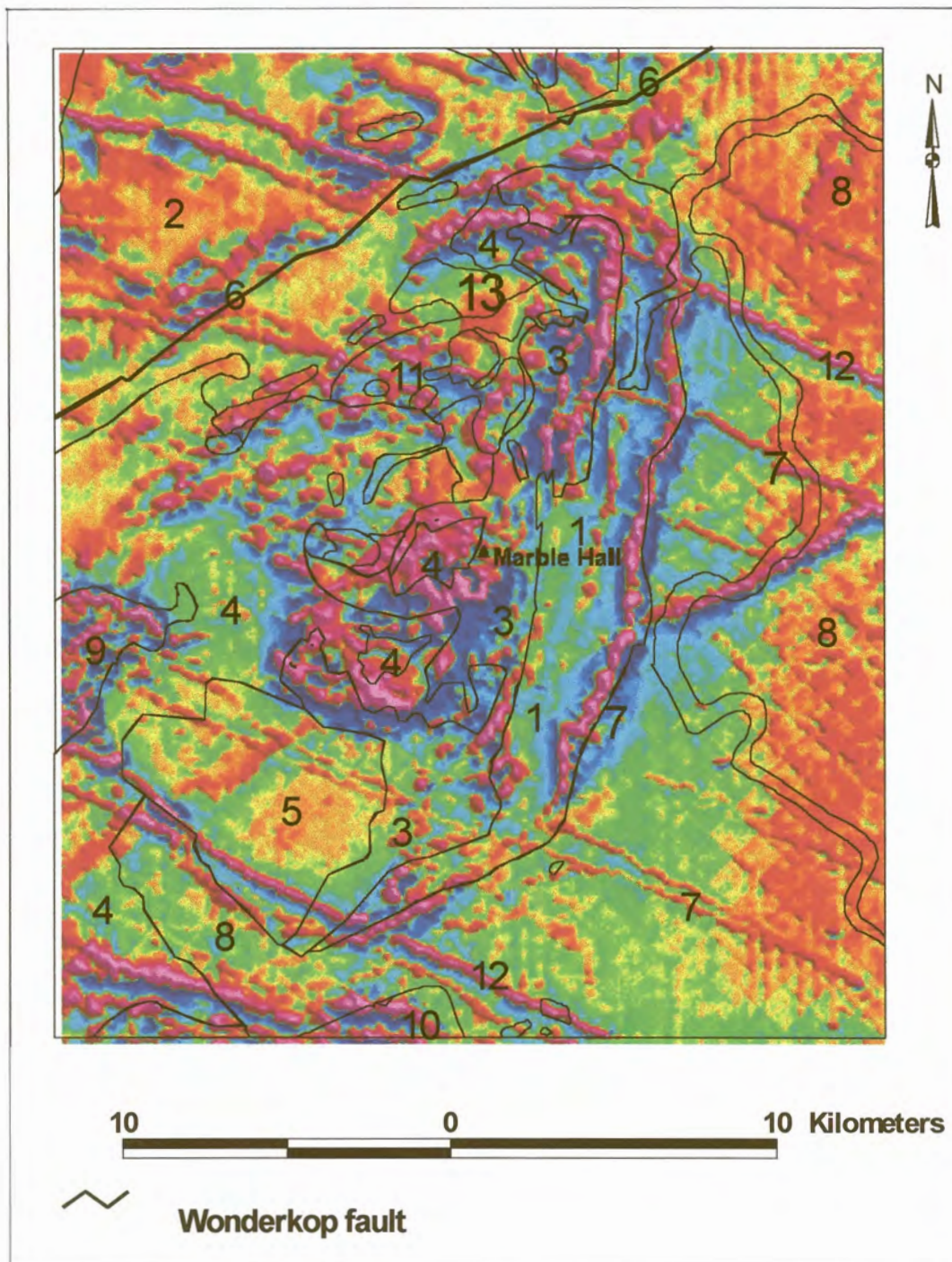


Figure 4.11. Features identified from the correlation of vertical derivative map with simplified geology

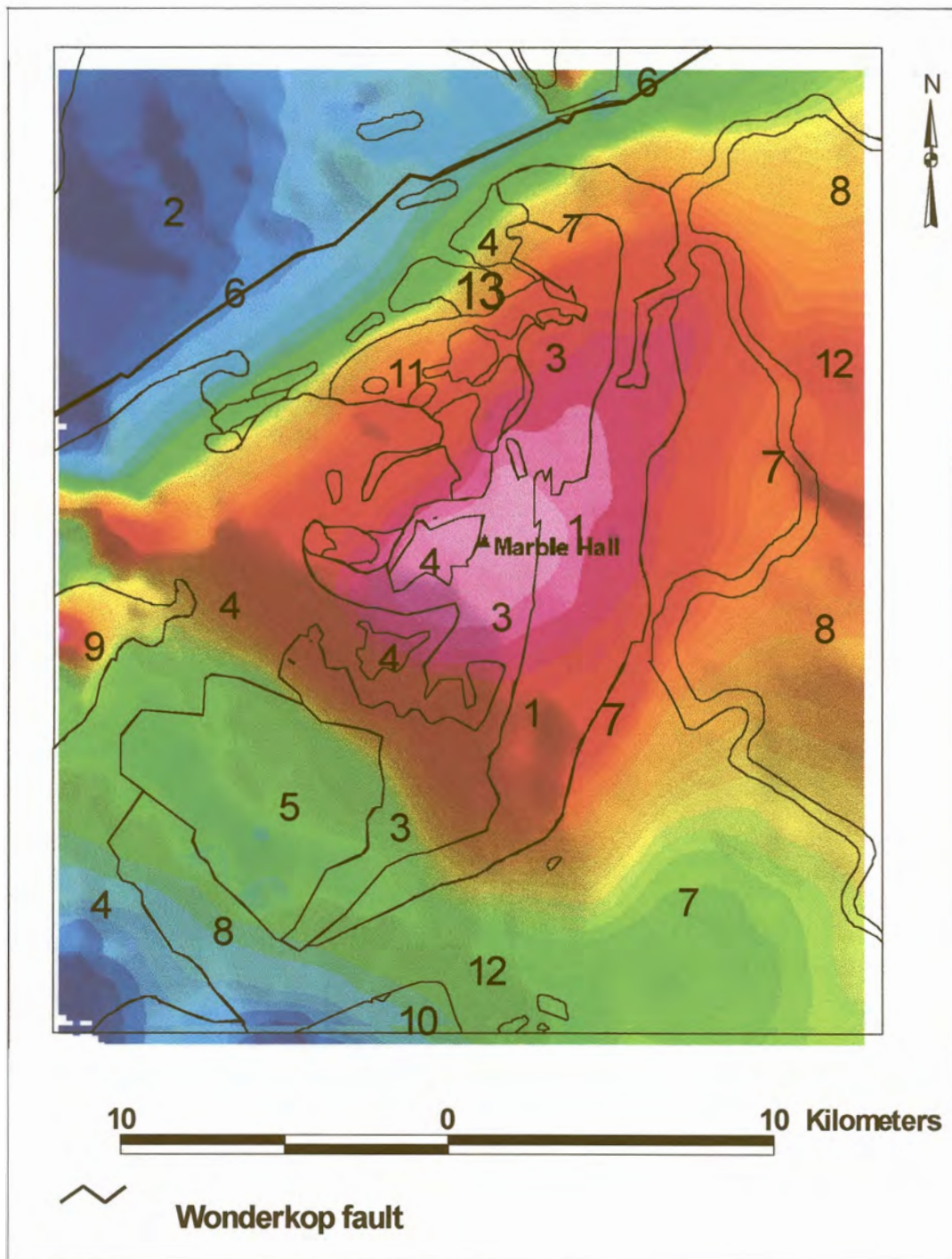


Figure 4.12. Bouguer gravity map with outline of simplified geology

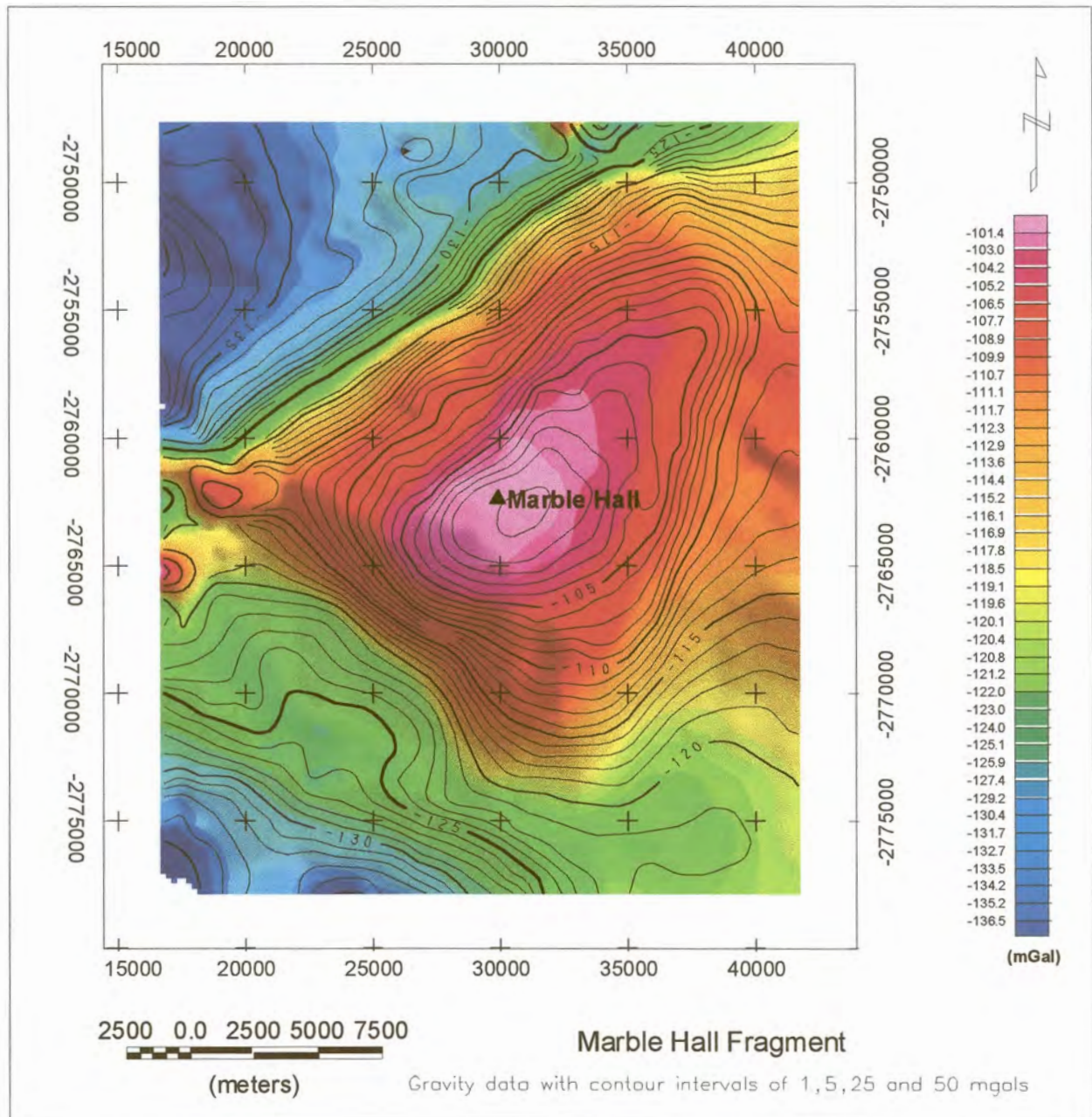


Figure 4.13: Bouguer gravity map with contour lines to emphasise the steepness of the gradient in some areas.

4.4.3. Structural interpretation of magnetic and gravity contour maps.

4.4.3.1. Gravity

There is a good measure of correlation between several of the mapped geological features and the observed gravity values. The very large anomaly has a shape which roughly follows the northeast-southwest trend of the Fragment. The maximum amplitude of the gravity high is in the order of 30 mgal. This is too high to relate to either the surface geology or the topography of the area.

The steep gravity gradient observed in the north-western corner (Figure 4.13), is interpreted as a fault controlled contact between two lithologies. The interpreted fault trends from the western boundary to the northeast at a strike angle of approximately 45 degrees and is interpreted as the Wonderkop fault delineated by Lee and Sharpe (1983) and many others.

The gravity data suggest the presence of high density rocks at the centre of the Marble Hall Fragment. This gravity high is situated between the prominent Wonderkop fault to the west and a suspected north-south trending fault to the east (see next section).

Though the Marble Hall Fragment is bordered to the east and north-east by the Bushveld Complex granite, both the magnetic and gravity data associated with the eastern and north-eastern parts of the Fragment suggest that the Bushveld granite in these areas is underlain by relatively thick mafic rocks at great depth.

4.4.3.2. *Magnetics*

To correlate observed magnetic features with topography, the magnetic data were draped over the topography using ERMMapper software. The Wonderkop fault and an interpreted north-south fault are shown in Figure 4.14.

A large number of dykes and faults have been identified using the various filtered airborne magnetic contour maps. These features are shown in Figure 4.15. In this figure, feature 1 is identified as the Wonderkop fault, while feature 2 is interpreted as the major north-south trending fault. This fault has no surface geological expression.

4.4.4. *2.5D modeling of selected profiles.*

Initially three east-west striking profiles were selected on both the total field magnetic data as well as the gravity data. These lines are labeled AA', BB', and CC' in Figures 4.16(a) and (b), where the relative positions of the profiles are indicated.

The software used for the interpretation of the data is MAGIXP (MAGIX^{PLUS}) which is an interactive, graphically oriented, modeling program designed for the interpretation of gravity and magnetic data (potential field data).

For the magnetic data, the magnetic susceptibility value for the background and each body comprising the model is expressed in SI units. A magnetic inclination and declination of -60° and -17° respectively were used. The susceptibilities used for the various lithological units are given in Table 7.

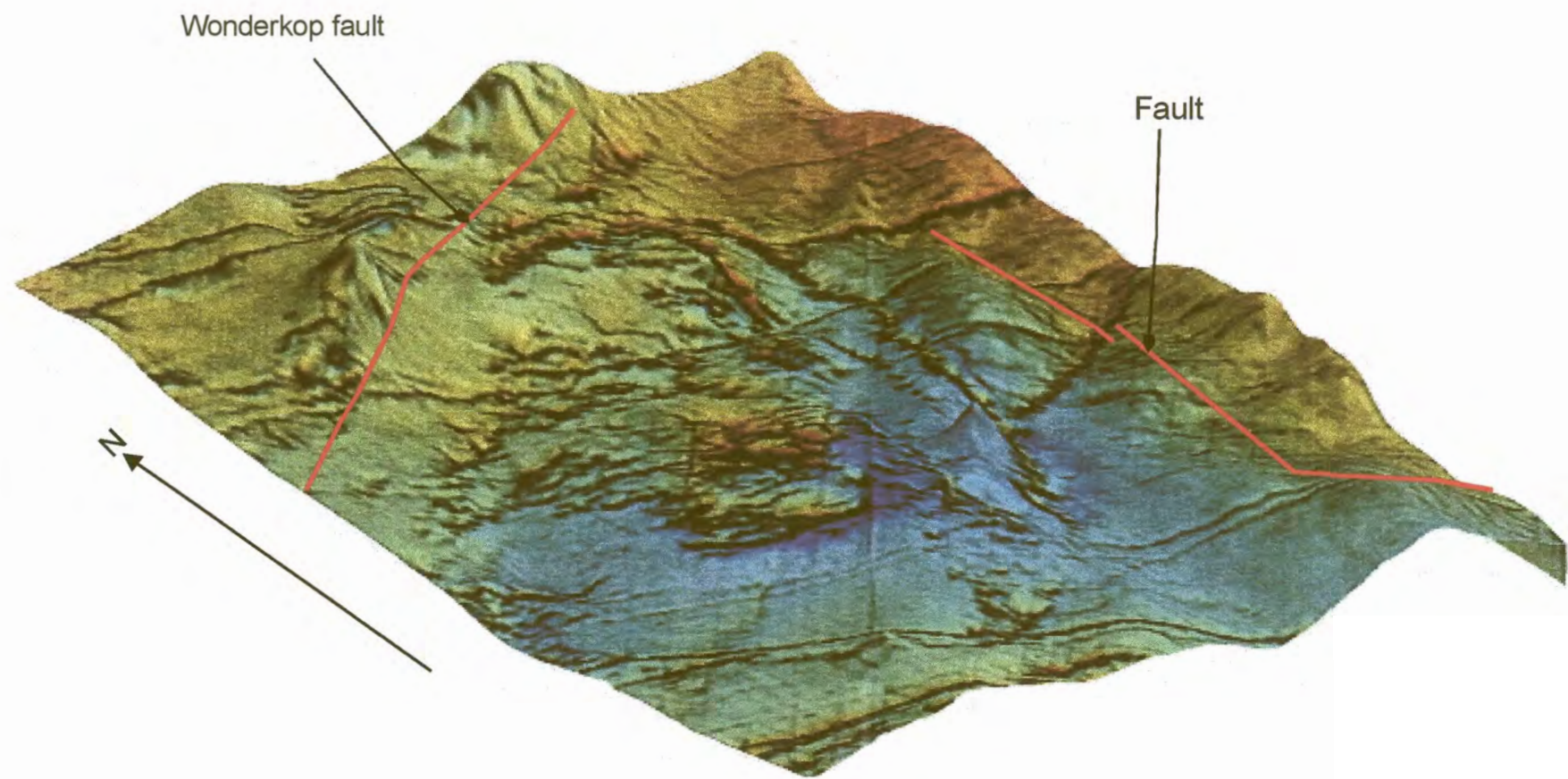


Figure 4.14. Total field magnetic data draped over the topography

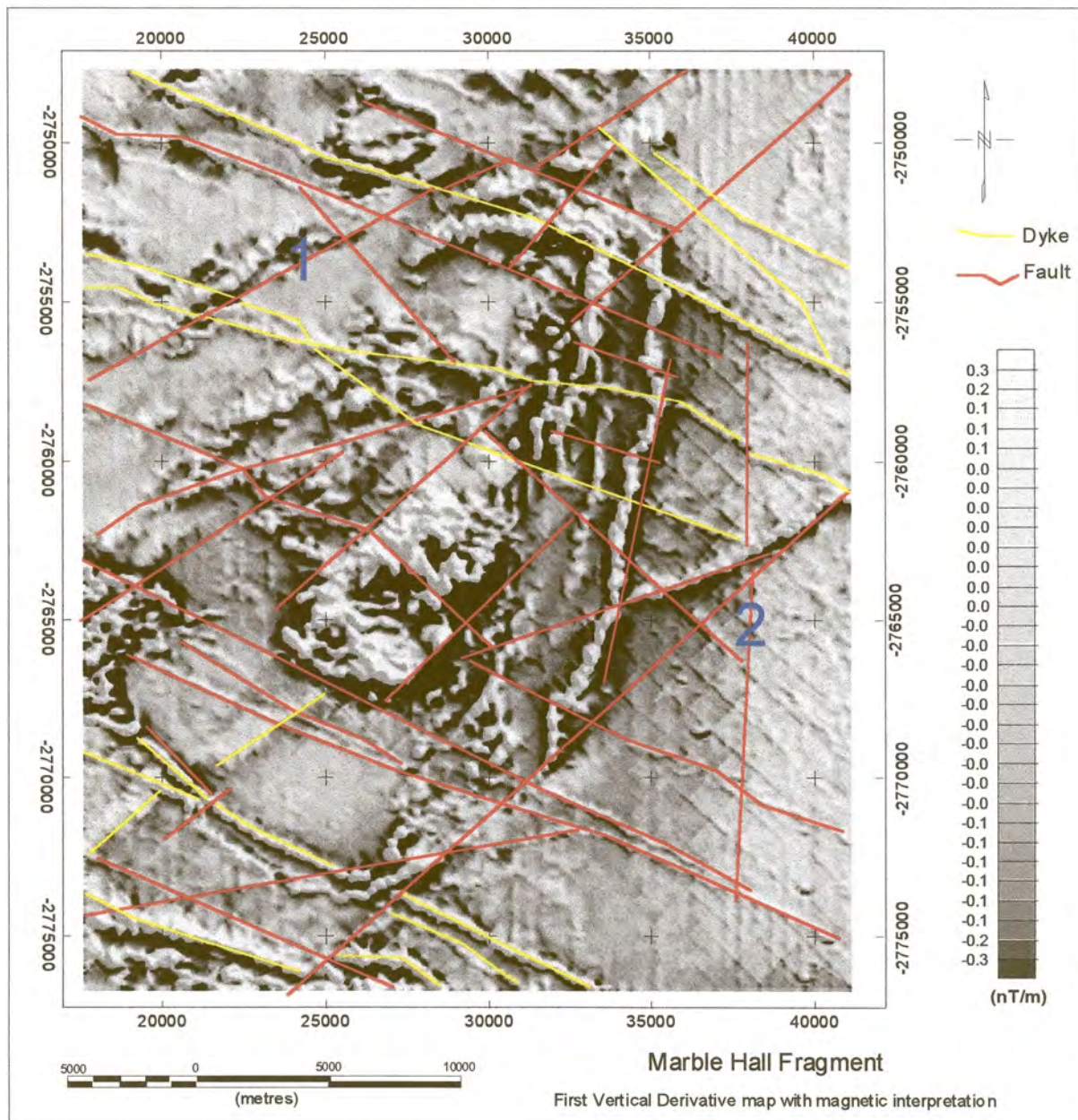


Figure 4.15. Interpreted structures from the vertical derivative map (grey scale)

A prominent magnetic signature with an amplitude in the order of 290 nT is observed in the centre of the Fragment, in about the same position as the gravity high. This anomaly remains prominent even when the data are upward continued to a height of 2000m, (Figure 4.6).

The KT-9 Kappmeter (susceptibility meter) supplied by the Council for Geoscience was used in determining the magnetic susceptibility of outcrops. Laboratory determination at the Council for Geoscience, of susceptibilities of rock samples taken from the few exposed outcrops, mostly granites and Transvaal Supergroup rocks, revealed that the samples were not remanently magnetised.

Hattingh (1991), however, described the dominance of remanent magnetism in all the structural mafic zones of the Bushveld Complex, except the weakly magnetic Critical Zone. The Main Zone has a low susceptibility despite having a high natural remanent magnetism (NRM) because the carriers of magnetisation are single domain grains which are very small with little or no contribution to the susceptibility of the rock unit (Hattingh, 1986b). Larger magnetic grains which can support higher susceptibilities are very scarce or in many cases absent Hattingh (1986a, b).

Hattingh (1989, 1991), indicated that the NRM in the Upper Zone is nearly 200% larger than the induced magnetisation and assumed that 80% of the NRM of the Upper Zone consist of random secondary magnetisation. This, according to Hattingh (1991), reflects that for the interpretation of magnetic anomalies associated with this zone, the induced component of the anomaly is more important than the permanent remanent magnetisation of the Upper Zone.

The susceptibilities of the Upper and Main Zones used in the modeling were taken from Hattingh (1991). Table 7 shows the susceptibilities of the various rock units.

Table 7: Susceptibilities used for rocks in the research area.

| Rock Formation | | Susceptibility (SI units) |
|-------------------------|------------|------------------------------|
| Makeckaan Formation | | 0,003 |
| Nebo Granite | | 0,002 |
| Pretoria Group | | 0,003 |
| Dolomite | | 0,000 |
| Bushveld basic rocks | Upper zone | 0,11129 |
| | Main Zone | 0,0025 |
| Bloempoot Formation | | 0,000 |
| Archaean Granite | | 0,000 |

The regional was estimated for the magnetic profiles by fitting a second order polynomial to the TMI contour map. For the gravity data a straight or very slow curving datum line, was subtracted from the data.

Starter models representing the structure of the Marble Hall Fragment as interpreted from surface geological mapping and excluding, on purpose, the mafic rocks known to exist in the central part of the Fragment, were used. The topography along these profiles are given in Figure 4.17. The gravity and magnetic data and the various geological cross sections are given in Figure 4.18 (a) and (b) for profiles AA', BB' and CC' respectively.

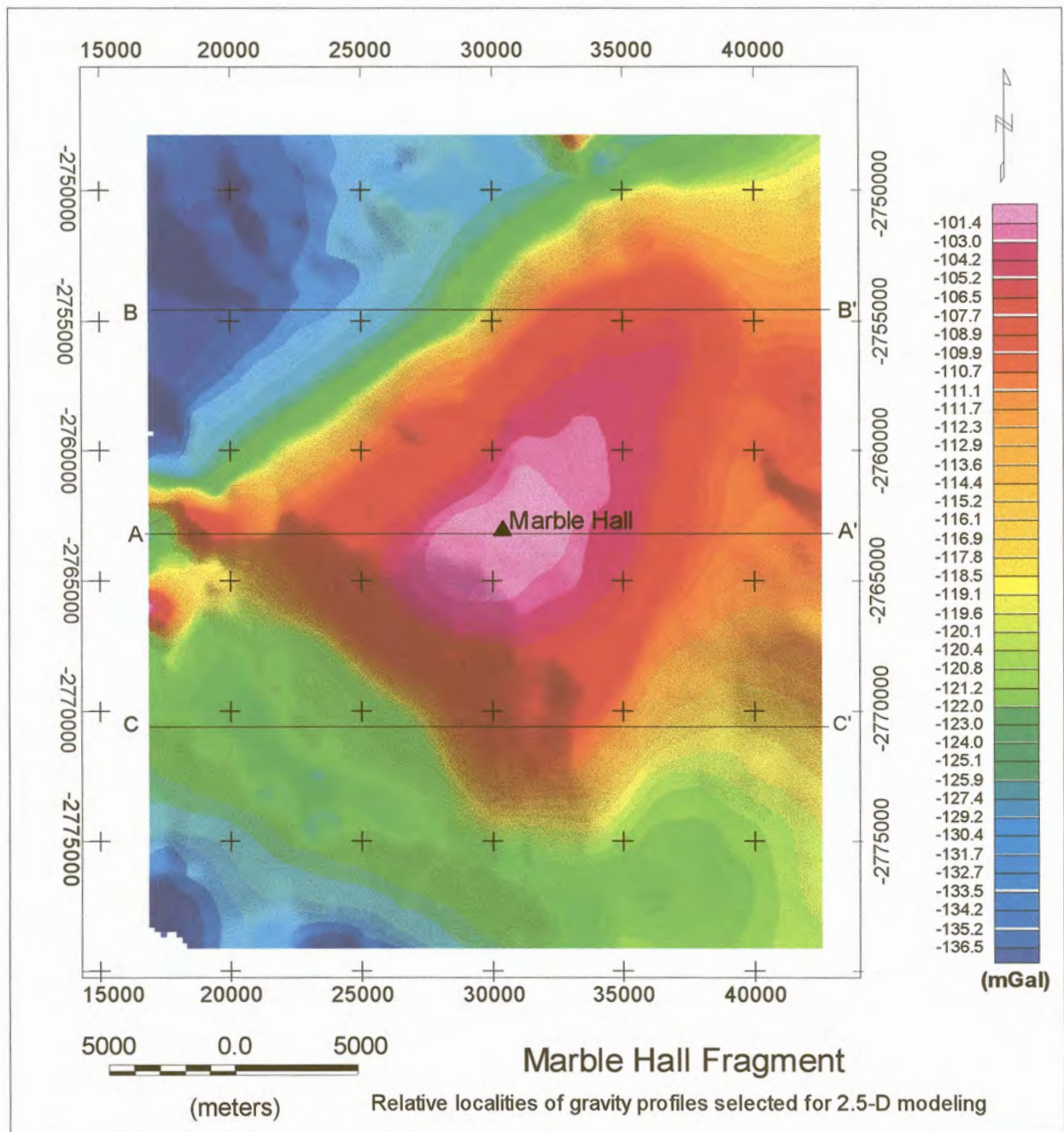


Figure 4.16a : Relative locality of gravity profiles selected for 2.5-D modeling

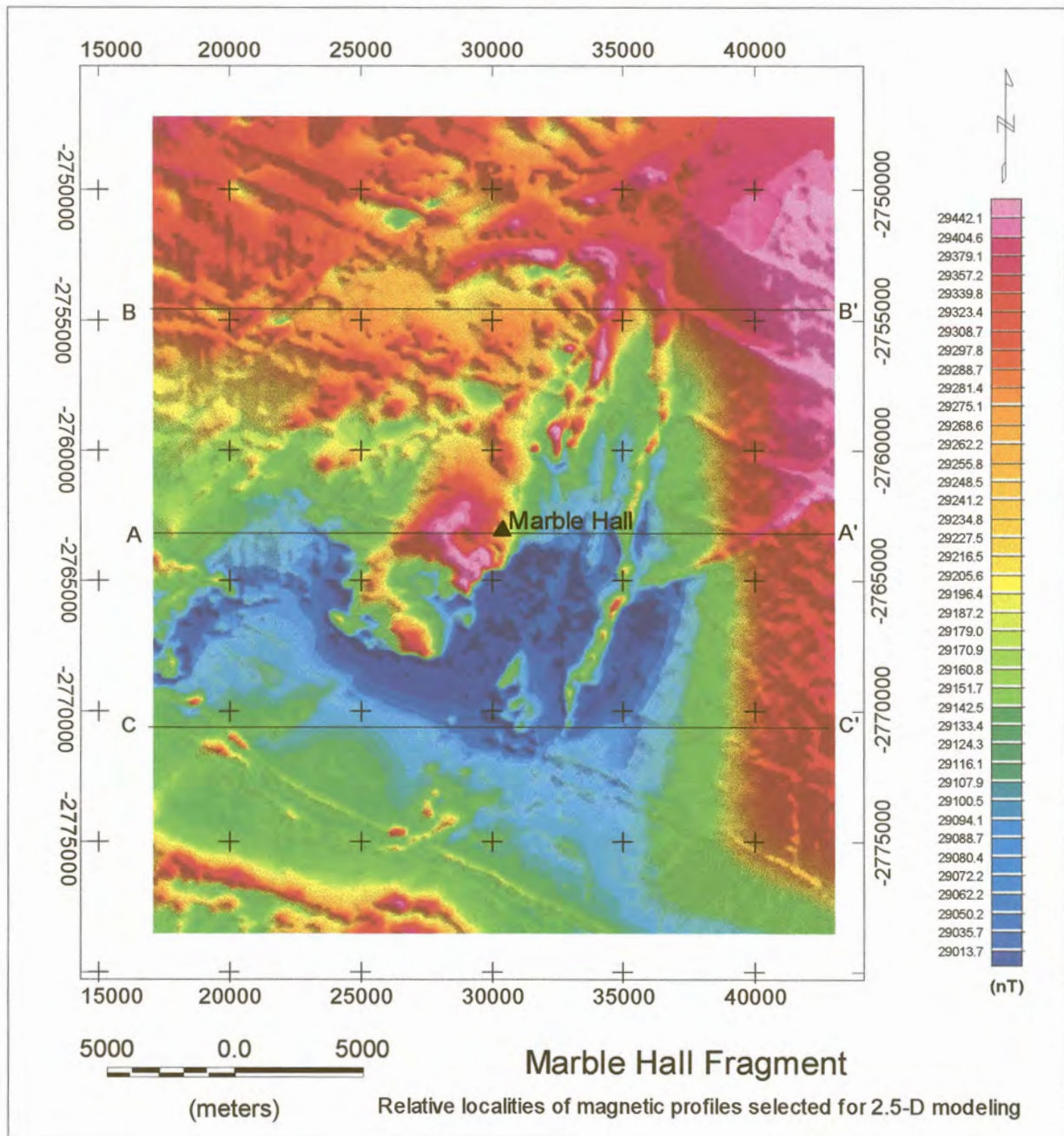


Figure 4.16b: Relative locality of magnetic profiles selected for 2.5-D modeling

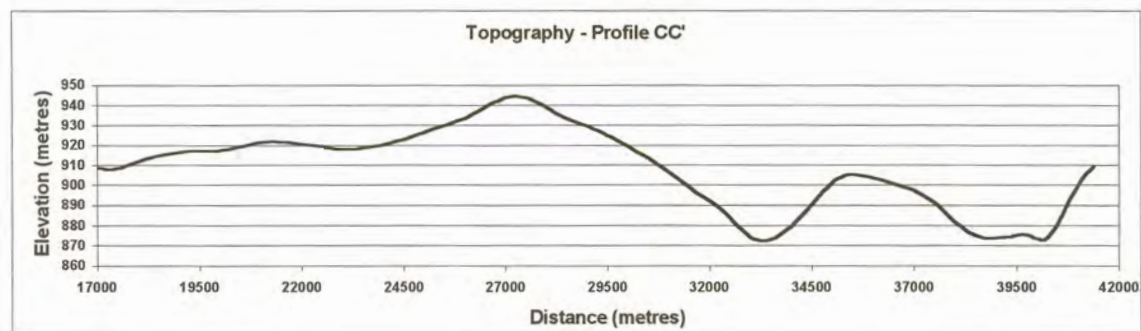
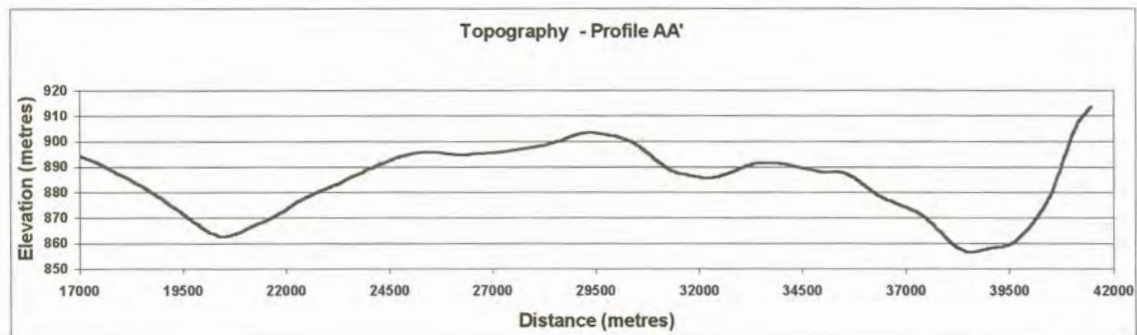
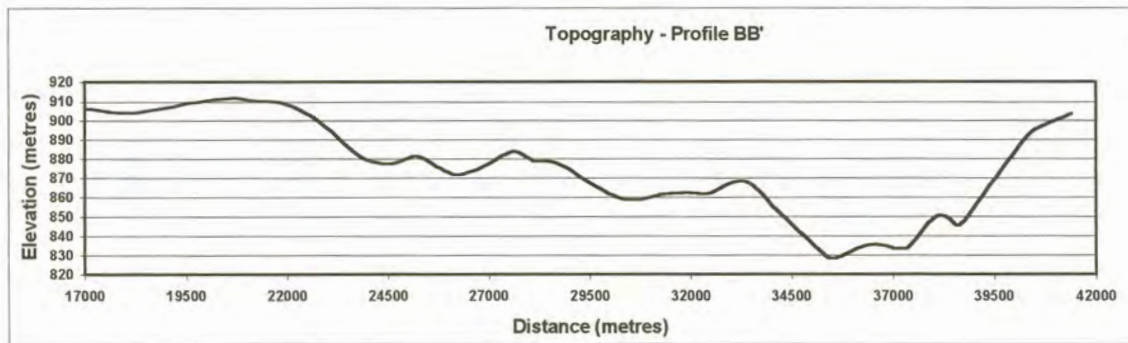


Figure 4.17: Topographic relief along profiles AA', BB' and CC'

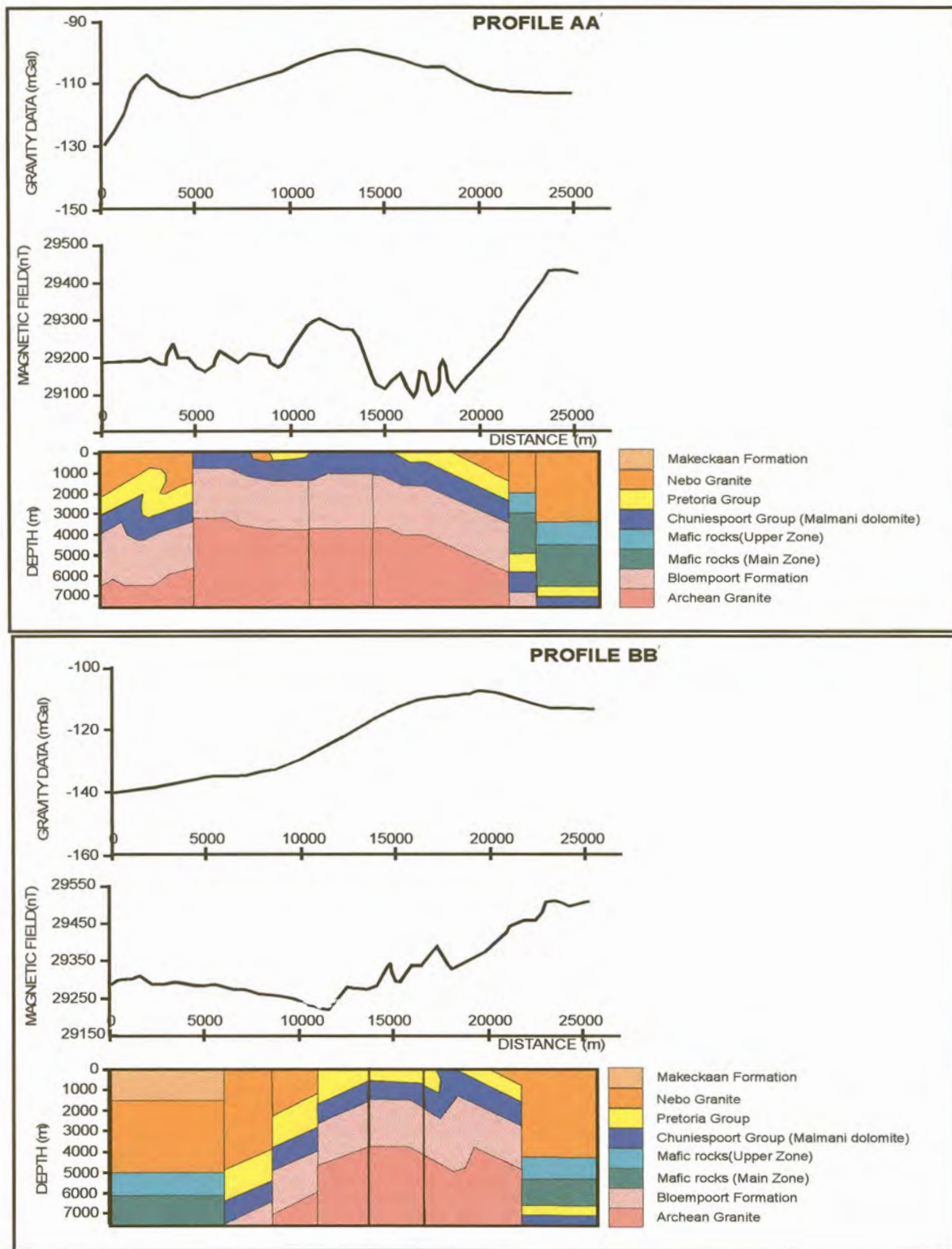


Figure 4.18 (a). Starting models for profiles AA' and BB' respectively.

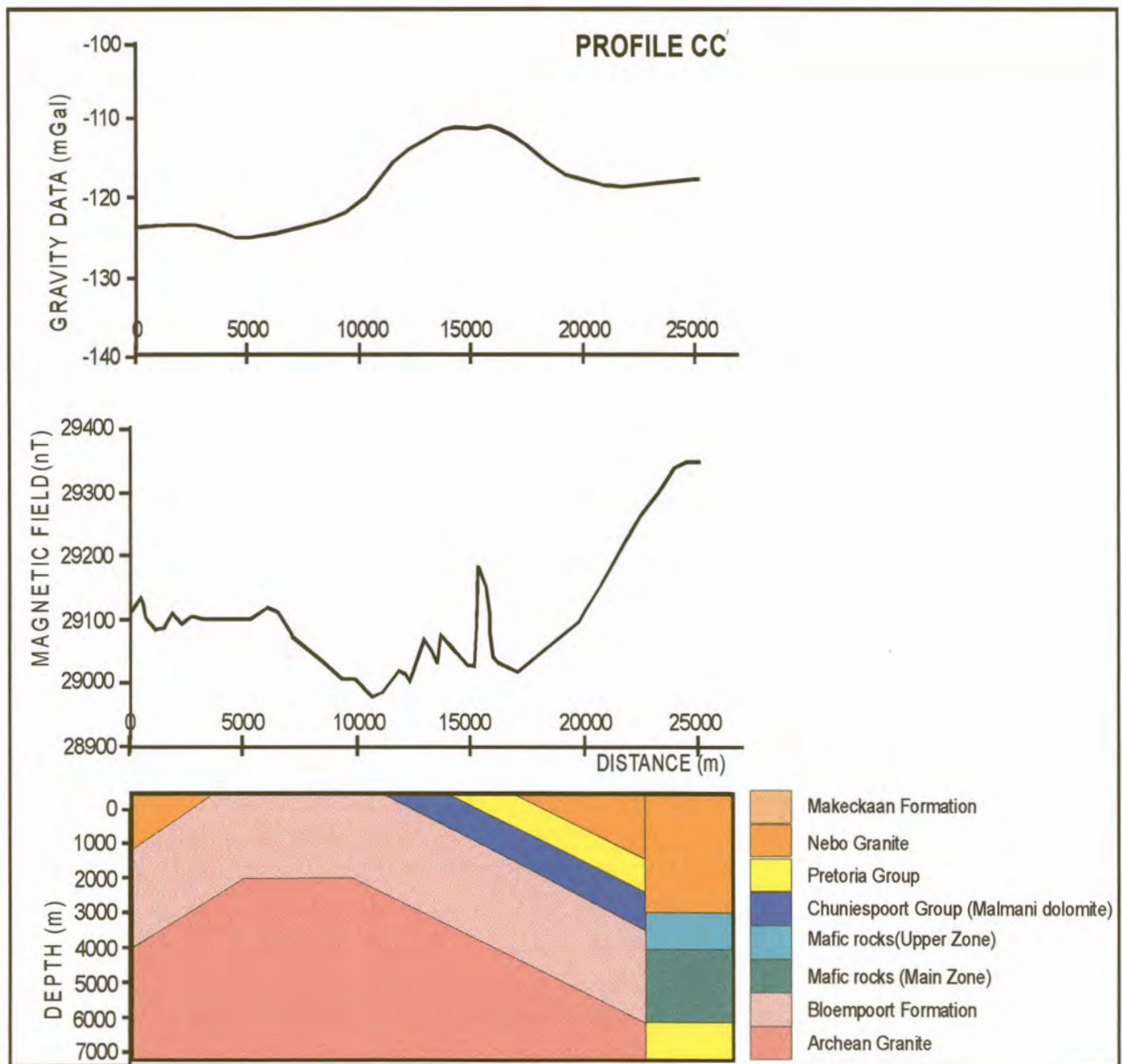


Figure 4.18b. Starting model for profile CC'

The geological models in Figures 4.18 (a) and (b), were then adjusted to fit the potential field data. The final geophysical models are given in Figures 4.19 (a) and (b).

Based on the interpreted profiles AA', BB', CC', Figures 4.19 (a),(b) and (c), it is possible to get an idea of the strike of the intrusive body. In order to confirm its linear trend and perhaps, the width, profiles DD' and EE' along the suspected strike and at right angle to the strike respectively, were drawn for modeling (Figures 4.20 (a) and (b)).

The geological cross-sections (Figure 4.21) along the profiles were used as starter models for profiles DD' and EE'. Again, the existence of mafic rocks in the central part of the Fragment is ignored in these profiles. The final geophysical models are given in Figures 4.22 and 4.23.

It is worthy of note that in the final geophysical models presented (Figures 4.19(a),(b), (c), 4.22 and 4.23), for the gravity models, background refers to Archaean Granite with a density of 2.67 g/cm^3 , while for the magnetic models, background refers to a combination of Archaean Granite, Malmani dolomite and the Bloempoot Formation as single model units, having magnetic susceptibilities of zero.

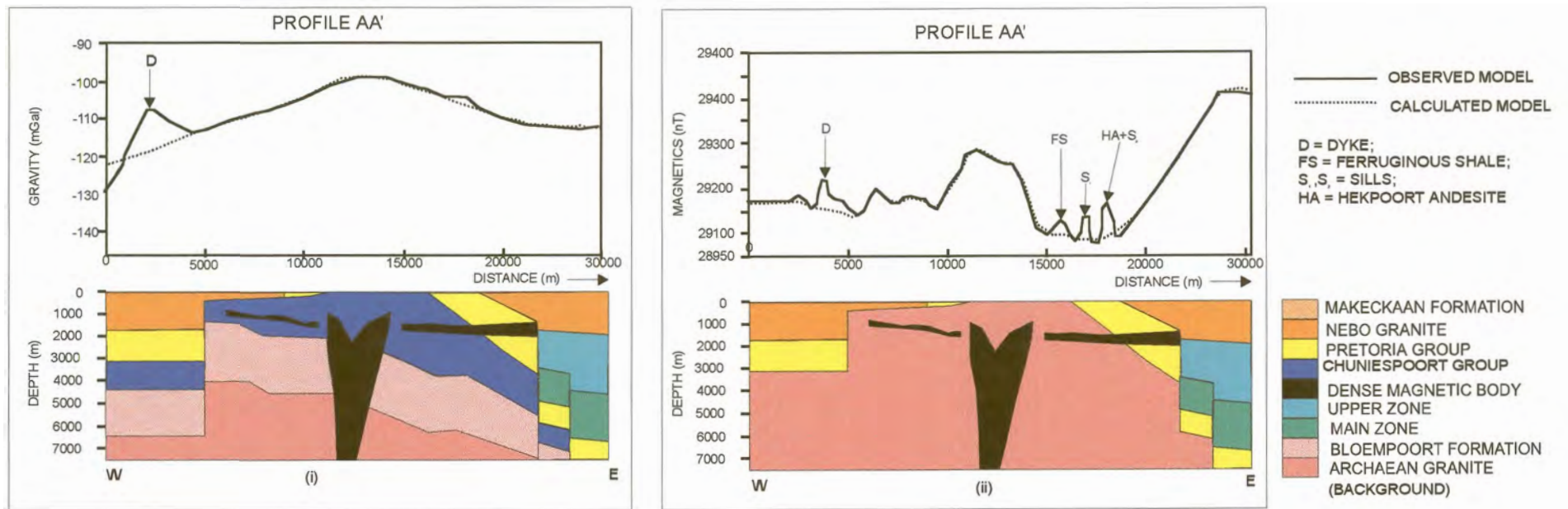


Figure 4.19a : Geophysical models for profiles AA' (i) the gravity and (ii) the magnetics

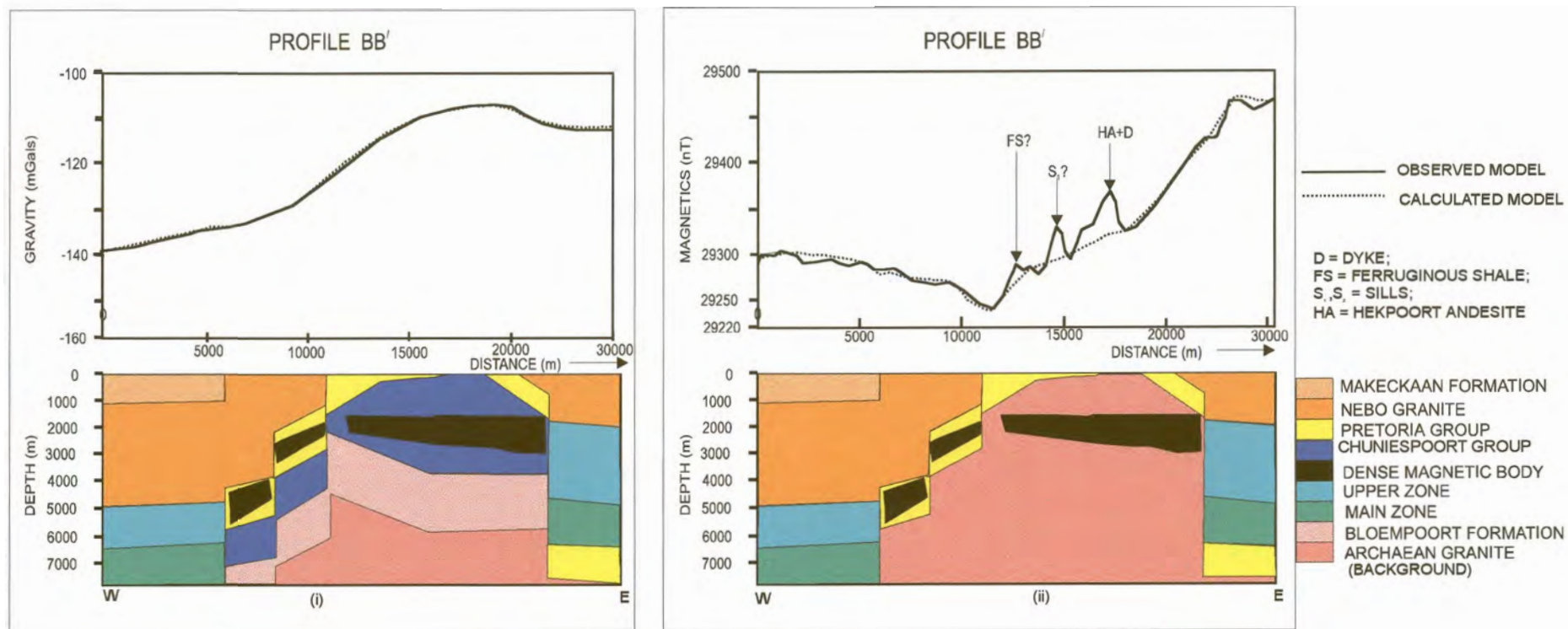


Figure 4.19b : Geophysical models for profiles BB' (i) the gravity and (ii) the magnetics

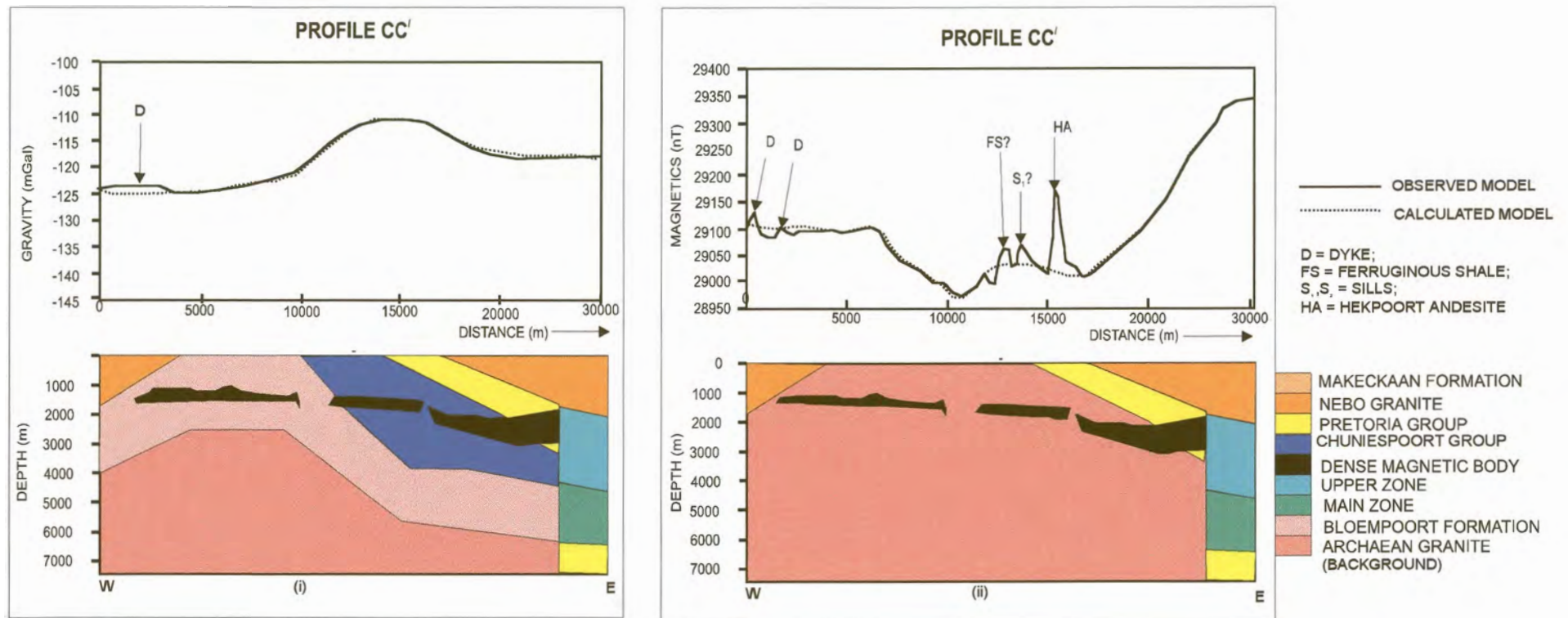


Figure 4.19c : Geophysical models for profiles CC' (i) the gravity and (ii) the magnetics

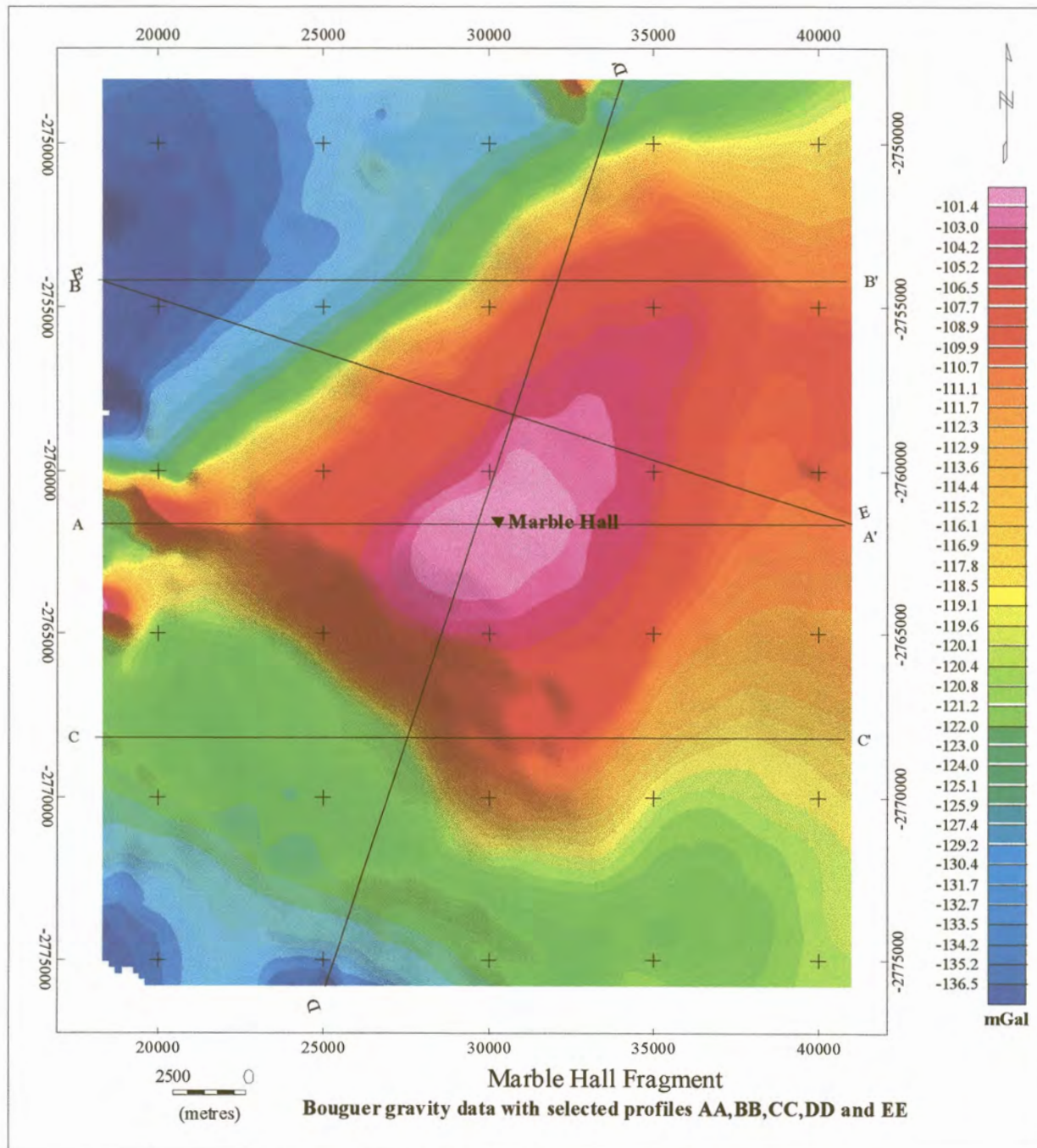


Figure 4.20a Gravity data showing the localities of profiles finally selected for 2.5-D modeling

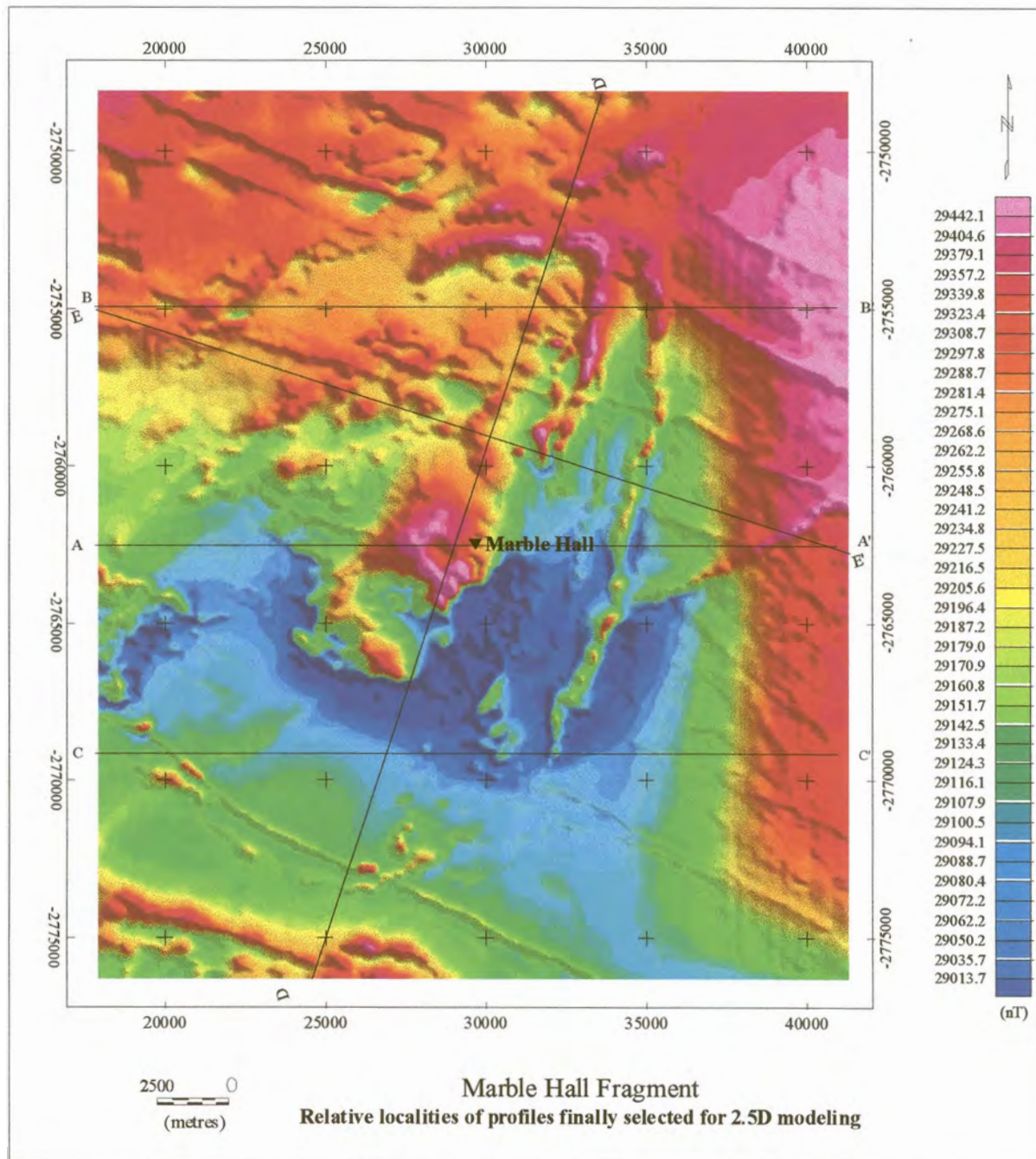


Figure 4.20b. Magnetic data showing the localities of profiles finally selected for 2.5-D modeling

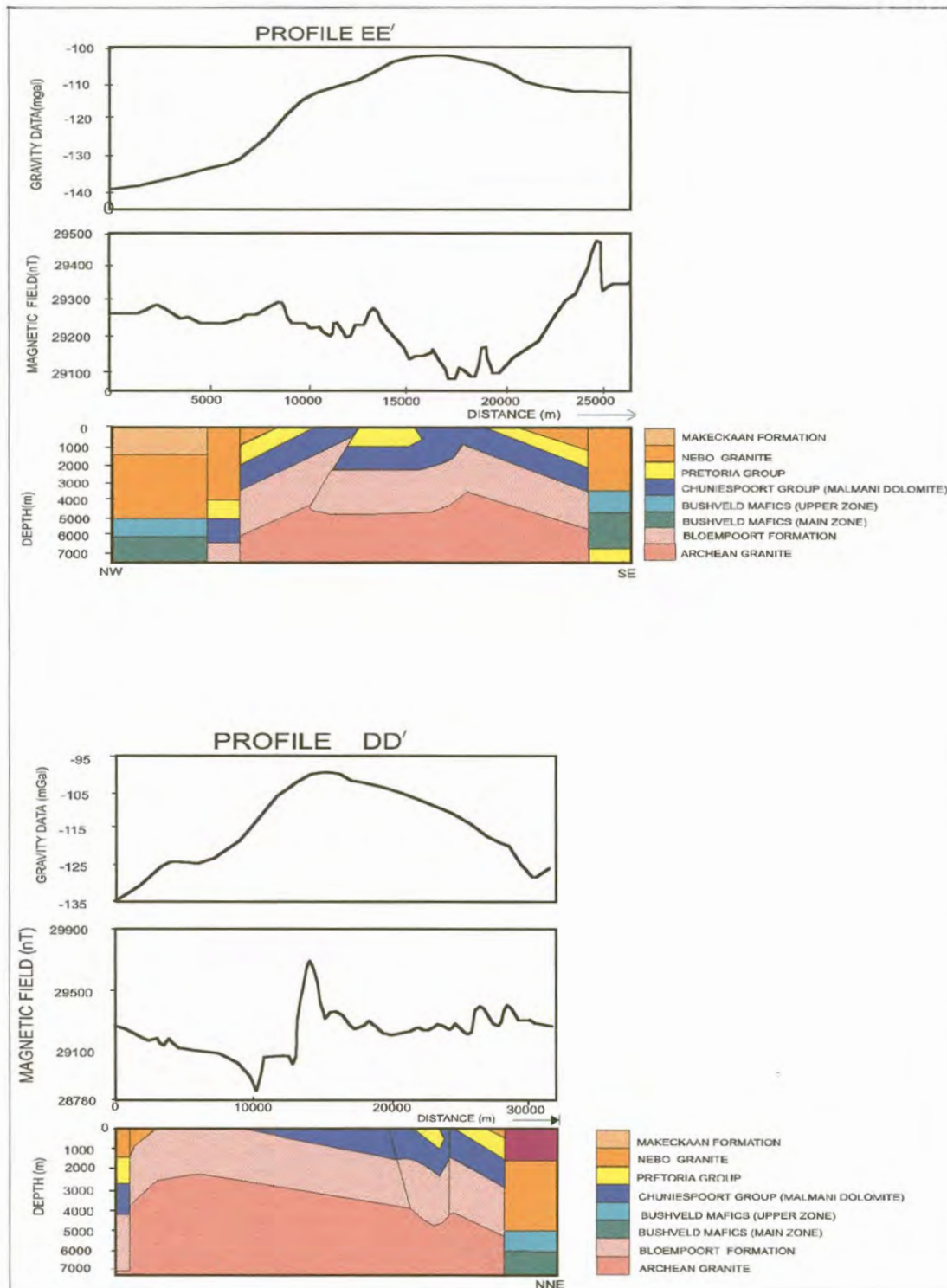


Figure 4.21 : Geological cross-sections gravity and magnetic data along profiles EE' and DD'.

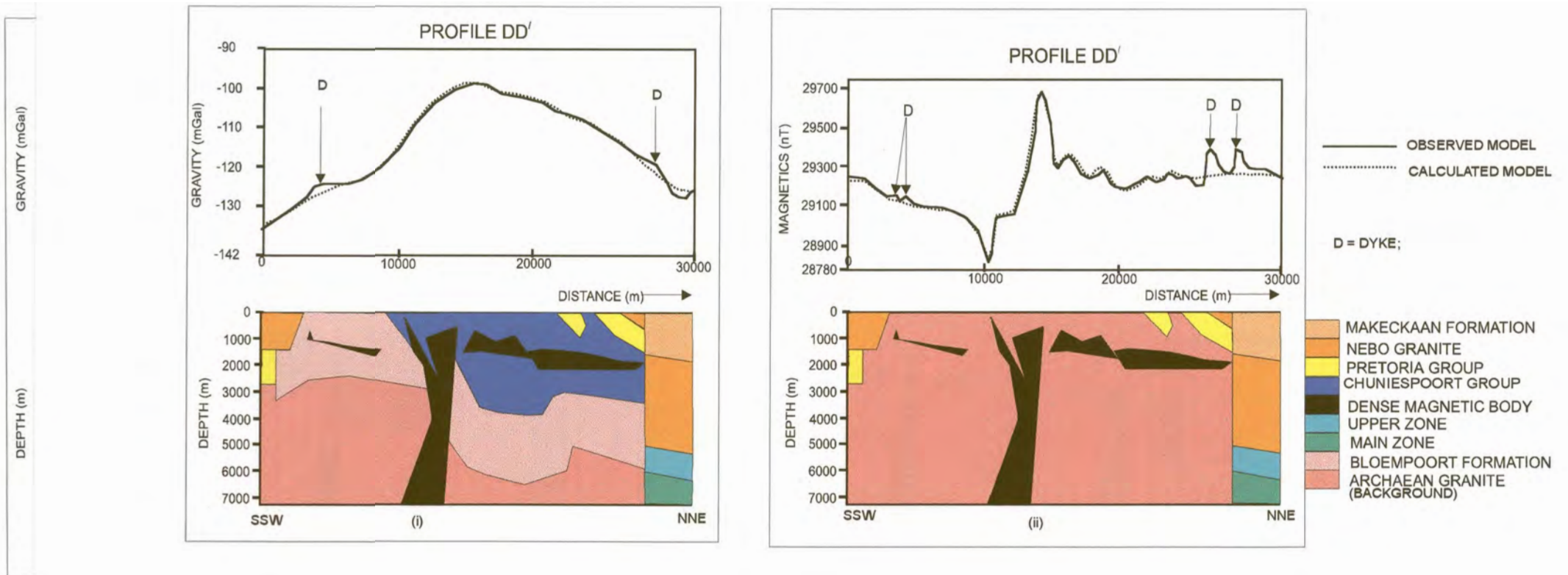


Figure 4.22: Geophysical models for profiles DD' (i) the gravity and (ii) the magnetics.

Fig

4.4.5. LIMITATIONS.

The process of quantitative interpretation of both gravity and magnetic anomalies endeavours to determine a source distribution whose anomalous field matches as closely as possible the actual field on the surface of measurement (Patterson and Reeves, 1985).

The interpretation is inherently ambiguous and this ambiguity arises because any given anomaly could be caused by an infinite number of possible sources. For example concentric spheres of constant mass but differing density and radius will all produce the same anomaly, since their mass acts as though located at the centre of the sphere. This ambiguity represents the inverse problem of potential field interpretation, which states that although the anomaly of a given body may be calculated uniquely, there are an infinite number of bodies that could give rise to any specified anomaly.

Another limitation to this interpretation is that a large deep body can also give the same anomaly as a small shallow body. This means that the amplitude and shape of an anomaly produced by a large body at great depth can be similar to that of a small body closer to the surface. In the same vein, a steeply dipping body and a vertical body might produce the same anomaly.

Removal of regional field to isolate the residual anomalies also provides a limitation in potential field interpretation especially in gravity surveying. This is because, if the regional field subtracted is too much, part of the residual anomalies of interest could be omitted and if too little a regional field is subtracted, fictitious residual anomalies could arise which are not supposed to be part of the anomalies of interest.

In this study, several samples of each particular rock type from surface outcrops have been

used for density determinations in order to obtain a reliable mean density and variance. In sedimentary rock sequences however, density tends to increase with depth due to compaction, and with age, due to progressive diagenesis, hence, non-availability of bore-hole information at depth from every part of the study area, might have an effect on the gravity models interpreted. A major consolation in this regard is that, the mean densities obtained for the different rock samples are compatible with that obtained in this area by Button (1973), Hattingh (1980), and Comer *et al.* (undated).

Due to non-uniqueness of potential field interpretation such as in the gravity and magnetic methods used in this study, constraints have been introduced in the form of simplification of geometry, limits to size or depth, range limits on density and susceptibility, location and extent of outcrops and other parameters seemed justifiable in the context of what is known or can be reasonably inferred about the Marble Hall geological environment.

4.5. CONCLUSIONS

Based on the data presented in the previous sections, the following conclusions can be made :

1. The high magnetic signature associated with the eastern limb of the Swartkop-Marble Hall Anticline, running from the south towards the north-east as observed on the total field map, is the surface expression of the Hekpoort Andesite Formation.
2. A well-defined fault, trending north-south, forms the eastern boundary of the Marble Hall Fragment. The dip of this fault could not be determined because there is no surface expression of the fault.

3. A highly magnetic, dense rock mass is situated in the centre of the Fragment. This rock mass is interpreted as an intrusive body with a central sub-vertical core section, surrounded at shallower levels, by sub-horizontal sill-like sections.
4. Due to non-uniqueness in potential field interpretation discussed above, the exact depth and thickness of the mafic sills cannot be categorically stated. It is conceivable that the sills might be thinner than indicated (Figures 4.19(a) and (b), 4.22, 4.23), but much closer to the surface.
5. The crescent shaped body with high magnetic signature along the axis of the Swartkop-Marble Hall Anticline and truncated by a fault to the north, is well defined but its origin is not obvious. The outcropping lithologies in that area can not explain the high magnetic signature. It is postulated that it might be a covered sill related to the Rustenburg Layered Suite.
6. Overall, the structure of the Marble Hall Fragment can be regarded as folded floor of Transvaal Supergroup rocks between two faults - the Wonderkop fault in the north-west and the delineated north-south trending fault in the east.
7. From model interpretations, it can be suggested that the intrusion of the Bushveld mafics post-dates the folding and perhaps some of the faults in the Fragment.
8. The dips of the faulting is given as vertical in this interpretation but it is conceivable that this might not be so.

Further investigation of the Marble Hall Fragment by other geophysical methods and finally drilling, will assist in confirming the presence and exact location in depth of the main intrusive mafic body which might have potential economic value.

REFERENCES

- Button, A.(1973). A regional study of the stratigraphy and the development of the Transvaal Basin in the eastern and north-eastern Transvaal, Ph.D Thesis, Univ. Witwatersrand, Johannesburg, 352 pp. (unpubl.)
- Button, A. (1976). Stratigraphy and relations of the Bushveld floor in the Eastern Transvaal Trans. Geol. Soc. S. Afr. **79**. 3 - 12.
- Cairncross, B. and Dixon, R. (1995). The Bushveld Complex . In : Minerals of South Africa. Published by Geological Society of South Africa. 79 - 87pp.
- Cameron, E.N. and Emerson, M.E. (1959). The origin of certain chromite deposits of the eastern part of the Bushveld Complex. : Econ. Geol., **54**, 1151 - 1213.
- Cameron, E.N. (1978). The lower zone of the eastern Bushveld Complex in the Olifants River trough. J. Petrol., **19**, 437 - 462.
- Cawthorn, R.G. and McCarthy, T.S. (1985). Incompatible trace element behaviour in the Bushveld Complex. Econ. Geol., **80**, 1016 - 1026.
- Coertzee, F.J. (1970). The geology of the western part of the Bushveld Igneous Complex. In: Symposium on the Bushveld Igneous Complex and other layered intrusions (Edited by Visser, D.J.L. and von Gruenewaldt, G.). 1 - 20 pp. Special Publication Geological Society South Africa, Johannesburg.
- Coertzee, F.J. (1974). The geology of the basic portion of the western Bushveld Igneous Complex: Mem. Geol. Surv. Soc. S. Afr., **66**, 148pp.
- Corner, B., Nkwana, M.M. and Antoine, L.A.G.(undated) Physical properties handbook of Southern African rocks. Bulletin of the Geological Survey of South Africa. Univ. of Witwatersrand, Geophysics Dept.(unpubl.)

- Cousins, C.A. (1959). The structure of the mafic portion of the Bushveld Igneous Complex.
Trans. Geol. Soc. S. Afr. **62**, 179 – 189.
- Daly, R.A. and Molengraaff, G.A.F. (1924). Structural relations of the Bushveld Igneous Complex, Transvaal: Jour. Geology, **32**, 1 - 35.
- Debeglia, N. and Corpeel, J. (1997). Automatic interpretation of potential field data using analytical signal derivatives. Geophysics, **62**, 87 - 96.
- De Waal, S.A. (1963). Die plooi-kompleks van die Sisteem Transvaal noord van Marble Hall en die meegande metamorfe in intrusiegesteentes. MSc. Thesis, University of Pretoria, Pretoria.
- De Waal, S.A. (1970). Interference-folding of Bushveld-Igneous-Complex age in the Transvaal System north of Marble Hall, Transvaal. In: Symposium on the Bushveld Igneous Complex and other layered intrusions. Geological Society South Africa, Special Publication, **1**, 283 – 298.
- De Waal, S.A. (1972). The Bushveld Granites in the Zaaipplaats area : Trans. Geol. Soc. S. Afr., **75**, 135 - 148.
- Eales, H.V., Marsh, J.S., Cox, K.G. (1984). The Karroo Igneous Province : An introduction. Spec. Publ. geol. Soc. S. Afr., **13**, 1 – 26.
- Eales, H.V., Botha, W.J., Hattingh, P.J., De Klerk, W.J., Maier, W.D. and Odgers, A.T.R. (1993) The mafic rocks of the Bushveld Complex: a review of emplacement and crystallisation history, and mineralisation, in the light of recent data. Journal of African Earth Sciences, Vol. **16**, No. 1/2, 121 – 142.
- Geosoft Inc. (1996) Data Processing System for Earth Science Applications, OASIS Montaj version 4.1 user guide.
- Hall, A.L. (1932). The Bushveld Igneous Complex of the Central Transvaal. Mem. Geol. Surv. S. Afr., **28**, 560pp.

- Hartzer, F.J. (1994) Geology of Transvaal inliers of the Bushveld Complex. Ph.D. Thesis (unpubl.). Rand Afrikaans University, 366 pp.
- Hamilton, P.J. (1977). Sr-isotope and trace element studies of the Great Dyke and the Bushveld mafic phase and their relation to early Proterozoic magma genesis in Southern Africa. *J. Petrol.*, **18**, 24 -52.
- Harmer, R.E. and Sharpe, M.R. (1985). Field relations and strontium isotope systematics of the marginal rocks of the eastern Bushveld Complex. *Econ. Geol.*, **80**, 813 - 837.
- Hatton, C.J. and Schweitzer, J.K. (1995). Evidence for synchronous extrusive and intrusive Bushveld magmatism. *Journal. African Earth Sciences*, **21**, 579 - 594.
- Hattingh, P.J.(1977). 'n Regionale gravitasie-opname van die Bosveldkompleks in die omgewing van Groblersdal, Lydenburg en Belfast. MSc. Thesis (unpubl.), Univ. Pretoria, 55 pp.
- Hattingh, P.J.(1980). The structure of the Bushveld Complex in the Groblersdal - Lydenburg-Belfast area of the eastern Transvaal as interpreted from a regional gravity survey. *Trans.Geol. Soc. S.Afr.* **83**, 125 – 133.
- Hattingh, P.J.(1983). A paleomagnetic investigation of the layered mafic sequence of the Bushveld Complex. PhD, Thesis, University of Pretoria(unpubl.).
- Hattingh, P.J.(1986a). The paleomagnetism of the Merensky reef footwall rocks of the Bushveld Complex. *Trans. Geol. Soc. S. Afr.* **89**, 1–8.
- Hattingh, P.J.(1986b). The paleomagnetism of the Main Zone in the western Bushveld Complex. *Tectonophysics* **79**, 441 - 452.
- Hattingh, P.J.(1986c). The paleomagnetism of the Main Zone of the eastern Bushveld Complex. *Tectonophysics* **124**, 271 – 295.
- Hattingh, P.J.(1989). The paleomagnetism of the Upper Zone of the Bushveld Complex. *Tectonophysics* **165**, 131 – 142.

- Hattingh, P.J.(1991). The magnetic susceptibility of the mafic rocks of the Bushveld Complex. South African Jour. of Geol. **94**, 132 - 136.
- Hunter, D.R.(1975) The regional geologic setting of the Bushveld Complex (An adjunct to the provisional tectonic map of the Bushveld Complex). Econ. Geol. Res. Unit, Univ. of Witwatersrand, 18pp.
- Jorssen, F. (1904) On the occurrence of the Dolomite and Chert Series in the Rustenburg district. Trans geol. Soc. S. Afr., **7**, 30 – 38.
- Kimbell, G.S., Burley, A.J., Parker, M.E., Pease, S.F., and Barton, K.J. (1984). The gravity survey of the Molopo Farms area, southern Botswana: Bull. **30**, Geol. Survey Dept., Botswana.
- Kleeman, G.J. & Twist, D. (1989). The compositionally-zoned sheet-like granite pluton of the Bushveld Complex : evidence bearing on the nature of the A-type magmatism. J. Petrol., **30**, 1383 – 1414.
- Klemm, D.D., Kettner, S., Reichardt, F., Steindl, J., and Weber-Diefenbach, K. (1985a). Implications of vertical and lateral compositional variations across the pyroxene marker and its associated rocks in the upper part of the Main Zone in the eastern Bushveld Complex. Econ. Geol., **80**, 1007 - 1015.
- Kleywegt, R.J. and Du Plessis, A.(1986). On the structure of the Bushveld Complex and the central Transvaal basin. Extd. Abst. Geocongress '86, Univ. of the Witwatersrand, Johannesburg, S. Afr.
- Kruger, F.J. and Corner, B.(1987). The tectonic setting of the Bushveld Complex and other layered intrusions in Southern Africa: Geophysical and Isotopic evidence. Indaba on the tectonic setting of layered intrusives. Geol. Soc. of South Africa, Pretoria, 31 – 32.
- Lee, C.A. and Sharpe, M.R.(1983) An interpretation of the structure of the Bushveld Complex aided by LANDSAT imagery. 15 pp., Institute Geological

Research Bushveld Complex, Pretoria University, South Africa.

- Lee, C.A. and Sharpe, M.R.(1986) The structural setting of the Bushveld Complex – an assessment aided by Landsat imagery. In: Anhausser C.R. and Maske,S. (eds.), Mineral deposits of Southern Africa 2, Geol. Soc. South Africa, 1031 – 1038.
- Lombaard, B.V. (1931) The geology of north-eastern Pretoria District and adjoining country. Explan. Sheet 18 (Moos River), Geol. Surv. S.Afr., 43 pp.
- Marlow, A.G. (1976). The geology of the Bushveld Complex on the Sekhukhune Plateau, Eastern Transvaal. MSc. Thesis (University of Pretoria).
- McCarthy, T.S. & Hasty, R.A.(1976). Trace elements distribution patterns and their relationship to the crystallisation of granitic melts. Geochim. Cosmochim. Acta, 40, 1351 – 1358.
- McCaskie, D.R. (1983). Differentiation of the Nebo Granite (main Bushveld granite), South Africa. Ph.D. thesis (unpubl.), Univ. Oregon, Corvallis, 121 pp.
- Mellor, E.T. (1906). The geology of the central portion of the Middleburg district. Ann. Rept. Geol. Surv. Transvaal, 55 – 71.
- Meyer, R.(1987). The structure of the Bushveld Complex: An evaluation of geophysical evidence. Indaba on the tectonic setting of layered intrusives. Geol. Soc. of South Africa, Pretoria, 18 – 21.
- Meyer, R. and de Beer, J.H.(1987). Structure of the Bushveld Complex from resistivity measurements. Nature **325**, 610 – 612.
- Molengraff, G.A.F. (1901). Géologie de la Republique Sud-Africaine du Transvaal. Bull. Soc. Geol. De France, 4 Ser Tome, 1, 13 - 92.
- Molengraff, G.A.F. (1902). Vice President's address. Trans geol. Soc. S. Afr., **5**, 69 – 75.
- Molyneux, T.G. (1974). A geological investigation of the Bushveld Complex in Sekhukhuneland and part of the Steelpoort valley: Trans. Geol. Soc.

S. Afr., **77**, 329 - 338.

Molyneux, T.G. and Klinkert, P.S.(1978). A structural interpretation of part of the eastern mafic lobe of the Bushveld Complex and its surrounds. Trans. Geol. Soc. S.Afr. **81**, 359 – 368.

Morelli, C., Ganter, C., Honkasalo, T., McConnell, R.K., Szabo, B., Tanner, J.G., Votila, U. & Whalen, C.T. (1974). The international gravity standardization net, 1971. Spec. Publ. Int. Assoc. Geod., Paris, **4**, 194 pp.

Moritz, H. (1968) The Geodetic Reference System (1967). Allgem. Vermessungs-Nachrichten, **2** – 7.

Nabighian, M.N. (1972) The analytical signal of two-dimensional magnetic bodies with polygonal cross-sections, its properties and use for automated anomaly interpretation, Geophysics, **37**, 507 – 517 pp.

Nabighian, M.N. (1984) Toward a three-dimensional automatic interpretation of potential field data via generalised Hilbert transforms. Fundamental relations. Geophysics, **49**, 780 – 786 pp.

Patterson, R.N., Reeves, C.V. (1985) Applications of gravity and magnetic surveys : The state-of -the-art in 1985. Geophysics, **50**, No. 12, 2558 - 2594 pp.

Reeves, C.V. (1985). The Kalahari Desert, central southern Africa : a case history of Regional gravity and magnetic exploration, in Hinze, W.J. Ed., The utility of regional gravity and magnetic anomaly maps: Soc. Explor. Geophys.

SACS (South African Committee for Stratigraphy) 1980. Stratigraphy of South Africa. Part 1 (Comp. L.E. Kent). Lithostratigraphy of the Republic of South Africa, South West Africa / Namibia, and the Republics of Bophuthatswana, Transkei and Venda. Geol. Surv. South Africa, Handbook **8**, 690 pp.

- Schreiber, U.M. (1991). A palaeoenvironmental study of the Pretoria Group in the eastern Transvaal. PhD. Thesis (unpubl.), University of Pretoria, Pretoria, South Africa.
- Schweitzer, J.K. and Hatton, C.J. (1995). Synchronous emplacement of the felsites, granophyres, granites and mafic intrusives of the Bushveld Complex. In: Extended Abstracts of the Centennial Geocongress (Edited by Barton, J.M. and Copperwaite, Y.E.) pp. 532 – 535. Geological Society of South Africa, Johannesburg.
- Schweitzer, J.K. and Hatton, C.J. and de Waal, S.A. (1995a). Economic potential of the Rooiberg Group: volcanic rocks in the floor and roof of the Bushveld Complex. *Mineralium Deposita* **30**, 168 – 177.
- Seigel, H.O. (1993). A guide to high precision land gravimeter surveys. Scintrex Limited, Ontario, Canada, 17 – 72pp.
- Sharpe, M.R. and Snyman, J. (1980). A model for the emplacement of the eastern compartment of the Bushveld Complex. *Tectonophysics*, **65**, 85 – 110.
- Sharpe, M.R. (1981). The chronology of magma influxes to the eastern compartment of the Bushveld Complex as exemplified by its marginal border group. *J. geol. Soc. Lond.*, **138**, 307 - 326.
- Sharpe, M.R., Bahat, D. and von Gruenewaldt, G. (1981). The concentric elliptical structure of feeder sites to the Bushveld Complex and possible economic implications. *Trans. Geol. Soc. S.Afr.* **84**, 239 - 244.
- Sharpe, M.R. (1985). Strontium isotope evidence for preserved density stratification in the Main Zone of the Bushveld Complex, South Africa. *Nature*, **316**, 119 – 126.
- Smit, P.J. (1961). Gravity Survey of the Republic of South Africa Part III – Interpretation of gravity anomalies. *Geol. Surv. S. Afr. Open File Report* **300**, 234pp.

- Smit, P.J., Hales, A.L. and Gough, D.I. (1962). The gravity survey of the Republic of South Africa. Handbook 3: Govt. Printer, Pretoria, S. Afr. 484 pp.
- Snyman, C.P. (1956). 'n Koepelstruktuur en die metamorfose van die sisteem Transvaal Suid van Marble Hall, Transvaal. M.Sc. thesis. Univ. Pretoria, Pretoria, 122 pp.
- Snyman, C.P. (1958) 'nGneis, 'n Koepelstruktuur en die metamorfose van die sisteem Transvaal suid van Marble Hall, Transvaal. Trans geol. Soc. S. Afr., 61, 225 - 262.
- Stoyer, C.H. (1988) Magix user's manual, Interpex Limited, Golden, Co, USA.
- Teigler, B. (1990). Mineralogy, petrology and geochemistry of the Lower and Critical Zones, north-western Bushveld Complex. PhD. Thesis, Rhodes University (unpubl.), 247 pp.
- Telford, W.M. et al. (1990) Applied geophysics, second edition. Cambridge University Press, Cambridge, New York, 62 – 134, 343 – 577 pp.
- Trimble Navigation Limited (1992). 4000SSE Geodetic Surveyor, operation manual, Revision A.
- Truter, F.C. (1955). Modern concepts of the Bushveld Igneous Complex. C.C.T.A. South Reg. Comm. Geol. 1, 77 - 87.
- Van der Merwe, M.J. (1976). The layered sequence of Potgietersrus limb of the Bushveld Complex: Econ. Geol., 71, 1337 - 1351.
- Vermaak, C.F. (1970). The geology of the lower portion of the Bushveld Complex and its relationship to the floor rocks in the area west of Pilannesburg, western Transvaal. Spec. Publ. Geol. Soc. S. Afr., 1, 242 - 262.
- Vermaak, C.F. (1976). The nickel pipes of Vlakfontein and vicinity, western Transvaal. Econ. Geol., 71, 261 - 268.
- Vermaak, C.F. and von Gruenewaldt, G. (1986). Introduction to the Bushveld Complex.

Mineral deposits of Southern Africa, 1021 – 1029 pp.

- Walraven, F.(1987a). Textural, geochemical and genetical aspects of the granophyric rocks of the Bushveld Complex. Mem. Geol. Surv. S. Afr., **72**, 145 pp.
- Walraven, F., Armstrong, R.A., and Kruger, F.J.(1988). A chronostratigraphic framework for the north-central Kaapvaal Craton, the Bushveld Complex and the Vredefort structure. Tectonophysics, **171**, 23 – 48.
- Walraven, F. and Hattingh, E. (1993). Geochronology of the Nebo Granite, Bushveld Complex. S.Afr., Vol. **96**, 31 – 41.
- Wagner, P.A. (1927) The geology of the north-eastern part of the Springbok Flats and surrounding country. Explan. Sheet 17 (Springbok Flats), Geol. Surv. S. Afr., 104 pp.
- Wessels, J.T. (1943) The geology of the Stavoren and Marble Hall Fragments. Report, Geol. Surv. S. Afr., Pretoria.
- Young, D.R. (1978). Explanatory notes for 1: 50000 sheets 2526BA (Kayakulu), 2526BB (Mabeskraal) and 2526BC (Lindleyspoort): (unpubl.) Rep. Geol. Surv. S.Afr.